Published for SISSA by Springer

Received: *November 12, 2024*
Accepted: *April 2, 2025*
Published: *May 8, 2025*

Search for vector-like leptons coupling to first- and second-generation Standard Model leptons in pp collisions at $\sqrt{s} = 13$ TeV with the ATLAS detector

The ATLAS collaboration

E-mail: atlas.publications@cern.ch

Abstract: A search for pair production of vector-like leptons coupling to first- and second-generation Standard Model leptons is presented. The search is based on a dataset of proton-proton collisions at $\sqrt{s} = 13$ TeV recorded with the ATLAS detector during Run 2 of the Large Hadron Collider, corresponding to an integrated luminosity of 140 fb^{-1}. Events are categorised depending on the flavour and multiplicity of leptons (electrons or muons), as well as on the scores of a deep neural network targeting particular signal topologies according to the decay modes of the vector-like leptons. In each of the signal regions, the scalar sum of the transverse momentum of the leptons and the missing transverse momentum is analysed. The main background processes are estimated using dedicated control regions in a simultaneous fit with the signal regions to data. No significant excess above the Standard Model background expectation is observed and limits are set at 95% confidence level on the production cross-sections of vector-like electrons and muons as a function of the vector-like lepton mass, separately for SU(2) doublet and singlet scenarios. The resulting mass lower limits are 1220 GeV (1270 GeV) and 320 GeV (400 GeV) for vector-like electrons (muons) in the doublet and singlet scenarios, respectively.

Keywords: Beyond Standard Model, Hadron-Hadron Scattering

ArXiv ePrint: 2411.07143

https://doi.org/10.1007/JHEP05(2025)075

JHEP05(2025)075

Contents

JHEP05(2025)075

1 Introduction

The Standard Model (SM) of particle physics is the most successful and tested theory of the known fundamental particles and their interactions. The last missing piece of the SM puzzle, the Higgs boson, was discovered in 2012 by the ATLAS and CMS Collaborations [1, 2] at the Large Hadron Collider (LHC) [3]. Despite its many achievements, the SM remains an incomplete theory, as it does not provide answers for open questions such as the structure of masses and mixings of elementary fermions (also known as the 'flavour puzzle'), the hierarchy and fine-tuning problems, the observed baryon asymmetry in the universe, and the nature of dark matter and dark energy. Many beyond-the-SM (BSM) theories, typically introducing new particles and interactions, or a new space-time structure, have been proposed to address these and other shortcomings of the SM.

Vector-like fermions are hypothetical particles whose left- and right-handed chiral components have the same transformation properties under the weak-isospin SU(2) gauge group [4–8]. Consequently, they have Dirac masses, without a Yukawa coupling proportional to their mass, becoming less constrained by Higgs boson measurements [9]. Vector-like fermions arise in many BSM scenarios, such as Composite Higgs models [10, 11], models

with extra spatial dimensions [12, 13], supersymmetric models [14, 15], and grand unified theories [16–18]. In particular, vector-like fermions can provide an explanation to the flavour puzzle via their mixings with SM fermions [19, 20], or even provide a dark matter candidate [21–24]. Naturalness arguments [25] require that quadratic divergences that arise from the radiative corrections to the Higgs boson mass are cancelled out by some new mechanism to avoid fine-tuning, and vector-like quarks play such role, e.g in Composite Higgs models. On the other hand, the observed tensions between the measured and predicted values of the muon [26, 27] and electron [28–30] anomalous magnetic moments or the so-called 'Cabibbo angle anomaly' [31–33] can be explained by BSM models including vector-like leptons (VLL) [34–38]. VLLs mixing with first-, second-, or third-generation SM leptons ($\ell = e, \mu, \tau$) are referred to as vector-like electrons, muons, or τ-leptons, respectively.

At the LHC, VLLs are predominantly produced in pairs via the electroweak interaction, and consequently have a considerably lower production cross-section than vector-like quarks, for which a broad search programme has been developed [39, 40]. In contrast, only few LHC searches for VLLs exist, which are summarised below. The production and decay modes for VLLs depend on the assumed SU(2) representation [41, 42]. In the doublet scenario, two mass-degenerate VLLs at tree level, one electrically charged ($L^{\pm}$) and one electrically neutral (N^0), form an SU(2) doublet (L, N^0). They can be produced in association via the exchange of a virtual W boson in the s-channel, $pp \to W^* \to L^+\bar{N}^0$,[1] or in pairs via a virtual Z-boson or photon exchange, $pp \to Z^*/\gamma^* \to L^+L^-$ and $pp \to Z^* \to N^0\bar{N}^0$. In the doublet scenario, the charged VLL decay modes are $L \to \ell Z$ and ℓH, where H is the SM Higgs boson, with branching ratios that depend on the VLL mass m_L and asymptotically reach 50% each for $m_L \gg m_H$, in accordance with the Goldstone boson equivalence theorem [43]; at lower masses, the branching ratio to ℓH decreases as it becomes kinematically disfavoured. In contrast, the neutral VLL decay mode is $N^0 \to \ell W$ with 100% branching ratio. In the singlet scenario, only the charged VLL is present and is also produced in pairs, $pp \to Z^*/\gamma^* \to L^+L^-$; its decay modes are $L \to \nu W$, ℓZ and ℓH, with branching ratios asymptotically reaching 50%, 25%, and 25%, respectively.

Searches by the L3 Collaboration at the LEP Collider excluded vector-like electrons, muons and τ-leptons with masses less than ∼100 GeV at the 95% confidence level (CL) [44]; the limits are similar for both the doublet and singlet scenarios. At the LHC, using a data sample of proton-proton (pp) collisions at a centre-of-mass energy of $\sqrt{s} = 8$ TeV corresponding to an integrated luminosity of 20.3 fb^{-1}, the ATLAS Collaboration excluded vector-like electrons (muons) in the mass range 129–176 GeV (114–168 GeV), except for the interval 144–163 GeV (153–160 GeV), in the singlet scenario [45]. Both the ATLAS and CMS Collaborations searched for vector-like τ-leptons using the full LHC Run 2 dataset at $\sqrt{s} = 13$ TeV, corresponding to about 140 fb^{-1}. Assuming the doublet scenario, the ATLAS search excluded vector-like τ-leptons in the mass range of 130–900 GeV [46]. The CMS search considered both the doublet and singlet scenarios, excluding vector-like τ-leptons in the mass ranges of 100–1045 GeV and 125–150 GeV, respectively [47].

This paper presents a search for doublet or singlet VLLs coupling to first- and second-generation SM leptons. Final states with two opposite-sign, three and four leptons are

[1]The charge-conjugate process, $pp \to W^* \to L^-N^0$, is also implied.

JHEP05(2025)075

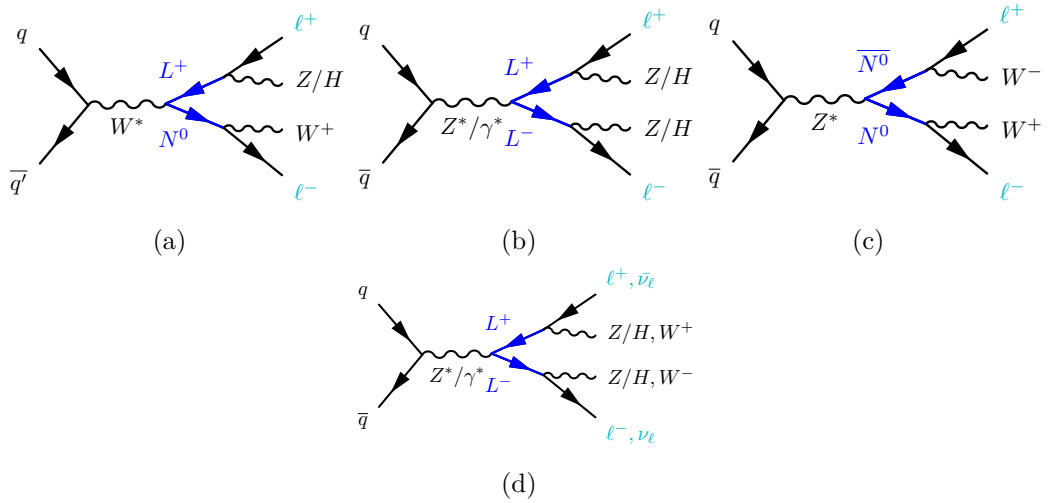

Figure 1. Feynman diagrams illustrating the pair production and decay of vector-like leptons: (a-c) refer to the doublet scenario, and (d) to the singlet scenario.

considered in the signal regions, where the leptons can originate from the VLL decays or the sub-sequent decays of the Z, H, or W bosons. Figure 1 illustrates the signal processes targeted in this analysis. The search is based on a dataset of pp collisions at $\sqrt{s} = 13$ TeV recorded with the ATLAS detector during Run 2 of the LHC, corresponding to an integrated luminosity of 140 fb^{-1}. A mass range between 150 GeV and 1600 GeV is considered for vector-like electrons (VLL$_e$) and vector-like muons (VLL$_\mu$). Vector-like leptons in the doublet scenario with mass values lower than 150 GeV would have already been seen by differential cross-section measurements in four-lepton events [48], and are therefore not considered in this analysis. A categorisation based on a deep neural network (DNN) is performed to enhance the purity of the various signal types and to discriminate signal against the SM background. Control regions (CRs), orthogonal to the signal regions (SRs), are defined to constrain the normalisation of the main backgrounds: $t\bar{t}$, Z + jets, $t\bar{t}W$, $t\bar{t}Z$, VV and non-prompt lepton backgrounds. A maximum-likelihood fit is performed across event categories to search for the signal and constrain several leading background processes simultaneously.

2 ATLAS detector

The ATLAS detector [49] at the LHC covers nearly the entire solid angle around the collision point.[2] It consists of an inner tracking detector surrounded by a thin superconducting solenoid, electromagnetic and hadronic calorimeters, and a muon spectrometer incorporating three large superconducting air-core toroidal magnets.

[2]ATLAS uses a right-handed coordinate system with its origin at the nominal interaction point (IP) in the centre of the detector and the z-axis along the beam pipe. The x-axis points from the IP to the centre of the LHC ring, and the y-axis points upwards. Polar coordinates (r, ϕ) are used in the transverse plane, ϕ being the azimuthal angle around the z-axis. The pseudorapidity is defined in terms of the polar angle θ as $\eta = -\ln\tan(\theta/2)$ and is equal to the rapidity $y = \frac{1}{2}\ln\left(\frac{E+p_z}{E-p_z}\right)$ in the relativistic limit. Angular distance is measured in units of $\Delta R \equiv \sqrt{(\Delta y)^2 + (\Delta\phi)^2}$.

JHEP05(2025)075

The inner-detector system (ID) is immersed in a 2 T axial magnetic field and provides charged-particle tracking in the range $|\eta| < 2.5$. The high-granularity silicon pixel detector covers the vertex region and typically provides four measurements per track, the first hit generally being in the insertable B-layer (IBL) installed before Run 2 [50]. It is followed by the SemiConductor Tracker (SCT), which usually provides eight measurements per track. These silicon detectors are complemented by the transition radiation tracker (TRT), which enables radially extended track reconstruction up to $|\eta| = 2.0$. The TRT also provides electron identification information based on the fraction of hits (typically 30 in total) above a higher energy-deposit threshold corresponding to transition radiation.

The calorimeter system covers the pseudorapidity range $|\eta| < 4.9$. Within the region $|\eta| < 3.2$, electromagnetic calorimetry is provided by barrel and endcap high-granularity lead/liquid-argon (LAr) calorimeters, with an additional thin LAr presampler covering $|\eta| < 1.8$ to correct for energy loss in material upstream of the calorimeters. Hadronic calorimetry is provided by the steel/scintillator-tile calorimeter, segmented into three barrel structures within $|\eta| < 1.7$, and two copper/LAr hadronic endcap calorimeters. The solid angle coverage is completed with forward copper/LAr and tungsten/LAr calorimeter modules optimised for electromagnetic and hadronic energy measurements respectively.

The muon spectrometer (MS) comprises separate trigger and high-precision tracking chambers measuring the deflection of muons in a magnetic field generated by the superconducting air-core toroidal magnets. The field integral of the toroids ranges between 2.0 and 6.0 T m across most of the detector. Three layers of precision chambers, each consisting of layers of monitored drift tubes, cover the region $|\eta| < 2.7$, complemented by cathode-strip chambers in the forward region, where the background is highest. The muon trigger system covers the range $|\eta| < 2.4$ with resistive-plate chambers in the barrel, and thin-gap chambers in the endcap regions.

The luminosity is measured mainly by the LUCID-2 [51] detector that records Cherenkov light produced in the quartz windows of photomultipliers located close to the beampipe.

Events are selected by the first-level trigger system implemented in custom hardware, followed by selections made by algorithms implemented in software in the high-level trigger [52]. The first-level trigger accepts events from the 40 MHz bunch crossings at a rate below 100 kHz, which the high-level trigger further reduces in order to record complete events to disk at about 1 kHz.

A software suite [53] is used in data simulation, in the reconstruction and analysis of real and simulated data, in detector operations, and in the trigger and data acquisition systems of the experiment.

3 Data and simulated event samples

This analysis uses data from pp collisions at $\sqrt{s} = 13$ TeV collected by the ATLAS experiment from 2015 to 2018. After the application of data-quality requirements [54] to ensure that all parts of the detector are operational during data-taking, the data sample corresponds to an integrated luminosity of 140 fb^{-1}. The number of additional pp interactions per bunch crossing (pile-up) in this sample ranges from about 8 to 70, with an average of 34. The trigger requirements are discussed in section 5.

JHEP05(2025)075

Monte Carlo (MC) simulation samples are produced for the different signal and background processes. Table 1 gives a detailed summary of all signal and SM background samples used in this analysis. All samples showered with Pythia use the A14 set of tuned parameters [55] (referred to as 'tune'), whereas those showered with Herwig use the H7-UE tune [56]. In all samples simulated with Sherpa [57], the matrix elements (MEs) are calculated with the Comix [58] and OpenLoops [59–61] libraries. They are matched with the Sherpa parton shower (PS) [62] using the MEPS@NLO prescription [63–66] with the set of tuned parameters developed by the Sherpa authors. Pile-up is modelled using events from minimum-bias interactions generated with Pythia 8.186 [67] with the A3 tune [68], and overlaid onto the simulated hard-scatter events according to the luminosity profile of the recorded data. All samples include leading-logarithm photon emission, either modelled by the PS generator or by Photos [69]. The mass of the top quark and SM Higgs boson are set to 172.5 GeV and 125 GeV, respectively. The generated events are processed through either a full simulation of the ATLAS detector geometry and response using Geant4 [70], or a faster simulation where the full Geant4 simulation of the calorimeter response is replaced by a detailed parameterisation of the shower shapes (ATLAS Fast Simulation) [71]. Both types of simulated events are processed through the same reconstruction software used for the pp collision data. Corrections are applied to the simulated events so that the particle candidates' selection efficiencies, energy scales and energy resolutions match those determined from data control samples. The simulated samples are normalised to their theoretical cross-sections, most of which are computed to the highest order available in perturbation theory.

Signal samples for VLL_e and VLL_μ from SU(() 2) singlet ($\mathrm{VLL}_e^{\mathrm{S}}$, $\mathrm{VLL}_\mu^{\mathrm{S}}$) and doublet ($\mathrm{VLL}_e^{\mathrm{D}}$, $\mathrm{VLL}_\mu^{\mathrm{D}}$) models are simulated using MadGraph5_aMC@NLO 2.9.5 [72] at next-to-leading-order (NLO) in QCD with the NNPDF3.0nlo PDF set [73] and Pythia 8.245 [74], and processed through the ATLAS Fast Simulation. The NLO cross-section obtained from MadGraph is used for the normalisation of the signals.

The production of $t\bar{t}$ events is modelled using the Powheg Box v2 [75–81] generator at NLO with the NNPDF3.0nlo PDF set. The events are interfaced to Pythia 8.230 to model the PS, hadronisation, and underlying event, using the NNPDF2.3lo set of PDFs. The decays of bottom and charm hadrons are performed by EvtGen 1.6.0 [82]. The $t\bar{t}$ process is modelled with the h_{damp} parameter[3] set to $1.5\,m_t$ [83]. The $t\bar{t}$ sample is normalised to the cross-section prediction at next-to-next-to-leading-order (NNLO) in QCD including the resummation of next-to-next-to-leading logarithmic (NNLL) soft-gluon terms calculated using Top++ 2.0 [84–90]. This cross-section is $\sigma(t\bar{t})_{\mathrm{NNLO+NNLL}} = 832 \pm 51\,\mathrm{pb}$.

The $Z/\gamma^* \to \ell\ell$ process (with $\ell = e, \mu, \tau$) is simulated with Sherpa 2.2.11 [57] using the NNPDF3.0nnlo PDF set [73]. For strong production of Z/γ^* + jets, where a QCD coupling facilitates the production of the additional jets, processes with up to two coloured partons are modelled at NLO in the strong coupling, while processes with up to five additional partons are modelled at leading-order (LO) accuracy. The Z+jets sample is normalised to the theoretical cross-section calculated at NLO accuracy in QCD [91].

[3]The h_{damp} parameter is a resummation damping factor and one of the parameters that controls the matching of Powheg MEs to the PS, thus effectively regulating the high-p_{T} radiation against which the hard-process system recoils.

JHEP05(2025)075

The samples used to model the $t\bar{t}W$ and the $t\bar{t}(Z/\gamma^* \to \ell^+\ell^-)$ backgrounds are simulated using Sherpa 2.2.10 [92] and Sherpa 2.2.11, where the MEs are calculated for up to one and zero additional partons at NLO in QCD, respectively, and up to two partons at LO in QCD. These samples are simulated using the NNPDF3.0nnlo PDF set. The invariant mass of the lepton pair ($m_{\ell^+\ell^-}$) in the $t\bar{t}(Z/\gamma^* \to \ell^+\ell^-)$ sample is set to be greater than 1 GeV. Both the factorisation and renormalisation scales are set to $\mu_r = \mu_f = m_T/2$ in the $t\bar{t}W$ sample, where m_T is defined as the scalar sum of the transverse masses $\sqrt{m^2 + p_T^2}$ of the particles generated from the ME calculation. In addition to this $t\bar{t}W$ prediction at NLO in QCD, higher-order corrections related to electroweak (EW) contributions are also included. First, event-by-event correction factors are applied that provide virtual NLO EW corrections of the order $\alpha^2\alpha_s^2$ derived using the formalism described in ref. [93] along with LO corrections of order α^3. Second, real emission contributions from the sub-leading EW corrections at order $\alpha^3\alpha_s$ [94] are simulated with Sherpa 2.2.10 produced at LO in QCD and included as a separate sample.

Diboson (VV) background processes are simulated with Sherpa 2.2.2 [92] and include $W^\pm Z$, ZZ, and W^+W^- processes. The ME is calculated with NLO accuracy in QCD for up to one additional parton and at LO accuracy for up to three additional partons. The NNPDF3.0nnlo set of PDFs is used. The simulation includes off-shell effects and Higgs boson contributions, where appropriate. Samples for the loop-induced processes $gg \to VV$ are simulated using LO-accurate MEs for up to one additional parton emission.

Samples for $t\bar{t}H$, and single top production are simulated using the NLO generator Powheg Box v2 and interfaced with Pythia 8 for the PS and fragmentation. These samples used the NNPDF3.0nlo PDF set. The decays of bottom and charm hadrons are performed by EvtGen 1.6.0. The production of a top quark in association with a W boson (tW) is modelled using the five-flavour scheme. The diagram removal scheme [95] is used to remove interference and overlap with $t\bar{t}$ production. Single-top s- and t-channel production is modelled using the five- and four-flavour schemes, respectively.

A dedicated $t\bar{t}$ sample including rare $t \to Wb\gamma^*(\to \ell^+\ell^-)$ radiative decays, $t\bar{t} \to W^+bW^-\bar{b}\ell^+\ell^-$, is simulated using a ME calculated at LO in QCD and requiring $m_{\ell^+\ell^-} > 1$ GeV. In this sample the photon can be radiated from the top quark, the W boson, or the b-quark. Both the $t\bar{t}(Z/\gamma^* \to \ell^+\ell^-)$ and $t\bar{t} \to W^+bW^-\bar{b}\ell^+\ell^-$ samples are combined and together form the '$t\bar{t}(Z/\gamma^*)$' sample. The contribution from internal photon conversions ($\gamma^* \to \ell^+\ell^-$, referred to as 'IntC') with $m_{\ell^+\ell^-} < 1$ GeV is modelled by QED multi-photon radiation via the PS in an inclusive $t\bar{t}$ sample. Dedicated Z+jets samples containing electrons from material photon conversion ($\gamma \to e^+e^-$, referred to as 'MatC') or internal photon conversion are generated with Powheg Box and interfaced with Pythia 8 for the PS and fragmentation. These samples are used to model the data in control regions enriched in material and internal conversion electrons, as explained in section 5.

The remaining rare background contributions listed in table 1 are normalised using their LO theoretical cross-sections, except for the $t\bar{t}t\bar{t}$, tZ, single top, W + jets and VH processes, for which a NLO cross-section is used.

JHEP05(2025)075

Process	Generator	ME order	PS	PDF	Tune
VLL signal	MG5_aMC	NLO	Pythia 8	NNPDF3.0nlo	A14
$t\bar{t}$	Powheg-BOX	NLO	Pythia 8	NNPDF3.0nlo	A14
	(Powheg-BOX)	(NLO)	(Herwig7.1.3)	(NNPDF3.0nlo)	(H7-UE-MMHT)
$Z \to \ell^+\ell^-$	Sherpa 2.2.11	MePs@Nlo	Sherpa	NNPDF3.0nlo	Sherpa default
$Z \to \ell^+\ell^-(\gamma \to e^+e^-)$	Powheg-BOX	NLO	Pythia 8	CTEQ6L1nlo [96]	A14
$Z \to \ell^+\ell^-(\gamma* \to e^+e^-)$	Powheg-BOX	NLO	Pythia 8	CTEQ6L1nlo	A14
$t\bar{t}W$	Sherpa 2.2.10	MePs@Nlo	Sherpa	NNPDF3.0nnlo	Sherpa default
	(MG5_aMC)	(NLO)	(Pythia 8)	(NNPDF3.0nlo)	(A14)
$t\bar{t}W$ (EW)	Sherpa 2.2.10	LO	Sherpa	NNPDF3.0nnlo	Sherpa default
	(MG5_aMC)	(LO)	(Pythia 8)	(NNPDF3.0nlo)	(A14)
$t\bar{t}(Z/\gamma^* \to \ell^+\ell^-)$	Sherpa 2.2.11	MePs@Nlo	Sherpa	NNPDF3.0nnlo	Sherpa default
	(MG5_aMC)	(NLO)	(Pythia 8)	(NNPDF3.0nlo)	(A14)
VV, VVV	Sherpa 2.2.2	MePs@Nlo	Sherpa	NNPDF3.0nnlo	Sherpa default
$t\bar{t}H$	Powheg-BOX	NLO	Pythia 8	NNPDF3.0nlo	A14
	(Powheg-BOX)	(NLO)	(Herwig7.0.4)	(NNPDF3.0nlo)	(H7-UE-MMHT)
	(MG5_aMC)	(NLO)	(Pythia 8)	(NNPDF3.0nlo)	(A14)
$t\bar{t}t\bar{t}$	MG5_aMC	NLO	Pythia 8	NNPDF3.1nlo [97]	A14
	(Sherpa 2.2.10)	(MePs@Nlo)	(Sherpa)	(NNPDF3.0nnlo)	(Sherpa default)
$t\bar{t} \to W^+bW^-\bar{b}\ell^+\ell^-$	MG5_aMC	LO	Pythia 8	NNPDF3.0lo	A14
$t(Z/\gamma^*)$	MG5_aMC	NLO	Pythia 8	NNPDF2.3lo	A14
$tW(Z/\gamma^*)$	MG5_aMC	NLO	Pythia 8	NNPDF2.3lo	A14
Single top (t-, Wt-, s-channel)	Powheg-Box	NLO	Pythia 8	NNPDF3.0nlo	A14
W+jets	Sherpa 2.2.1	MePs@Nlo	Sherpa	NNPDF3.0nlo	Sherpa default
VH	Powheg-BOX	NLO	Pythia 8	NNPDF3.0nlo	A14
$t\bar{t}t$	MG5_aMC	LO	Pythia 8	NNPDF2.3lo	A14
$t\bar{t}W^+W^-$	MG5_aMC	LO	Pythia 8	NNPDF2.3lo	A14
$t\bar{t}ZZ$	MG5_aMC	LO	Pythia 8	NNPDF2.3lo	A14
$t\bar{t}HH$	MG5_aMC	LO	Pythia 8	NNPDF2.3lo	A14
$t\bar{t}WH$	MG5_aMC	LO	Pythia 8	NNPDF2.3lo	A14

Table 1. Simulated signal and background event samples, with the corresponding ME generator, ME order (which is the order in the strong coupling constant of the perturbative calculation), PS generator, the generator PDF sets and the underlying set of tuned parameters of the PS generator used. The samples used to estimate the systematic uncertainties are indicated in parentheses and grey. V refers to production of an electroweak boson (W or Z/γ^*). The '$t\bar{t}W$ (EW)' sample also includes next-to-leading-order electroweak corrections. MG5_aMC refers to MadGraph5_aMC@NLO 2.2, 2.3, or 2.6; Pythia 8 refers to version 8.2; MePs@Nlo is the method used in Sherpa to match the ME to the PS.

JHEP05(2025)075

4 Event reconstruction and object identification

Candidate events are required to have at least one pp interaction vertex. Interaction vertices are reconstructed from at least two tracks with transverse momentum p_{T} larger than 500 MeV that are consistent with originating from the beam collision region in the x-y plane. If more than one primary vertex is found in the event, the candidate with the highest scalar sum of the squared transverse momenta of the associated tracks is selected as the hard-scatter primary vertex [98].

Electron candidates are reconstructed from energy clusters in the electromagnetic calorimeter matched to a track in the ID [99]. They are required to satisfy $p_{\mathrm{T}} > 10\,\mathrm{GeV}$ and $|\eta_{\mathrm{cluster}}| < 2.47$, excluding the transition region between the endcap and barrel calorimeters ($1.37 < |\eta_{\mathrm{cluster}}| < 1.52$). "Loose" and "Tight" electron identification working points are used, based on a likelihood discriminant employing calorimeter, tracking and combined information that provide separation between electrons and jets.

The reconstruction of muon candidates is based on tracking information from the MS and the ID, as well as energy deposits in the calorimeter system [100]. Muons are required to satisfy $p_{\mathrm{T}} > 10$ GeV and $|\eta| < 2.5$. "Loose" and "Medium" muon identification working points are used.

Electron (muon) candidates are matched to the primary vertex by requiring that the significance of their transverse impact parameter, d_0,[4] satisfies $|d_0|/\sigma(d_0) < 5\,(3)$, where $\sigma(d_0)$ is the measured uncertainty in d_0, and by requiring that their longitudinal impact parameter, z_0,[5] satisfies $|z_0 \sin\theta| < 0.5$ mm.

Lepton candidates are also required to be isolated in the tracker and in the calorimeter to further suppress leptons from heavy-flavour (HF) hadron decays, misidentified jets, or photon conversions (collectively referred to as "non-prompt leptons"). The track-based lepton isolation criterion is based on the quantity $I_R = \sum p_{\mathrm{T}}^{\mathrm{trk}}$, where the scalar sum includes all tracks (excluding the lepton candidate itself) within a cone of size $\Delta R < R_{\mathrm{cut}}$ around the direction of the lepton. The value of R_{cut} is the smaller of r_{min} and $10\ \mathrm{GeV}/p_{\mathrm{T}}^{\ell}$, where r_{min} is set to 0.2 (0.3) for electron (muon) candidates and p_{T}^{ℓ} is the lepton's p_{T}. All lepton candidates must satisfy $I_R/p_{\mathrm{T}}^{\ell} < 0.15$. They are also required to satisfy a calorimeter-based isolation criterion: the sum of the transverse energy within a cone of size $\Delta R = 0.2$ around the lepton, after subtracting contributions from pile-up and the energy deposit of the lepton itself, is required to be less than 20% (30%) of the electron's (muon's) p_{T}^{ℓ}.

These selection criteria largely suppress the contribution from non-prompt leptons. However, several channels considered in this search have additional suppression requirements targeting the main types of non-prompt leptons. Non-prompt leptons from hadron decays that contain bottom- or charm-quarks (referred to as "HF non-prompt leptons") are further rejected using a boosted decision tree (BDT) discriminant (referred to as the non-prompt-lepton BDT [101]), based on isolation and lifetime information about a track-jet that matches the selected electron or muon (referred to as a "light lepton"). Three working points (WPs)

[4] The transverse impact parameter, d_0, is defined in the x-y plane as the distance of closest approach of the track to the beamline.

[5] The longitudinal impact parameter, z_0, is defined as the distance in z between the primary vertex and the point on the track used to evaluate d_0.

JHEP05(2025)075

based on the non-prompt-lepton BDT are used: *Tight*, *VeryTight*, and *Tight-not-VeryTight*. The *Tight* WP allows prompt muons (barrel/endcap electrons) satisfying the calorimeter- and track-based isolation criteria to be selected with an efficiency that is about 60% (60%/70%) for $p_{\mathrm{T}} \sim 20$ GeV and reaches a plateau of 95% (95%/90%) for $p_{\mathrm{T}} \sim 40$ (40/65) GeV. The prompt-lepton efficiency of the *VeryTight* WP for muons (barrel/endcap electrons) that satisfy the calorimeter- and track-based isolation criteria is approximately 55% (55%/60%) for $p_{\mathrm{T}} \sim 20$ GeV and reaches a plateau of 90% (85%/83%) for $p_{\mathrm{T}} \sim 40$ (40/65) GeV. The corresponding rejection factor[6] for muons (electrons) from the decay of b-hadrons ranges from 33 to 50 (20 to 50) for the *Tight* WP, and from 50 to 100 (33 to 66) for the *VeryTight* WP, depending on p_{T} and η, after resolving ambiguities between overlapping reconstructed objects. The *Tight-not-VeryTight* WP allows the selection of non-prompt leptons and is part of the event selection for control regions enriched in HF non-prompt-lepton background, as described in section 6.

To suppress electrons with an incorrect charge assignment, a BDT discriminant based on calorimeter and tracking quantities [99] is used. An efficiency of approximately 96% in the barrel region and 81% in the endcaps is obtained, with rejection factors of 19 in the barrel region and 40 in the endcaps. The electron candidates are separated into three classes: "material conversion", "internal conversion", and "non-conversion". Most electrons arising from material conversions, i.e. from photon conversions in the detector material, are rejected by the standard electron identification selection, but additional requirements are imposed to remove residual material-conversion candidates. These candidates have a reconstructed displaced vertex with radius $r > 20$ mm that includes the track associated with the electron.[7] The invariant mass of the associated track and the closest (in $\Delta\eta$) opposite-sign charge track reconstructed in the silicon detector, calculated at the conversion vertex, is required to be lower than 100 MeV. Internal conversion candidates, which correspond to the internal photon conversions ($\gamma^* \to \ell^+\ell^-$), must fail to satisfy the requirements for material conversions, and the di-track invariant mass, calculated here at the primary vertex, is also required to be lower than 100 MeV.

The various requirements applied to the different lepton categories used are summarised in table 2. After the initial categorisation based on "loose" leptons (corresponding to L), the best lepton working point to further optimise the event selection is chosen depending on the main background processes and available number of data events in each category. The various choices for the signal and control regions are described in section 5.

The constituents for jet reconstruction are identified by combining measurements from both the ID and the calorimeter using a particle flow (PFlow) algorithm [102]. Jet candidates are reconstructed from these PFlow objects using the anti-k_{T} algorithm [103, 104] with a radius parameter of $R = 0.4$. They are corrected to particle level by the application of jet energy scale (JES) and resolution (JER) calibrations, derived from 13 TeV data and simulation [105]. Only jet candidates with $p_{\mathrm{T}} > 25$ GeV and within $|\eta| < 2.5$ are selected. To reduce the effect of pile-up, each jet with $p_{\mathrm{T}} < 60$ GeV and $|\eta| < 2.4$ is required to have an origin compatible with the primary vertex, as defined by the jet vertex tagger (JVT) [106]

[6]The rejection factor is defined as the reciprocal of the efficiency.

[7]The beampipe and insertable B-layer inner radii are 23.5 mm and 33 mm, respectively.

JHEP05(2025)075

	Electron					Muon				
Lepton definition	L	$L*$	M	M_{ex}	T	L	$L*$	M	M_{ex}	T
Identification	Loose	Tight				Loose	Medium			
$\lvert d_0\rvert/\sigma_{d_0}$	< 5					< 3				
$\lvert z_0 \sin\theta\rvert$ [mm]	< 0.5									
Isolation	Yes					Yes				
Non-prompt lepton WP	—		*Tight*	*Tight-not-VeryTight*	*VeryTight*	—		*Tight*	*Tight-not-VeryTight*	*VeryTight*
Charge-misassignment veto	—		Yes			—				
Conversion candidate veto	—	Yes (except e^*)				—				

Table 2. Description of the loose inclusive (L), loose with tighter identification ($L*$), medium inclusive (M), medium exclusive (M_{ex}), and tight (T) lepton definitions. The electron e^* is required to fulfil, in addition to the corresponding lepton definition requirements, those corresponding to an internal or material conversion candidate.

criteria. A set of quality criteria is also applied to reject events containing at least one jet arising from non-collision sources or detector noise [107].

Jets containing b-hadrons are identified (b-tagged) via an algorithm [108] that uses a deep-learning neural network based on the distinctive features of b-hadron decays, primarily the impact parameters of tracks and the displaced vertices reconstructed in the ID. Additional input to this network is provided by discriminating variables constructed by a recurrent neutral network, which exploits the spatial and kinematic correlations between tracks originating from the same b-hadron. A multivariate b-tagging discriminant value is calculated for each jet. In this search, a jet is considered b-tagged if it passes the working point corresponding to 85%, 77%, 70%, or 60% average expected efficiency to tag a b-quark jet, with a light-jet[8] rejection factor of about 40 to 2500, and a charm-jet (c-jet) rejection factor of about 3 to 40, as determined for jets with $p_{\text{T}} > 20$ GeV and $|\eta| < 2.5$ in simulated $t\bar{t}$ events. The b-tagging distribution obtained by ordering the resulting five exclusive bins from the four working points from higher to lower b-jet efficiency is referred to as 'pseudo-continuous' b-tagging score, and it is used as input to the multivariate analysis discriminant described in section 5. The notation $b^{85\%}$, $b^{77\%}$, $b^{70\%}$, and $b^{60\%}$ is used to denote a b-tagged jet (b-jet) that satisfies the corresponding working point. Correction factors derived from dedicated calibration samples enriched in b-jets, c-tagged jets, or light-tagged jets, are applied to the simulated event samples [109–111].

To uniquely identify objects, a sequential "overlap removal" procedure is performed. Electrons and muons that satisfy the L criteria are considered in this procedure, as well as jets that satisfy the JVT requirement.

If two electrons are separated by $\Delta R < 0.1$, only the one with the higher p_{T} is kept. If an electron and a muon overlap within $\Delta R < 0.1$, the muon is removed if it is reconstructed only from an ID track and calorimeter energy deposits consistent with a minimum-ionising particle (i.e. if it is "calo-tagged"), otherwise the electron is removed. If an electron and a selected jet are found within $\Delta R < 0.2$, the jet is removed. For each electron in the event a p_{T}-dependent

[8] 'Light jet' refers to a jet originating from the hadronisation of a light quark (u, d, s) or a gluon.

JHEP05(2025)075

variable-size cone of maximum size $\Delta R = 0.4$ is defined. If a selected jet, surviving all previous overlap criteria, is found in this cone, the lepton is rejected. The same procedure is also applied between jets and muons, with the exception that, if a muon and a jet overlap with $\Delta R < 0.2$, the jet is removed, unless the number of tracks in the jet is more than two.

The missing transverse momentum $\vec{p}_{\mathrm{T}}^{\,\mathrm{miss}}$ (with magnitude $E_{\mathrm{T}}^{\mathrm{miss}}$) is defined as the negative vector sum of the p_{T} of all selected and calibrated objects in the event that fulfilled the overlap removal procedure, and an additional term to account for the momenta of soft particles that are not associated with any of the selected objects [112]. This soft term is calculated from inner-detector tracks matched to the primary vertex, which makes it more resilient to contamination from pile-up interactions.

5 Search strategy

Events are firstly required to satisfy a minimal preselection and then are categorised into orthogonal SRs based on different criteria such as number of leptons and a multi-class DNN classifier. This categorisation provides a set of regions that are sensitive to all the signal production and decay modes considered in this search. Orthogonal CRs are defined to constrain the normalisation of the main backgrounds. Dedicated kinematic selections are applied to the CRs to improve the purity of the targeted backgrounds. A maximum-likelihood fit is performed across the electron (muon) SRs to test for a possible VLL_e (VLL_μ) signal, together with the CRs to constrain in situ the leading backgrounds simultaneously.

Candidate events are selected by a combination of single-lepton and dilepton triggers, requiring the electrons or muons to satisfy identification criteria similar to those used in the offline reconstruction and isolation requirements [113, 114]. Single-electron triggers require a minimum p_{T} threshold of 24 (26) GeV in the 2015 (2016, 2017 and 2018) data-taking period(s), while single-muon triggers have a lowest p_{T} threshold of 20 (26) GeV in 2015 (2016–2018). The dielectron triggers require two electrons with minimum p_{T} thresholds ranging from 12 GeV in 2015 to 24 GeV in 2017–2018, whereas the dimuon triggers use asymmetric p_{T} thresholds for leading (subleading) muons: 18 (8) GeV in 2015 and 22 (8) GeV in 2016–2018. Finally, an electron+muon trigger requires events to have an electron candidate with a 17 GeV threshold and a muon candidate with a 14 GeV threshold for all periods.

In the offline selection at least two leptons in the event are required to be matched, within $\Delta R < 0.15$, to the corresponding leptons reconstructed by the trigger and to have a p_{T} exceeding the trigger p_{T} threshold by at least 1 GeV.

Three orthogonal event categories are defined according to the number of L leptons in the event: opposite-sign charge dilepton (2ℓOS), three-lepton (3ℓ), and four-lepton (4ℓ) categories. The four-lepton category is inclusive and contains events with higher lepton multiplicity, while the other two are exclusive. VLL signals from both doublet and singlet models can be classified into distinct topologies in the 2ℓOS and 3ℓ channels. Signals from the VLL doublet model are characterised mostly by low $E_{\mathrm{T}}^{\mathrm{miss}}$, while those from the singlet model can have larger $E_{\mathrm{T}}^{\mathrm{miss}}$ due to a neutrino from the VLL in the final state. To minimise the migration of signal events in each decay mode across categories while maximising rejection against the SM background, the analysis uses a multi-class DNN, trained separately in the 2ℓOS and 3ℓ channels to classify events into the background or one of the signal categories.

JHEP05(2025)075

Variable
Number of jets (N_{jets})
Sum of pseudo-continuous b-tagging scores of jets
Number of hadronic W/Z bosons
Number of hadronic H bosons
Missing transverse energy ($E_{\text{T}}^{\text{miss}}$)

Table 3. Input variables to the DNN trainings in the 2ℓOS and 3ℓ channels.

The training of the DNN is done using the Keras library [115] with Tensorflow as a backend [116] and Adam optimiser [117]. The networks consist of five input features, two dense fully connected layers of 22 (30) nodes with rectified linear units as activation functions, interleaved with a drop-out layer with 20% rate, and six (four) output nodes with a soft-max activation function for the categorisation of 2ℓOS (3ℓ) events. The network is trained with a batch size of 2000 and up to 100 epochs, using all the available signal mass points. To avoid discarding signal events in the evaluation, a two-fold cross-validation is used with the events divided by even/odd event number.

The five input features are the number of jets, the sum of the pseudo-continuous b-tagging scores of all jets, the number of hadronic W/Z bosons, the number of hadronic H bosons, and the event $E_{\text{T}}^{\text{miss}}$, as shown in table 3. The hadronic H boson candidates are reconstructed by requiring one (for boosted scenarios) or two $b^{85\%}$ jets to have an invariant mass within 90–140 GeV, compatible with the Higgs boson mass. The hadronic W/Z boson candidates are similarly identified by requiring one or two jets to have an invariant mass within 60–110 GeV, compatible with the W or Z boson mass. The order in which the matching of jet(s) as originating from H or W/Z bosons is tested is the following: 1 jet matched to H boson candidate, 2 jets matched to H boson candidate, 1 jet matched to W/Z boson candidate, 2 jets matched to W/Z boson candidate. These variables are independent of lepton flavour and independent of the mass of the VLL, ensuring the same training can be used for both VLL_e and VLL_μ for all mass points. Good modelling of the input variables is observed in the $t\bar{t}$ and Z + jets correction regions as defined in section 6.

The output categories correspond to the signal topologies, with an additional category in each channel corresponding to the 'SM-like' events, defined to capture events that fall into none of the other signal categories. Each event is categorised according to the highest class probability.

In the 2ℓOS channel, three low-$E_{\text{T}}^{\text{miss}}$ and two high-$E_{\text{T}}^{\text{miss}}$ signal topologies are defined, sensitive to both VLL models:

- $\ell\ell$HH: low-$E_{\text{T}}^{\text{miss}}$ topology targeting two hadronic Higgs boson candidates. Characterised by a high number of b-tagged jets.
- $\ell\ell$HV: low-$E_{\text{T}}^{\text{miss}}$ topology targeting a hadronic Higgs boson candidate and a hadronic W/Z boson candidate. Characterised by a high number of light- and heavy-flavour jets.
- $\ell\ell$VV: low-$E_{\text{T}}^{\text{miss}}$ topology targeting two hadronic W/Z boson candidates. Characterised by a high number of light-flavour jets.

JHEP05(2025)075

- $\ell\nu$HW: high-$E_{\mathrm{T}}^{\mathrm{miss}}$ topology targeting a hadronic Higgs boson candidate and a leptonic W boson candidate. Characterised by heavy-flavour jets.

- $\ell\nu$WZ: high-$E_{\mathrm{T}}^{\mathrm{miss}}$ topology targeting a hadronic Z boson candidate and a leptonic W boson candidate. Characterised by light-flavour jets.

Similarly in the 3ℓ channel, two low-$E_{\mathrm{T}}^{\mathrm{miss}}$ and one high-$E_{\mathrm{T}}^{\mathrm{miss}}$ signal topologies are defined:

- $\ell\ell$HH + HW: low-$E_{\mathrm{T}}^{\mathrm{miss}}$ topology targeting a hadronic Higgs boson candidate and a leptonic W boson candidate (prompt or from the other Higgs boson decay). Characterised by a high number of b-tagged jets.

- $\ell\ell$HV + VV: low-$E_{\mathrm{T}}^{\mathrm{miss}}$ topology targeting a Higgs boson $H \to WW$ candidate, with one of the W bosons decaying into a lepton and a neutrino, and a hadronic W/Z boson candidate. Characterised by a high number of light-flavour jets.

- $\ell\nu$HV: high-$E_{\mathrm{T}}^{\mathrm{miss}}$ topology targeting a Higgs boson $H \to WW$ candidate, with both W bosons decaying into a lepton and a neutrino, and a hadronic W/Z boson candidate. Characterised by a low number of jets.

The advantage of this classification is that the analysis is sensitive to not only the VLL doublet and singlet models, but also to any similar non-VLL topology that fulfils one of the above descriptions. In the training all background processes are included, normalised to their respective cross-sections and including the corrections described in section 6, as well as the VLL_e or VLL_μ signal samples in the doublet and singlet scenarios for all masses, sub-divided using truth information into the aforementioned signal templates.

The 'SM-like' categories in 2ℓOS and 3ℓ are expected to be low in signal yield but capture a significant contribution of the SM background. These categories are not included in the final fit to the data, rejecting a large fraction of the SM background contamination.

The 4ℓ channel is subdivided into four signal categories based on the presence of one or two opposite-sign charge same-flavour (OSSF) lepton pairs, and the multiplicity of electrons or muons. Table 4 shows a summary of the signal region categories.

Multiple CRs are defined to fit the normalisation of the leading backgrounds. These regions are orthogonal to the signal regions and among each other based on different requirements on the lepton working points, dilepton invariant mass, and jet and b-jet multiplicities. First, a region enriched in $t\bar{t}W$ is defined by selecting two same-sign leptons with the tight definition and at least two $b^{60\%}$ jets. A region enriched in $W^{\pm}Z$ and $t\bar{t}Z$ is defined by selecting events with three leptons (a same-sign pair of M leptons and an opposite-sign charge $L*$ lepton), from which one OSSF lepton pair is required to be compatible with a Z boson, $|m_{\ell^+\ell^-}^{\mathrm{OSSF}} - m_Z| < 10$ GeV. A dedicated region dominated by ZZ is defined by requiring four $L*$ leptons where both OSSF pairs fulfil $|m_{\ell^+\ell^-}^{\mathrm{OSSF}} - m_Z| < 10$ GeV. Two CRs enriched in photon conversions from $Z \to \mu\mu\gamma^*(\to ee)$ are defined, according to the identification of the electron as a material conversion or internal conversion candidate. Finally, four CRs enriched in HF non-prompt leptons are defined, requiring exactly one $b^{60\%}$ jet to be orthogonal to the $t\bar{t}W$ CR. Events with two same-sign leptons are categorised according to the criteria (T, M_{ex}) and $(T, L*)$ for the leading and subleading leptons in p_{T}, and further split according

JHEP05(2025)075

Signal regions	2ℓOS	3ℓ	4ℓ
Lepton flavour	e: (ee)	e: $(2e1\mu + 3e)$	e: $(2e2\mu + 3e1\mu + 4e)$
	μ: $(\mu\mu)$	μ: $(2\mu1e + 3\mu)$	μ: $(2\mu2e + 3\mu1e + 4\mu)$
Lepton definition	$(L*, L*)$	$(L*, M, M)$	$(L*, L*, L*, L*)$
Minimum lepton p_{T} [GeV]	(20, 20)	(10, 20, 20)	(10, 10, 10, 10)
$m^{\mathrm{OSSF}}_{\ell^+\ell^-}$ [GeV]	> 15	—	
$\lvert m^{\mathrm{OSSF}}_{\ell^+\ell^-} - m_Z\rvert$ [GeV]	> 10	> 10	> 10 for at least 1 OSSF pair
N_{jets}	≥ 2	≥ 1	≥ 0 (1OSSF)
			≥ 1 (2OSSF)
Other	$\Delta R(\ell, \ell) > 1$	Total lepton charge $= \pm 1$	Total lepton charge $= 0$
Region split	($\ell\ell$HH, $\ell\ell$HV, $\ell\ell$VV, $\ell\nu$HV, $\ell\nu$VV) $\times$ (e, μ)	($\ell\ell$HH + HV, $\ell\ell$HV + VV, $\ell\nu$HV) $\times$ (e, μ)	(1OSSF, 2OSSF) $\times$ (e, μ)
Region naming	2$\ell(e)\ell\ell$HH, 2$\ell(\mu)\ell\ell$HH	3$\ell(e)\ell\ell$HH + HW, 3$\ell(\mu)\ell\ell$HH + HW	4$\ell(e)$1OSSF, 4$\ell(\mu)$1OSSF
	2$\ell(e)\ell\ell$HV, 2$\ell(\mu)\ell\ell$HV	3$\ell(e)\ell\ell$HV + VV, 3$\ell(\mu)\ell\ell$HV + VV	4$\ell(e)$2OSSF, 4$\ell(\mu)$2OSSF
	2$\ell(e)\ell\ell$VV, 2$\ell(\mu)\ell\ell$VV	3$\ell(e)\ell\nu$HV, 3$\ell(\mu)\ell\nu$HV	
	2$\ell(e)\ell\nu$HW, 2$\ell(\mu)\ell\nu$HW		
	2$\ell(e)\ell\nu$WZ, 2$\ell(\mu)\ell\nu$WZ		

Table 4. Event selection summary in the signal regions. Leptons are ordered by decreasing p_{T} in the 2ℓOS and 4ℓ regions. In the 3ℓ regions the lepton with opposite-sign charge is taken first, followed by the two same-sign leptons in decreasing p_{T} order. In $2e2\mu$ ($2\mu2e$) events the sum of the p_{T} of the two electrons (muons) is larger than the sum of the p_{T} of the two muons (electrons). The splitting of regions are based on DNN classifications in the 2ℓOS and 3ℓ regions, where 'H' ('V') stands for the Higgs boson (W and Z bosons).

to the fake-lepton-candidate flavour, which is assumed to be the subleading lepton. These two CRs allow to derive constraints on the background from HF non-prompt leptons for the 3ℓ channel and for the 2ℓOS and 4ℓ channels, respectively.

The full description of the kinematic selections applied to each CR is given in table 5. As described in section 6, background corrections are derived in orthogonal regions and applied to the corresponding simulated processes before the simultaneous fit to data.

Figure 2 illustrates the categorisation and definition of the SRs and CRs that are fitted simultaneously. A total of 19 analysis regions are defined for each VLL search (electron or muon), with 10 SRs (5 for 2ℓOS, 3 for 3ℓ, and 2 for 4ℓ) and 9 CRs. In each region, a given kinematic variable is fitted to improve the sensitivity to the targeted signal process (in the case of the SRs) or to improve the modelling of a particular background process (in the case of the CRs). The sum of the p_{T} of the leptons plus the event $E_{\mathrm{T}}^{\mathrm{miss}}$ ($H_{\mathrm{T}}^{\mathrm{lep}} + E_{\mathrm{T}}^{\mathrm{miss}}$) is fitted in the signal regions and is connected to the VLL mass; the b-jet multiplicity ($N_{b-\mathrm{jets}}$) is fitted in the diboson and $t\bar{t}Z$ CR and provides discrimination between these two background processes; the total event yield is fitted in the other CRs.

6 Background estimation

Section 6.1 describes the irreducible backgrounds, where prompt leptons are produced from W/Z boson decays, leptonic τ-lepton decays, or internal conversions. Section 6.2 introduces the reducible backgrounds, containing prompt leptons with misassigned charge or at least one non-prompt lepton in the event.

JHEP05(2025)075

Control regions	$t\bar{t}W$	$W^{\pm}Z$ and $t\bar{t}Z$	ZZ	Conversions	HF non-prompt
N_{jets}	≥ 2	≥ 0			≥ 2
$N_{b-\text{jets}}$	≥ 2 $b^{60\%}$	—		0 $b^{60\%}$	1 $b^{60\%}$
Lepton requirement	2ℓSS	3ℓ	2e2μ, 4e, 4μ	$\mu\mu e^{*}$	2ℓSS
Lepton definition	(T, T)	$(L*, M, M)$	$(L*, L*, L*, L*)$	$(L*, M, M)$	(T, M_{ex}), $(T, L*)$
Minimum lepton p_{T} [GeV]	(20, 20)	(10, 20, 20)	(10, 10, 10, 10)	(10, 20, 20)	(20, 20)
$m^{\text{OSSF}}_{\ell^+\ell^-}$ [GeV]	> 15	—			
$\lvert m^{\text{OSSF}}_{\ell^+\ell^-} - m_Z\rvert$ [GeV]	—	< 10		> 10	—
$\lvert m_{\ell\ell\ell} - m_Z\rvert$ [GeV]	—			< 10	—
Region split	—			internal / material	subleading $e/\mu \times ((T, M_{\text{ex}}), (T, L*))$
Region naming	2ℓttW	3ℓVV+ttZ	4ℓZZ	3ℓIntC	2ℓtt(e)$_{(T,M_{\text{ex}})}$, 2ℓtt(e)$_{(T,L*)}$
				3ℓMatC	2ℓtt(μ)$_{(T,M_{\text{ex}})}$, 2ℓtt(μ)$_{(T,L*)}$

Table 5. Event selection summary in the CRs. The notation e^{*} is used to denote material conversion or internal conversion candidates, as described in section 4. Leptons are ordered by decreasing p_{T} in the 2ℓSS and 4ℓ regions. In the 3ℓ regions the lepton with opposite-sign charge is taken first, followed by the two same-sign leptons in decreasing p_{T} order. In the HF non-prompt lepton region naming, '2ℓtt(e)' ('2ℓtt(μ)') is the CR enriched in non-prompt electrons (muons) from semileptonic b-decays originating mostly from $t\bar{t}$ and with the lepton flavours for the leading and subleading leptons corresponding to '$ee, \mu e$' ('$\mu\mu, e\mu$'). The additional (T, M_{ex}) and $(T, L*)$ subscripts refer to the lepton definitions required for the leading and subleading leptons in each region.

Correction regions	$t\bar{t}$	Z + jets	$W^{\pm}Z$
Lepton flavour	2ℓOS $e\mu$	2ℓOS ee, $\mu\mu$	3ℓ
Lepton definition	$(L*, L*)$	$(L*, L*)$	$(L*, T, T)$
Minimum lepton p_{T} [GeV]	(20, 20)		(10, 20, 20)
$m_{\ell^+\ell^-}$ [GeV]	> 15 (OS)	> 15 (OSSF)	—
$\lvert m_{\ell^+\ell^-} - m_Z\rvert$ [GeV]	> 10 (OS)	< 10 (OSSF)	
N_{jets}	≥ 2		≥ 1
$N_{b-\text{jets}}$	—		0 $b^{77\%}$

Table 6. Event selection summary in the regions used for deriving data-driven corrections and for cross-checks of the $t\bar{t}$, Z + jets and $W^{\pm}Z$ background processes. Leptons are ordered by decreasing p_{T} in the 2ℓOS regions. In the 3ℓ region the lepton with opposite-sign charge is taken first, followed by the two same-sign leptons in decreasing p_{T} order.

All background processes are estimated by using the simulation samples described in section 3. Before the simultaneous fit to data, the event kinematics of the simulated $t\bar{t}$, Z + jets and VV backgrounds require dedicated corrections derived from data control samples (described in table 6) to better describe the data. During the simultaneous fit to data discussed in section 8, the yields of $t\bar{t}W$, $t\bar{t}Z$, $W^{\pm}Z$, ZZ and non-prompt-lepton backgrounds, are adjusted via normalisation factors.

JHEP05(2025)075

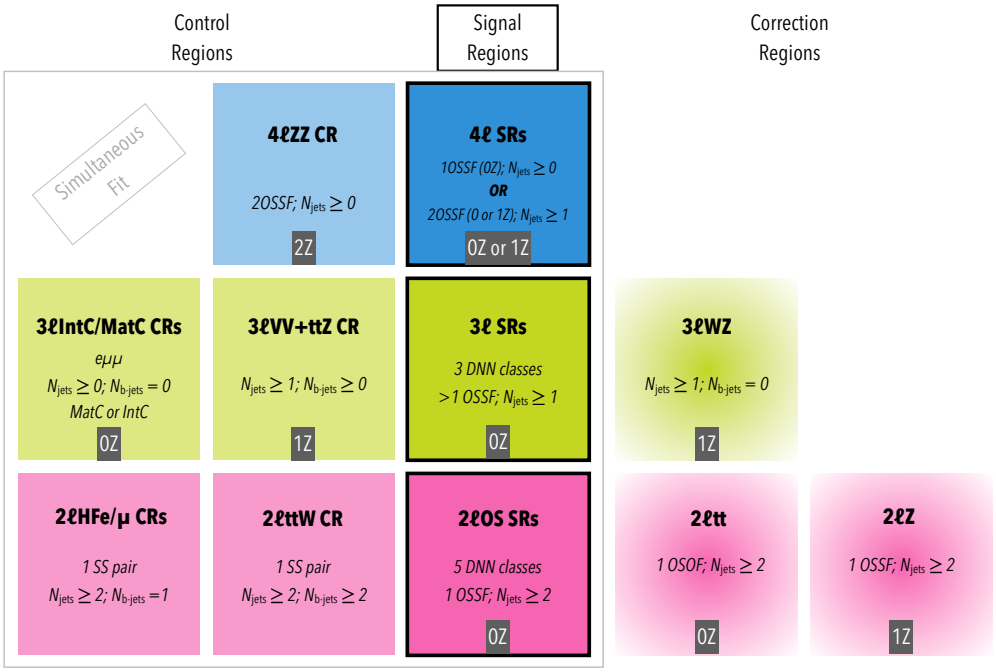

Figure 2. Illustrative sketch of the definition of the SRs and CRs. The $2\ell\text{HF}_{e/\mu}$ CRs include the $2\ell\text{tt(e)}_{(T,M_{ex})}$, $2\ell\text{tt(e)}_{(T,L*)}$, $2\ell\text{tt}(\mu)_{(T,M_{ex})}$, and $2\ell\text{tt}(\mu)_{(T,L*)}$ regions. The 2ℓOS, 3ℓ and 4ℓ SRs include the various regions shown in table 4. The control regions correspond to those described in table 5 and the correction regions are presented in table 6. The terms 'OSSF' and 'OSOF' refer to opposite-sign charge lepton pairs with same and opposite lepton flavours, respectively, whereas 'SS' refers to a same-sign charge lepton pair.

6.1 Irreducible backgrounds

Background contributions with prompt leptons originate from a wide range of physics processes with the relative importance of individual processes varying by channel. The main irreducible backgrounds originate from $t\bar{t}$, Z + jets, $t\bar{t}W$, $t\bar{t}(Z/\gamma^*)$, $W^{\pm}Z$ and ZZ production, and have final states and kinematic properties similar to the VLL signal. Smaller contributions originate from the following rare processes: $t\bar{t}H$, $t\bar{t}t\bar{t}$, tZ, tW, tWZ, $t\bar{t}WW$, VVV, and $t\bar{t}t$ production.

6.1.1 $t\bar{t}$ background

The $t\bar{t}$ process is one of the main prompt backgrounds in the 2ℓOS signal regions. Three distinct corrections are applied: first a theory-based correction to correct the distributions of the p_{T} and of the invariant mass of the $t\bar{t}$ system ($m(t\bar{t})$) at parton level, then data-driven corrections to improve the modelling of the number of extra HF jets and the jet multiplicity in different corners of the $E_{\text{T}}^{\text{miss}}$ phase space.

Previous studies [118] have shown that the latest theoretical predictions at NNLO QCD and NLO EW for the top quark p_{T} are significantly softer than the spectrum from the nominal Powheg+Pythia8 and alternate Monte Carlo samples considered in this analysis,

JHEP05(2025)075

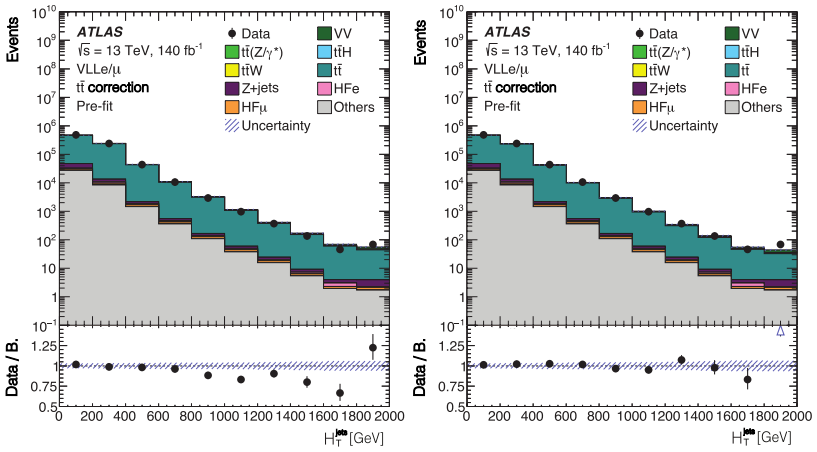

Figure 3. Distributions of $H_{\mathrm{T}}^{\mathrm{jets}}$ before the fit to data in the $t\bar{t}$ correction region (a) before any corrections are applied and (b) after the theory-based $t\bar{t}$ corrections are implemented. The ratio of the data to the background prediction ('B.') is shown in the lower panel. The 'Others' contribution is dominated by the tW production. Only statistical uncertainties are shown. The last bin in each distribution contains the overflow.

and significantly different in $d\sigma(t\bar{t})/dm(t\bar{t})$. An iterative, recursive reweighting procedure is used to correct the parton level distributions of $p_{\mathrm{T}}(t)$, $p_{\mathrm{T}}(\bar{t})$, $m(t\bar{t})$ and $p_{\mathrm{T}}(t\bar{t})$ in each of the $t\bar{t}$ MC samples. Figure 3 shows the sum of the p_{T} of the jets ($H_{\mathrm{T}}^{\mathrm{jets}}$) distributions before and after the corrections are applied.

Even though significant improvement in the agreement of MC to data is observed after the reweighting in many kinematic variables related to the top/anti-top p_{T}, the agreement in jet multiplicity and multiplicity of b-tagged jets remains suboptimal. Additional data-driven corrections are derived for these distributions in the $t\bar{t}$ $e\mu$ correction region (see table 6) in an iterative procedure. First, corrections to the fractions of $t\bar{t}$ + light flavour jets ($t\bar{t}$ + LF), $t\bar{t}$ + b-tagged jets ($t\bar{t}+b$) and $t\bar{t}$ + c-tagged jets ($t\bar{t}+c$) are estimated with dedicated normalisation factors, by fitting the sum of pseudo-continuous b-tagging scores to data. The resulting values are 0.98 ± 0.01 for $t\bar{t}$ + LF, 1.30 ± 0.04 for $t\bar{t}$ + b and 1.40 ± 0.05 for $t\bar{t}$ + c. Second, a bin-to-bin rescaling to data is performed for the jet multiplicity in four $E_{\mathrm{T}}^{\mathrm{miss}}$ bins: 0–100 GeV, 100–200 GeV, 200–300 GeV, and >300 GeV. The derived correction is less than 1% for 2 or 3 jets and up to 10% for 6 jets in the regions with $E_{\mathrm{T}}^{\mathrm{miss}} < 300$ GeV. For higher jet multiplicities and higher $E_{\mathrm{T}}^{\mathrm{miss}}$, the correction can be up to 48%. After correcting for the number of jets, a fit to the sum of pseudo-continuous b-tagging scores is repeated to check that the best-fit values of $t\bar{t}$ + LF, $t\bar{t}$ + b and $t\bar{t}$ + c are not affected.

The distributions of the fitting variable, $H_{\mathrm{T}}^{\mathrm{lep}} + E_{\mathrm{T}}^{\mathrm{miss}}$, in the different 2$\ell$OS DNN classes (see table 4) in the $t\bar{t}$ correction region (see table 6) are shown in figure 4.

Four normalisation factors affecting the $t\bar{t}$ contributions in the corresponding 2ℓOS categories are free-floated in the simultaneous fit to data using the CRs and the VLL$_e$ (VLL$_\mu$) SRs and measured to be for the background-only hypothesis: $\hat{\lambda}_{t\bar{t}_{\ell\ell\mathrm{HH}}} = 0.98 \pm 0.07$ (0.92 ± 0.06), $\hat{\lambda}_{t\bar{t}_{\ell\ell\mathrm{HV}}} = 0.97 \pm 0.08$ (0.91 ± 0.06), $\hat{\lambda}_{t\bar{t}_{\ell\nu\mathrm{VV},\ell\ell\mathrm{VV}}} = 1.01 \pm 0.07$ (1.06 ± 0.07)

JHEP05(2025)075

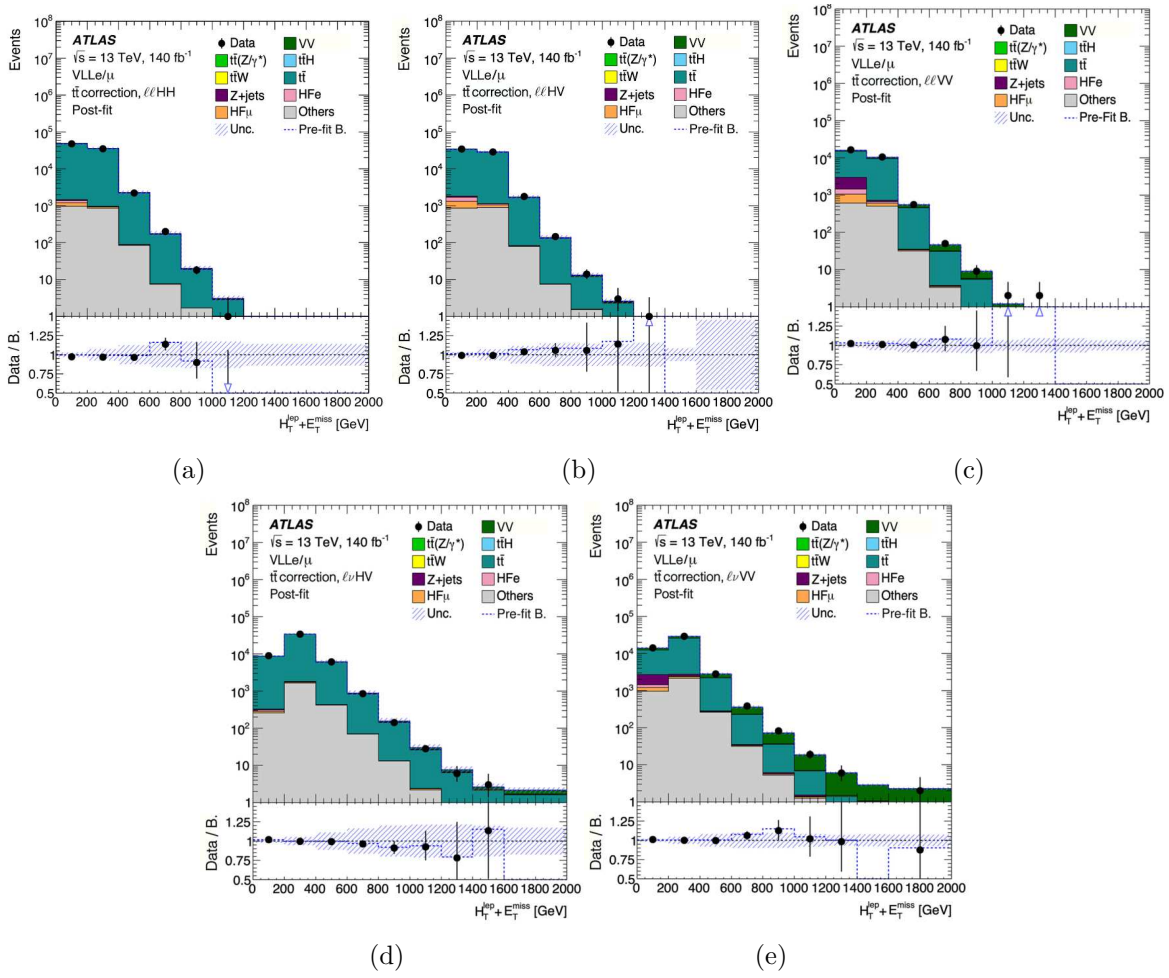

Figure 4. Distributions of the fitting variable, $H_{\mathrm{T}}^{\mathrm{lep}} + E_{\mathrm{T}}^{\mathrm{miss}}$, before the fit to data in the different DNN classes within the $t\bar{t}$ 2ℓOS correction region ((a) $\ell\ell HH$, (b) $\ell\ell HV$, (c) $\ell\ell VV$, (d) $\ell\nu HV$, (e) $\ell\nu VV$) after all $t\bar{t}$ corrections are applied. The background contributions after the likelihood fit to data ('post-fit') for the background-only hypothesis are shown as filled histograms. The ratio of the data to the background prediction ('B.') is shown in the lower panel, separately for post-fit background (black points) and pre-fit background (dashed blue line). The 'Others' contribution is dominated by the tW production. The blue hashed band shows both statistical and systematic uncertainties.

and $\hat{\lambda}_{t\bar{t}_{\ell\nu\mathrm{HV}}} = 0.98 \pm 0.04$ (1.00 ± 0.04), where the uncertainty includes both statistical and systematic contributions. The $t\bar{t}$ events satisfying the 3ℓ and 4ℓ selections contain at least one non-prompt lepton. The normalisation of these events is treated separately and discussed in section 6.2.1.

6.1.2 Z + jets background

Two types of data-driven corrections are derived for Z + jets in the corresponding correction region from table 6: first, the jet multiplicity is corrected to data, followed by a correction to the angular separation between the leptons coming from the Z boson ($\Delta R_{\ell\ell}$).

The number of jets distribution exhibits good MC agreement with data at low jet multiplicities but requires a correction of up to 25% at high jet multiplicities. A data-driven correction is then derived per bin in the jet multiplicity distribution.

JHEP05(2025)075

Next, the $\Delta R_{\ell\ell}$ distribution is examined in different bins of jet multiplicity. The $\Delta R_{\ell\ell} < 1$ region shows poorly modelled MC background for all jet multiplicities, most likely originating from a suboptimal modelling of the boosted Z/γ^*+jets process, and therefore events in this region are vetoed from the 2ℓOS SRs. For the remaining bins, a bin-by-bin correction is derived as a function of jet multiplicity, with corrections as large as 13%(25%) at low (high) $\Delta R_{\ell\ell}$.

Two normalisation factors are assigned to the Z + jets contributions in the 2ℓOS categories with the largest contamination from this background process ($2\ell(e)\ell\ell$VV, $2\ell(\mu)\ell\ell$VV, $2\ell(e)\ell\nu$WZ, $2\ell(\mu)\ell\nu$WZ) and measured to be for the background-only hypothesis using the CRs and the VLL$_e$ (VLL$_\mu$) SRs: $\hat{\lambda}_{Z+\text{jets}_{\ell\ell\text{VV}}} = 0.90 \pm 0.14$ (0.81 ± 0.11) and $\hat{\lambda}_{Z+\text{jets}_{\ell\nu\text{VV}}} = 0.77 \pm 0.19$ (0.70 ± 0.14), where the uncertainty includes both statistical and systematic contributions.

6.1.3 $t\bar{t}W$ background

Despite the use of state-of-the-art simulations, accurate modelling of additional QCD and QED radiation in $t\bar{t}W$ production remains challenging. Disagreement between the data and the pre-fit prediction from the simulation is observed in the $t\bar{t}W$ CR. Therefore, an overall normalisation factor is assigned to the $t\bar{t}W$ background, and is determined during the likelihood fit. The measured normalisation factor for the background-only hypothesis using the CRs and the VLL$_e$ (VLL$_\mu$) SRs is $\hat{\lambda}_{t\bar{t}W} = 1.33 \pm 0.22$ (1.31 ± 0.22), where the uncertainty includes both statistical and systematic contributions. This measured normalisation factor is compatible with the one determined by the $t\bar{t}W$ production cross-section measurement [119].

6.1.4 VV and $t\bar{t}(Z/\gamma^*)$ backgrounds

A data-driven correction to the VV jet multiplicity spectrum is derived from the $W^\pm Z$ correction region described in table 6. This region is enriched in $W^\pm Z$ + LF jets; however the jet multiplicity mismodelling is assumed to be independent from the flavour of the additional jets in the event.

The 3ℓVV+ttZ and 4ℓZZ CRs are used in the likelihood fit to improve the prediction of the background contribution from the $W^\pm Z$ + LF jets, $W^\pm Z$ + HF jets, ZZ, and $t\bar{t}(Z/\gamma^*)$ processes. The number of b-jets provides good discrimination in the 3ℓVV+ttZ CR between the $W^\pm Z$ and $t\bar{t}(Z/\gamma^*)$ processes and is the variable used in this region in the fit. The event yields are fitted in the 4ℓZZ CR. The measured normalisation factors for the background-only hypothesis using the CRs and the VLL$_e$ (VLL$_\mu$) SRs are: $\hat{\lambda}_{W^\pm Z\,+\,\text{LF}} = 0.99 \pm 0.06$ (0.97 ± 0.06), $\hat{\lambda}_{W^\pm Z\,+\,\text{HF}} = 0.96 \pm 0.29$ (0.83 ± 0.26), $\hat{\lambda}_{ZZ} = 1.03 \pm 0.03$ (1.03 ± 0.03), and $\hat{\lambda}_{t\bar{t}Z} = 1.25 \pm 0.17$ (1.20 ± 0.16), where the uncertainty includes both statistical and systematic contributions.

Figure 5 shows the b-jet multiplicity distribution in the 3ℓVV+ttZ CR after the likelihood fit to data.

6.1.5 Other irreducible backgrounds

The rate of the background from internal conversions with $m(e^+e^-) < 1$ GeV is estimated by using the two dedicated CRs, 3ℓIntC and 3ℓMatC, with a purity of 86% and 14%, respectively. The total yield in each category is used in the likelihood fit to determine the normalisation factor, which is measured for the background-only hypothesis using the CRs and the VLL$_e$

JHEP05(2025)075

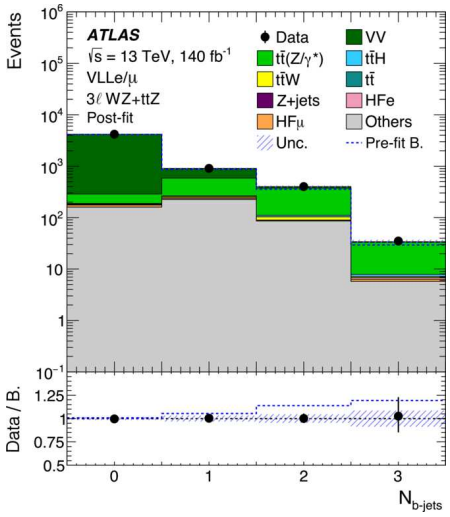

Figure 5. Comparison between data and the background prediction for the distribution of the b-jet multiplicity in the 3ℓVV+ttZ CR after the VV jet multiplicity correction. The background contributions after the likelihood fit to data ('post-fit') for the background-only hypothesis are shown as filled histograms. The ratio of the data to the background prediction ('B.') is shown in the lower panel, separately for post-fit background (black points) and pre-fit background (dashed blue line). The 'Others' contribution is dominated by the tZ production. The size of the combined statistical and systematic uncertainty in the background prediction is indicated by the blue hatched band. The last bin contains the overflow.

(VLL$_\mu$) SRs to be $\hat{\lambda}_e^{\text{IntC}} = 1.04 \pm 0.13$ (1.04 ± 0.14), where the main contribution to the uncertainty comes from the statistics. The contribution from muons from internal conversions for $m(\mu^+\mu^-) < 1$ GeV is negligible in this analysis.

6.2 Reducible backgrounds

6.2.1 Non-prompt leptons

Non-prompt leptons originate from material conversions, LF and HF hadron decays, or the improper reconstruction of other particles, and their relative composition depends on the lepton quality requirements and event categories. These backgrounds are generally small in all SRs and CRs and thus are estimated from simulation, with the normalisation determined by the likelihood fit. The main contribution to the non-prompt-lepton background is from $t\bar{t}$ production, with much smaller contributions from V+jets and single-top-quark processes. The non-prompt leptons in the simulated samples are labelled according to whether they originate from HF or LF hadron decays, or from a material conversion candidate. The HF category includes leptons from both bottom and charm decays.

Several of the event categories introduced in section 5 are designed to be enriched in specific processes and are used to derive normalisation factors to improve their modelling by the simulation. The 3ℓMatC CR is enriched in material conversions with a purity of 85% and only the total event yield is used.

Given the different lepton quality requirements used in the 2ℓOS and 4ℓ SRs compared with the 3ℓ SR, as well as in the CRs, four 2ℓ CRs enriched in contributions from HF

JHEP05(2025)075

non-prompt leptons in $t\bar{t}$ events are defined requiring a leading T lepton, with two of them using the M_{ex} lepton definition for the subleading lepton and the other two using the looser lepton definition $L*$. Normalisation factors for five non-prompt-lepton background contributions are estimated from the likelihood fit. The normalisation factor for HF non-prompt leptons is estimated separately for electrons and muons, and for joint (M, M_{ex}, T) lepton definitions (denoted by 'tight') and for $L*$ (denoted by 'loose'), i.e. $\lambda^{\text{had}}_{e,\text{tight}}$, $\lambda^{\text{had}}_{e,\text{loose}}$, $\lambda^{\text{had}}_{\mu,\text{tight}}$, and $\lambda^{\text{had}}_{\mu,\text{loose}}$. An additional normalisation factor is determined for the material conversions background, $\lambda^{\text{MatC}}_{e}$. The measured normalisation factors for the background-only hypothesis using the CRs and the VLL$_e$ (VLL$_\mu$) SRs are: $\hat{\lambda}^{\text{had}}_{e,\text{tight}} = 0.88 \pm 0.27$ (0.88 ± 0.28), $\hat{\lambda}^{\text{had}}_{e,\text{loose}} = 0.90 \pm 0.03$ (0.90 ± 0.04), $\hat{\lambda}^{\text{had}}_{\mu,\text{tight}} = 0.99 \pm 0.11$ (1.00 ± 0.11), $\hat{\lambda}^{\text{had}}_{\mu,\text{loose}} = 1.00 \pm 0.03$ (0.99 ± 0.03), $\hat{\lambda}^{\text{MatC}}_{e} = 1.16 \pm 0.08$ (1.16 ± 0.08), where the uncertainties include systematic effects but are dominated by the statistical uncertainty.

Backgrounds with leptons with the charge incorrectly assigned affect primarily the same-sign 2ℓ $t\bar{t}W$ and HF non-prompt lepton control regions and predominantly arise from $t\bar{t}$ production, where one electron undergoes a hard bremsstrahlung and an asymmetric conversion ($e^{\pm} \to e^{\pm}\gamma^* \to e^{\pm}e^+e^-$) or a mismeasured track curvature. This background process has negligible contributions in this analysis and is estimated from MC simulation. The muon charge misassignment rate is also negligible in the p_{T} range relevant to this analysis.

7 Systematic uncertainties

Several sources of systematic uncertainty may affect the signal and background yields in each signal and control region and are described in the following subsections. Given the low background yields and good signal-to-background separation provided by the final discriminating variable used in the signal-enriched event categories, the search sensitivity is limited by the number of data events rather than by the systematic uncertainties in the background estimate.

7.1 Experimental uncertainties

Experimental systematic uncertainties related to the trigger efficiency, lepton reconstruction, identification and isolation, jet calibration, b-tagging calibration, and $E^{\text{miss}}_{\text{T}}$ measurement are considered in the search.

The uncertainty in the measurement of the combined 2015–2018 integrated luminosity is 0.83% [120], obtained using the LUCID-2 detector [51] for the primary measurements, complemented by the ones using the inner detector and calorimeters.

Uncertainties associated with the lepton selection arise from the trigger, reconstruction, identification and isolation efficiencies, and the lepton momentum scale and resolution [99, 100, 121, 122]. Uncertainties in the calibration of the non-prompt lepton BDT are estimated through a $Z \to \ell\ell$ tag-and-probe method and cover uncertainties related to the $Z(\to \ell\ell)$+jets MC modelling, the template cut/shape, the $m_{\ell\ell}$ window, the tag-and-probe lepton selections, the multijet background, the non-prompt lepton background, the luminosity, the cross-sections of the considered processes, and the limited number of events in simulation and data.

Uncertainties associated with the jet selection arise from the JES, the JVT requirement and the JER [105, 106]. The JES and its uncertainties are derived by combining information

JHEP05(2025)075

from test-beam data, collision data and simulation [105]. The JES (JER) have 30 (13) components included in the fit. The uncertainties in the JES, JER and JVT increase at lower jet p_{T}.

The efficiency of the flavour-tagging algorithm is measured for each jet flavour using control samples in data and in simulation. From these measurements, correction factors are derived to correct the tagging rates in the simulation [109–111]. Experimental uncertainties in these correction factors are taken as uncorrelated between b-jets, c-jets, and light-flavour jets. An additional uncertainty is assigned to account for the extrapolation of the b-tagging efficiency measurement from the p_{T} region used to determine the correction factors to regions with higher transverse momentum.

The treatment of the uncertainties associated with reconstructed objects is common to all analysis channels and applies to all signal and background samples and thus these are considered as fully correlated among different analysis regions and samples.

7.2 Theoretical uncertainties

The modelling uncertainties in the main irreducible backgrounds are assessed through comparisons with alternative MC samples, as listed in table 1. Additional uncertainties are evaluated from renormalisation and factorisation scale variations by a factor of 0.5 and 2, relative to the nominal scales, for the $t\bar{t}$, Z + jets, $t\bar{t}W$, $t\bar{t}Z$, and diboson samples. An additional 20% uncertainty is assigned to the $t\bar{t}W$ electroweak contribution [123].

For the $t\bar{t}$ process, four additional uncertainties are considered related to the reweighting method itself, derived by comparing the nominal reweighted SM $t\bar{t}$ sample to a sample obtained through the alternative reweighting obtained by varying the renormalisation and the factorisation scales separately by a factor of 0.5 and 2, applied on the (anti-)top quark p_{T} or on the $m(t\bar{t})$ distribution independently. Related to the reweighting of the $t\bar{t}$ + LF, $t\bar{t}$ + b and $t\bar{t}$ + c contributions, uncertainties of 3% and 4% are assigned to events originating from $t\bar{t} + \geq 1b$ and $t\bar{t} + \geq 1c$, respectively. The statistical uncertainty related to reweighting the jet multiplicity distribution is expected to be very small due to the large statistics of $t\bar{t}$ in the VR and is not considered. All alternative $t\bar{t}$ MC samples are reweighted to the same higher-order predictions as the nominal Powheg v2 +Pythia 8.230 MC sample. In addition to the comparison to the alternative MC sample shown in table 1, the nominal predictions are also compared with those obtained from an alternative sample generated as the nominal sample but setting the $p_{\mathrm{T}}^{\mathrm{hard}}$ parameter in Pythia to 1 instead of 0 [124]. This parameter regulates the definition of the vetoed region of the showering to avoid holes or overlaps in the phase space filled by Powheg and Pythia. An uncertainty related to the choice of the h_{damp} parameter is estimated by comparing the predictions of the nominal sample to those obtained with an alternative sample with the h_{damp} parameter increased by a factor of 1.5 compared with its nominal value. Variations in the initial state radiation (ISR) are estimated by varying the factorisation and renormalisation scales independently up and down by a factor of two. Similarly, the uncertainty related to final-state radiation (FSR) is assessed by varying the renormalisation scale for final-state parton-shower emissions up and down by a factor of two. Finally, the uncertainty associated with the A14 tune is

JHEP05(2025)075

derived by varying the A14 tune (Var3c), which affects the renormalisation scale variations in the ISR PS. No theory reweighting is applied to this systematic.

For the Z + jets process, the uncertainty related to the upper cut-off of perturbative calculations for PS evolution is known as the re-summation scale (QSF). This uncertainty is evaluated at truth level by varying the nominal value of 2 GeV by a factor of 4 up and 1/4 down. Fiducial cuts are applied at truth level to define a phase space close to that used at reconstruction level in the signal regions where Z + jets is a dominant background. Additionally, the uncertainty related to the choice of the CKKW merging scale, i.e. the scale for calculating the overlap between jets from the ME and the PS, is derived similarly; the nominal value of 20 GeV is varied down to 15 GeV and up to 30 GeV and differences relative to the nominal distribution are evaluated at truth level.

The statistical uncertainty in the fitted parameters for the VV jet-multiplicity correction is propagated as an uncertainty in the diboson background. Finally, additional normalisation uncertainties are included for all processes whose normalisation is not obtained from the fit. In particular, for the $t\bar{t}t\bar{t}$, $t\bar{t}H$, and tZ processes, cross-section uncertainties of 20% [94], 11% [125], and 5% [126] are assigned, respectively, while for $t\bar{t}t$, tWZ, $t\bar{t}WW$, and triboson backgrounds a 50% cross-section uncertainty is assigned as a conservative estimate, since they are small backgrounds and have low impact on the search.

Uncertainties in the modelling of the signal samples are evaluated through independent variations of the factorisation and renormalisation scales by a factor of two. Additional uncertainties due to PDF effects are estimated through an ensemble of eigenvariations of the NNPDF set, and by taking the differences relative to alternative PDF sets [127].

7.3 Reducible background uncertainties

The normalisation of HF non-prompt leptons for processes where the non-prompt lepton is M or T is obtained from regions including one sub-leading M_{ex} lepton. An uncertainty of 20% in the extrapolation from M_{ex} to M and T leptons is applied from the comparison of the relative efficiency between nominal and alternative $t\bar{t}$ MC samples. Validation regions with looser lepton requirements and further enriched in non-prompt leptons are defined. A good agreement between data and background prediction is observed in all kinematic variables except for the number of b-jets. Based on this disagreement, an $N_{b-\text{jets}}$-dependent uncertainty is added to the HF non-prompt background, ranging from 6%–40% for 1–3 additional b-jets in the non-prompt muon regions, and 10%–80% in the non-prompt electron regions.

The modelling of internal and material conversions is tested in dedicated validation regions with two tight same-sign leptons, requiring one of them to be a conversion candidate. Additional uncertainties of 10% and 50% are assigned to the material and internal conversion backgrounds, respectively, evaluated from the data to background agreement in the validation regions.

A systematic uncertainty of 20% is assigned to the background from electrons with a misidentified charge and accounts for the disagreement observed between the MC simulation for this background and data in the same-sign charge ee inclusive region.

JHEP05(2025)075

8 Results

A maximum-likelihood fit is performed on all bins in the 19 signal and control regions considered in this search to simultaneously determine the signal and background yields that are most consistent with the data. The $H_{\mathrm{T}}^{\mathrm{lep}} + E_{\mathrm{T}}^{\mathrm{miss}}$ is used as the discriminating variable in the signal regions, while the $N_{b-\mathrm{jets}}$ and the total event yield are fitted in control regions. Two separate fits are performed for the VLL$_e$ and VLL$_\mu$ signal hypotheses, and for each of the two fits the 10 SRs for electrons or the 10 SRs for muons introduced in table 4 are simultaneously fitted with the 9 CRs to data.

The likelihood function $\mathcal{L}(\mu, \vec{\lambda}, \vec{\theta})$ is constructed as a product of Poisson probability terms over all bins considered in the search, and depends on: the signal-strength parameter, μ, a multiplicative factor applied to the predicted yield for the VLL signal; $\vec{\lambda}$, the normalisation factors for several backgrounds; $\vec{\theta}$, a set of nuisance parameters (NPs), encoding systematic uncertainties in the signal and background expectations [128]. Systematic uncertainties can impact the estimated signal and background rates, the migration of events between categories, and the shape of the fitted distributions. Both μ and $\vec{\lambda}$ are treated as free parameters in the likelihood fit. The NPs $\vec{\theta}$ allow variations of the expectations for signal and background according to the systematic uncertainties, subject to Gaussian or Poisson constraints in the likelihood fit. Their fitted values represent the deviations from the nominal expectations that globally provide the best fit to the data. Statistical uncertainties in each bin due to the limited size of the simulated samples are taken into account by dedicated parameters using the Beeston-Barlow 'lite' technique [129].

The test statistic q_μ is defined as the profile likelihood ratio: $q_\mu = -2\ln(\mathcal{L}(\mu, \hat{\hat{\vec{\lambda}}}_\mu, \hat{\hat{\vec{\theta}}}_\mu)/\mathcal{L}(\hat{\mu}, \hat{\hat{\vec{\lambda}}}_{\hat{\mu}}, \hat{\hat{\vec{\theta}}}_{\hat{\mu}}))$, where $\hat{\mu}$, $\hat{\hat{\vec{\lambda}}}_{\hat{\mu}}$, and $\hat{\hat{\vec{\theta}}}_{\hat{\mu}}$ are the values of the parameters that maximise the likelihood function, and $\hat{\hat{\vec{\lambda}}}_\mu$ and $\hat{\hat{\vec{\theta}}}_\mu$ are the values of the parameters that maximise the likelihood function for a given value of μ. The test statistic q_μ is evaluated with the RooFit package [130]. A related statistic is used to determine the probability that the observed data are incompatible with the background-only hypothesis (i.e. the discovery test) by setting $\mu = 0$ in the profile likelihood ratio (q_0). The p-value (referred to as p_0) representing the probability of the data being compatible with the background-only hypothesis is estimated by integrating the distribution of q_0 from background-only pseudo-experiments, approximated using the asymptotic formulae given in ref. [131], above the observed value of q_0. Some model dependence exists in the estimation of the p_0, as a given signal scenario must be assumed in the calculation of the denominator of q_0, even if the overall signal normalisation is allowed to float and is fitted to data. The observed p_0 is checked for each explored signal scenario. Upper limits on the signal production cross-section for each of the signal scenarios considered are derived by using q_μ in the CL$_\mathrm{s}$ method [132, 133]. For a given signal scenario, values of the production cross-section (parameterised by μ) yielding CL$_\mathrm{s} < 0.05$, where CL$_\mathrm{s}$ is computed using the asymptotic approximation [131], are excluded at $\geq 95\%$ CL.

A comparison of the predicted numbers of background events, obtained from the combined likelihood fit in the background-only hypothesis, and the observed data is shown in figures 6(a) and 6(b) for the 10 VLL$_e$ and 10 VLL$_\mu$ SRs, respectively, and in figure 6(c) for the 9 CRs. The corresponding post-fit yields for the VLL$_e$ and VLL$_\mu$ SRs are reported in tables 7 and 8.

JHEP05(2025)075

Comparisons between data and the background prediction for the $H_{\mathrm{T}}^{\mathrm{lep}} + E_{\mathrm{T}}^{\mathrm{miss}}$ distributions used in the different SRs are shown in figures 7 and 8 for the VLL$_e$ and VLL$_\mu$ searches, respectively. The binning used for the $H_{\mathrm{T}}^{\mathrm{lep}} + E_{\mathrm{T}}^{\mathrm{miss}}$ distributions in the different SRs represents a compromise between preserving enough discrimination in the fit between the background and the signal and keeping the MC statistical uncertainty in the background prediction per bin below 30%. As shown in section 6, the fitted normalisation factors for each background are compatible between the VLL$_e$ and VLL$_\mu$ searches.

No significant deviations from the SM expectations are observed in any of the SRs considered. The smallest p-value for each of the signal benchmarks considered is 0.34 (0.40) for VLL$_e^{\mathrm{S}}$ 800 GeV (VLL$_e^{\mathrm{D}}$ 1.3 TeV) and 0.14 (0.18) for VLL$_\mu^{\mathrm{S}}$ 150 GeV (VLL$_\mu^{\mathrm{D}}$ 150 GeV), which corresponds to a local significance of 0.42σ (0.25σ) and 1.07σ (0.91σ), respectively. Limits at 95% CL on the cross-section of a VLL$_e$ or a VLL$_\mu$ signal as a function of the mass of the VLL are set. Figures 9(a), 9(b), 9(c) and 9(d) show the limits on the cross-section for the models: VLL$_e^{\mathrm{S}}$, VLL$_e^{\mathrm{D}}$, VLL$_\mu^{\mathrm{S}}$, and VLL$_\mu^{\mathrm{D}}$. The VLL$_e^{\mathrm{S}}$ is observed (expected) to be excluded at 95% CL for masses up to 320 (300) GeV while the VLL$_e^{\mathrm{D}}$ is observed (expected) to be excluded at 95% CL for masses up to 1220 (1230) GeV. The VLL$_\mu^{\mathrm{S}}$ is observed (expected) to be excluded at 95% CL for masses up to 400 (330) GeV while the VLL$_\mu^{\mathrm{D}}$ is observed (expected) to be excluded at 95% CL for masses up to 1270 (1250) GeV. The search is dominated by statistical uncertainties: the expected limits obtained when including only statistical uncertainties represent approximately 90% of the total limits throughout the probed mass range. Within the systematic uncertainties, the leading ones for the search of a VLL$_e^{\mathrm{D}}$ or VLL$_\mu^{\mathrm{D}}$ with a 600 GeV mass are the Z + jets QSF and signal PDF and scale variation uncertainties. The 2ℓOS channel is the most sensitive signal region at high VLL masses, whereas the 3ℓ (4ℓ) channel sets stronger expected exclusion limits at lower VLL masses in the VLL doublet (singlet) scenario.

JHEP05(2025)075

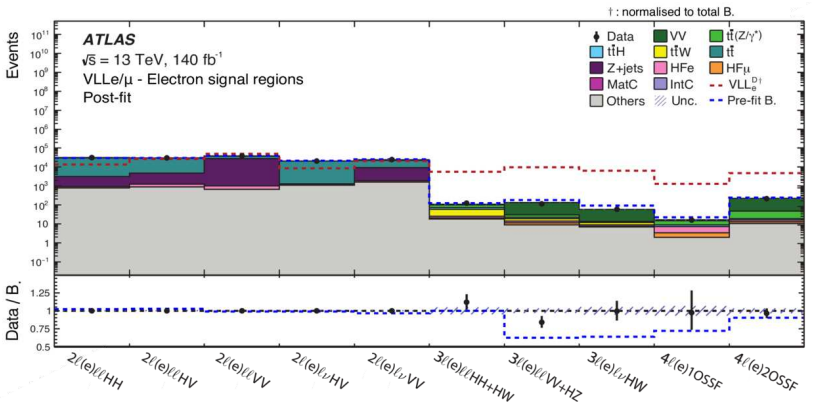

(a)

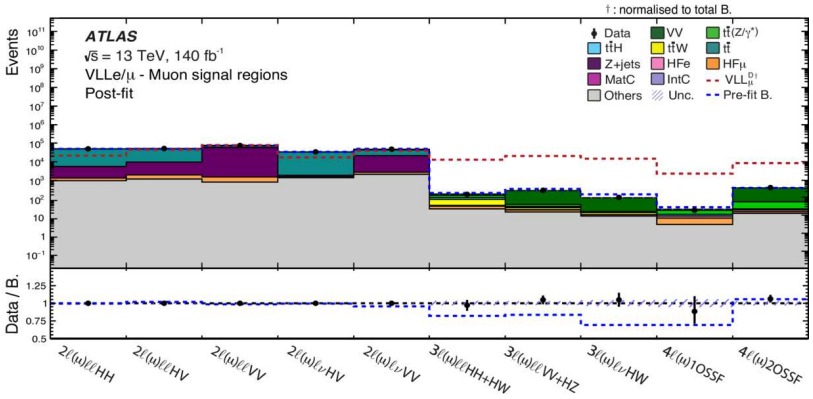

(b)

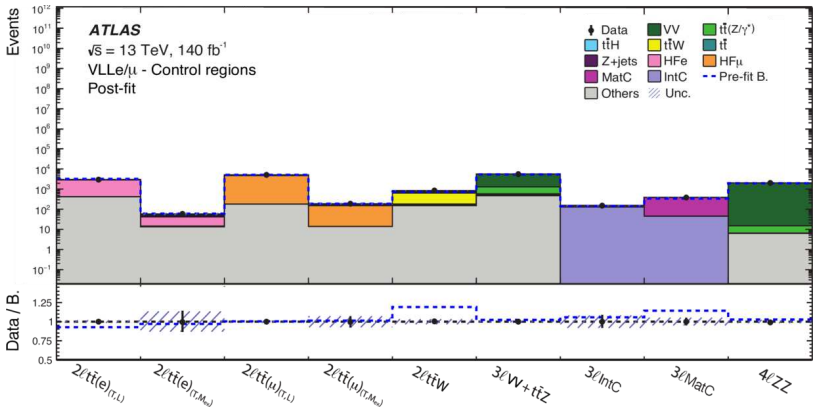

(c)

Figure 6. Comparison between data and the background prediction for the event yields in the (a) 10 VLL_e SRs, (b) 10 VLL_μ SRs, and (c) 9 CRs, after a background-only fit to data ('post-fit') in the (a) VLL_e SRs and CRs and (b, c) VLL_μ SRs and CRs. The background contributions in the CRs after the likelihood fit to data in the VLL_e SRs and CRs are comparable to those in (c). Distributions for the $\mathrm{VLL}_e^{\mathrm{D}}$ and $\mathrm{VLL}_\mu^{\mathrm{D}}$ signal points for a VLL mass of 600 GeV are overlaid for comparison in (a) and (b), respectively. The lower panels show the ratio of data to the background estimate ('B.'), separately for post-fit background (black points) and pre-fit background (dashed blue line). The size of the combined statistical and systematic uncertainty in the background prediction is indicated by the blue hatched band.

JHEP05(2025)075

Channel	$2\ell(e)\ell\ell$HH	$2\ell(e)\ell\ell$HV	$2\ell(e)\ell\ell$VV	$2\ell(e)\ell\nu$HW	$2\ell(e)\ell\nu$WZ
VV	53.5 ± 8.4	98 ± 18	1124 ± 72	148 ± 11	2336 ± 54
$t\bar{t}(Z/\gamma^*)$	165 ± 93	182 ± 92	54 ± 26	59 ± 42	30 ± 21
$t\bar{t}H$	106 ± 15	56.5 ± 8.4	12.4 ± 2.1	14.9 ± 1.9	5.49 ± 0.85
$t\bar{t}W$	119 ± 16	140 ± 17	39.6 ± 6.3	57.5 ± 5.9	29.8 ± 4.3
$t\bar{t}$	27630 ± 680	25530 ± 720	8970 ± 510	19460 ± 340	13360 ± 380
Z+jets	2160 ± 640	3410 ± 720	27070 ± 560	101 ± 34	7260 ± 360
HFe	156.6 ± 6.0	377 ± 14	356 ± 14	77.7 ± 3.0	269 ± 10
HFμ	—	—	—	—	—
Others	770 ± 170	890 ± 170	654 ± 69	1110 ± 320	1620 ± 180
Total	31160 ± 180	30670 ± 190	38280 ± 210	21020 ± 150	24900 ± 160
Data	31162	30677	38279	21022	24890
$\mathrm{VLL}_e^{\mathrm{S}}$ 200 GeV	63.8 ± 2.9	88.8 ± 5.0	137.2 ± 7.7	34.9 ± 1.7	119.5 ± 2.8
$\mathrm{VLL}_e^{\mathrm{D}}$ 600 GeV	67.2 ± 3.2	132.1 ± 6.9	244 ± 12	42.4 ± 1.9	100.7 ± 4.3

Channel	$3\ell(e)\ell\ell$HH + HW	$3\ell(e)\ell\ell$HV + VV	$3\ell(e)\ell\nu$HV	$4\ell(e)$1OSSF	$4\ell(e)$2OSSF
VV	10.7 ± 1.1	106.8 ± 3.3	45.2 ± 2.5	2.10 ± 0.19	174.8 ± 6.9
$t\bar{t}(Z/\gamma^*)$	26.8 ± 3.2	7.4 ± 1.5	1.28 ± 0.19	5.47 ± 0.60	27.7 ± 2.8
$t\bar{t}H$	13.8 ± 1.9	2.70 ± 0.49	0.58 ± 0.10	1.75 ± 0.24	2.95 ± 0.42
$t\bar{t}W$	32.9 ± 3.1	4.99 ± 0.71	3.10 ± 0.37	—	—
$t\bar{t}$	—	—	—	—	—
Z+jets	—	—	—	—	—
HFe	5.4 ± 1.7	2.87 ± 0.90	1.18 ± 0.37	3.89 ± 0.29	3.11 ± 0.13
HFμ	2.33 ± 0.27	2.25 ± 0.26	0.73 ± 0.10	1.33 ± 0.10	2.64 ± 0.10
Others	17.6 ± 4.9	8.9 ± 1.9	6.7 ± 1.4	1.94 ± 0.35	10.3 ± 2.3
Total	109.2 ± 5.3	135.4 ± 4.2	58.5 ± 3.1	16.4 ± 1.1	221.2 ± 7.3
Data	122	114	58	16	213
$\mathrm{VLL}_e^{\mathrm{S}}$ 200 GeV	3.35 ± 0.27	10.51 ± 0.57	3.66 ± 0.21	1.94 ± 0.16	35.0 ± 1.0
$\mathrm{VLL}_e^{\mathrm{D}}$ 600 GeV	27.8 ± 1.4	47.7 ± 2.4	31.7 ± 1.6	6.35 ± 0.34	23.7 ± 1.2

Table 7. Summary of observed and predicted yields in the ten VLL_e signal region categories. The background prediction is shown after the combined likelihood fit to data under the background-only hypothesis across all control region and signal region categories. The expected signal yields for $\mathrm{VLL}_e^{\mathrm{S}}$ and $\mathrm{VLL}_e^{\mathrm{D}}$ for a VLL mass of 200 GeV and 600 GeV, respectively, that are obtained by using their theoretical cross-sections are also shown with their pre-fit uncertainties, assuming μ=1. The uncertainties correspond to the combined statistical and systematic uncertainties in the predicted yields. The 'Others' contribution is dominated by tW, VVV, and tWZ in the 2ℓ, 3ℓ, and 4ℓ SRs, respectively. Dashes refer to components that are negligible or not applicable.

JHEP05(2025)075

Channel	$2\ell(\mu)\ell\ell$HH	$2\ell(\mu)\ell\ell$HV	$2\ell(\mu)\ell\ell$VV	$2\ell(\mu)\ell\nu$HW	$2\ell(\mu)\ell\nu$WZ
VV	69 ± 10	124 ± 22	1580 ± 110	230 ± 17	3940 ± 120
$t\bar{t}(Z/\gamma^*)$	250 ± 160	250 ± 140	75 ± 43	77 ± 60	39 ± 29
$t\bar{t}H$	159 ± 21	86 ± 12	18.5 ± 3.1	19.9 ± 2.5	7.4 ± 1.1
$t\bar{t}W$	178 ± 25	215 ± 28	58 ± 11	77.0 ± 8.1	40.2 ± 6.4
$t\bar{t}$	43840 ± 920	41000 ± 1000	15740 ± 740	32350 ± 540	22530 ± 510
Z+jets	4340 ± 910	8000 ± 1000	57000 ± 800	282 ± 88	18910 ± 480
HFe	—	—	—	—	—
HFμ	377 ± 11	765 ± 23	725 ± 21	181.4 ± 5.4	637 ± 19
Others	970 ± 230	1180 ± 250	800 ± 110	1390 ± 460	2160 ± 260
Total	50175 ± 240	50970 ± 260	75990 ± 330	34610 ± 190	48260 ± 230
Data	50178	50968	75976	34605	48276
VLL_μ^S 200 GeV	95.6 ± 4.7	135.1 ± 6.9	199 ± 12	51.1 ± 1.9	178.3 ± 4.7
VLL_μ^D 600 GeV	83.9 ± 3.8	167.9 ± 8.1	305 ± 14	66.5 ± 2.9	150.8 ± 6.2

Channel	$3\ell(\mu)\ell\ell$HH + HW	$3\ell(\mu)\ell\ell$HV + VV	$3\ell(\mu)\ell\nu$HV	$4\ell(\mu)$1OSSF	$4\ell(\mu)$2OSSF
VV	23.0 ± 1.9	235.0 ± 6.8	97.9 ± 4.2	3.75 ± 0.27	326 ± 11
$t\bar{t}(Z/\gamma^*)$	45.2 ± 4.6	12.5 ± 2.2	1.88 ± 0.27	9.5 ± 1.0	40.7 ± 4.0
$t\bar{t}H$	21.4 ± 2.8	4.18 ± 0.89	0.77 ± 0.11	2.90 ± 0.44	3.73 ± 0.49
$t\bar{t}W$	50.5 ± 4.7	7.4 ± 1.3	4.22 ± 0.69	—	—
$t\bar{t}$	—	—	—	—	—
Z+jets	—	—	—	—	—
HFe	2.76 ± 0.88	0.94 ± 0.30	0.39 ± 0.13	2.87 ± 0.20	4.39 ± 0.17
HFμ	12.6 ± 1.4	6.61 ± 0.75	1.97 ± 0.23	5.24 ± 0.27	3.98 ± 0.12
Others	29.2 ± 3.3	19.9 ± 3.2	12.3 ± 2.3	4.35 ± 0.51	17.4 ± 3.8
Total	183.0 ± 6.0	283.9 ± 7.2	117.5 ± 5.0	28 ± 1.6	395 ± 11
Data	177	297	123	25	420
VLL_μ^S 200 GeV	6.34 ± 0.44	18.72 ± 0.78	5.85 ± 0.28	2.96 ± 0.17	55.8 ± 1.2
VLL_μ^D 600 GeV	51.2 ± 2.3	81.4 ± 3.4	58.0 ± 2.6	8.88 ± 0.40	32.9 ± 1.4

Table 8. Summary of observed and predicted yields in the ten VLL_μ signal region categories. The background prediction is shown after the combined likelihood fit to data under the background-only hypothesis across all control region and signal region categories. The expected signal yields for VLL_μ^S and VLL_μ^D for a VLL mass of 200 GeV and 600 GeV, respectively, that are obtained by using their theoretical cross-sections are also shown with their pre-fit uncertainties, assuming μ=1. The uncertainties correspond to the combined statistical and systematic uncertainties in the predicted yields. The 'Others' contribution is dominated by tW, VVV, and tWZ in the 2ℓ, 3ℓ, and 4ℓ SRs, respectively. Dashes refer to components that are negligible or not applicable.

JHEP05(2025)075

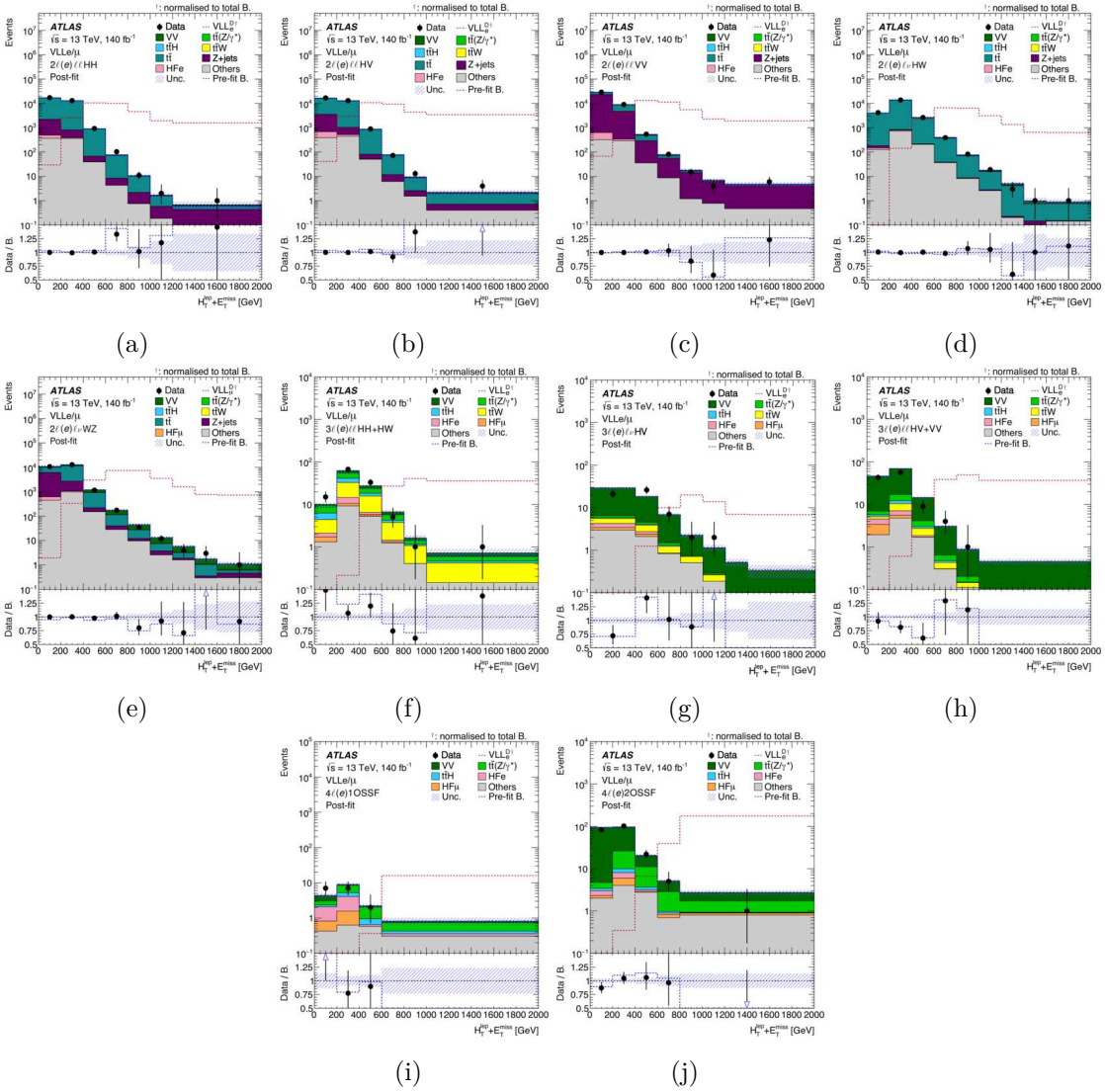

Figure 7. Comparison between data and the background estimate for the $H_{\mathrm{T}}^{\mathrm{lep}} + E_{\mathrm{T}}^{\mathrm{miss}}$ distribution used in different VLL$_e$ signal region categories: (a) $2\ell(e)\ell\ell$HH, (b) $2\ell(e)\ell\ell$HV, (c) $2\ell(e)\ell\ell$VV, (d) $2\ell(e)\ell\nu$HW, (e) $2\ell(e)\ell\nu$WZ, (f) $3\ell(e)\ell\ell$HH + HW, (g) $3\ell(e)\ell\nu$HV, (h) $3\ell(e)\ell\ell$HV + VV, (i) $4\ell(e)$1OSSF, (j) $4\ell(e)$2OSSF. Distributions for one VLL$_e^{\mathrm{D}}$ signal point for a VLL mass of 600 GeV normalised to the total background yields are overlaid for comparison. The lower panels show the ratio of data to the background estimate ('B.'), separately for post-fit background (black points) and pre-fit background (dashed blue line). The size of the combined statistical and systematic uncertainty in the signal-plus-background prediction is indicated by the blue hatched band.

JHEP05(2025)075

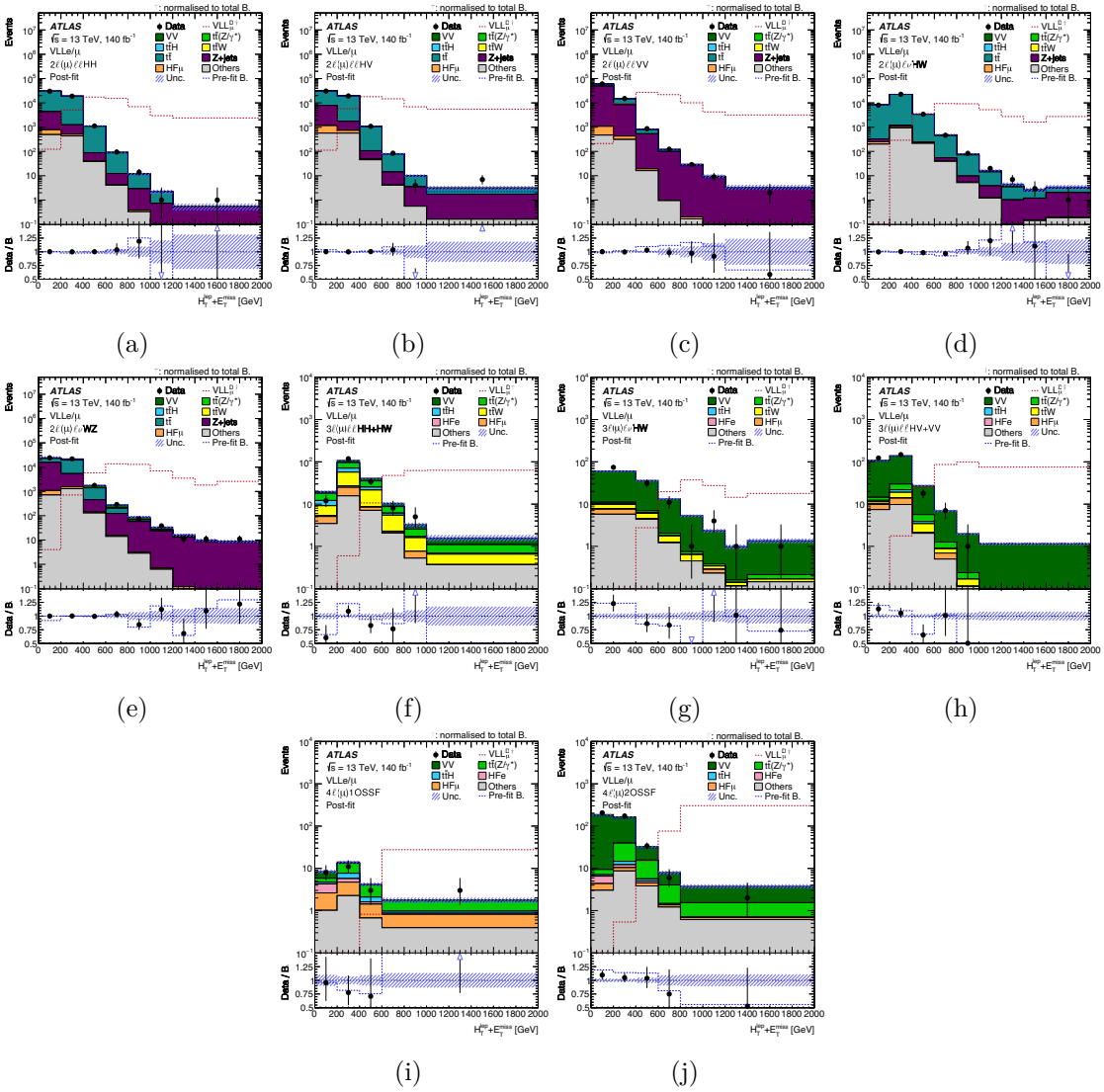

Figure 8. Comparison between data and the background estimate for the $H_{\mathrm{T}}^{\mathrm{lep}} + E_{\mathrm{T}}^{\mathrm{miss}}$ distribution used in different VLL_{μ} signal region categories: (a) $2\ell(\mu)\ell\ell\mathrm{HH}$, (b) $2\ell(\mu)\ell\ell\mathrm{HV}$, (c) $2\ell(\mu)\ell\ell\mathrm{VV}$, (d) $2\ell(\mu)\ell\nu\mathrm{HW}$, (e) $2\ell(\mu)\ell\nu\mathrm{WZ}$, (f) $3\ell(\mu)\ell\ell\mathrm{HH} + \mathrm{HW}$, (g) $3\ell(\mu)\ell\nu\mathrm{HV}$, (h) $3\ell(\mu)\ell\ell\mathrm{HV} + \mathrm{VV}$, (i) $4\ell(\mu)1\mathrm{OSSF}$, (j) $4\ell(\mu)2\mathrm{OSSF}$. Distributions for one $\mathrm{VLL}_{\mu}^{\mathrm{D}}$ signal point for a VLL mass of 600 GeV normalised to the total background yields are overlaid for comparison. The lower panels show the ratio of data to the background estimate ('B.'), separately for post-fit background (black points) and pre-fit background (dashed blue line). The size of the combined statistical and systematic uncertainty in the signal-plus-background prediction is indicated by the blue hatched band.

JHEP05(2025)075

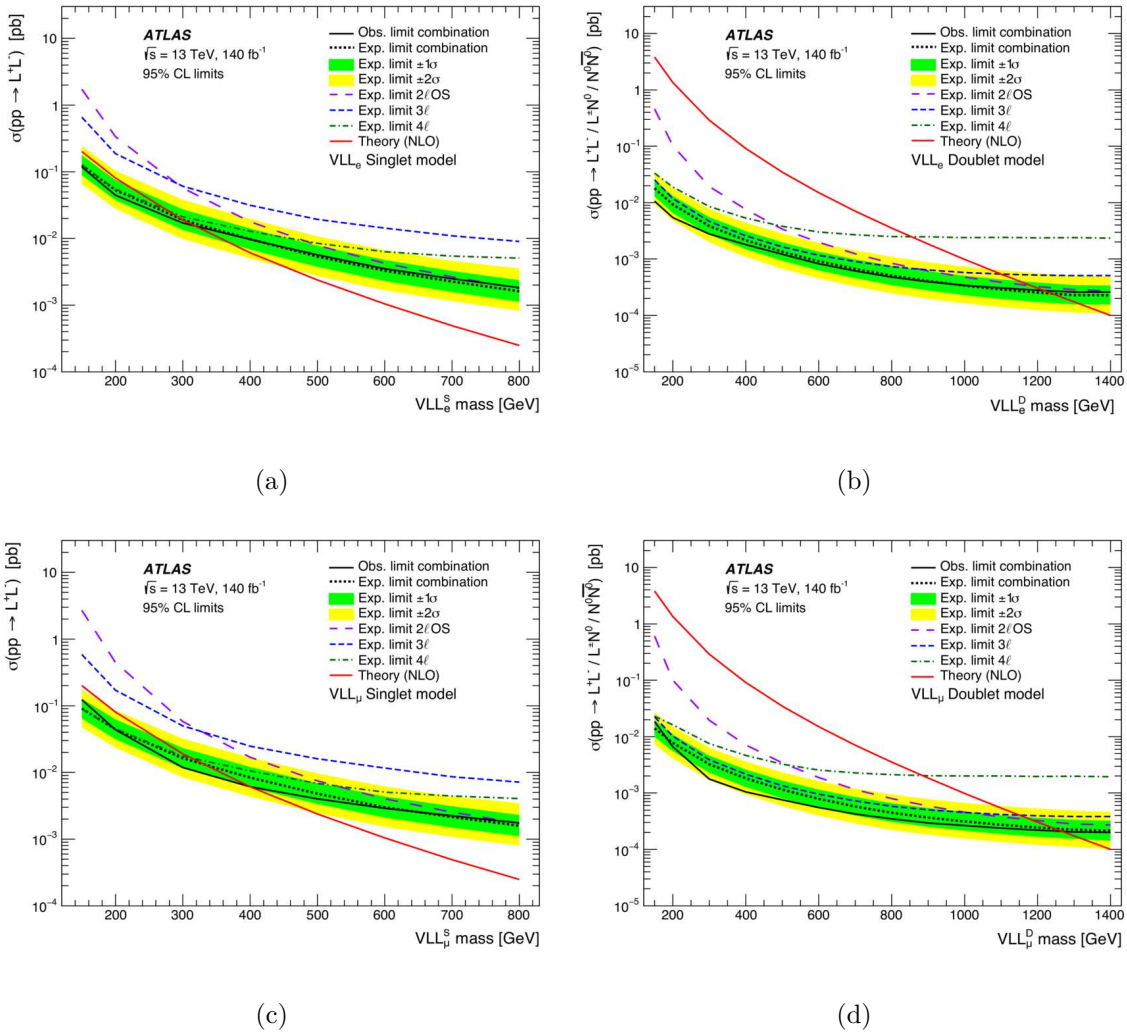

Figure 9. Combined observed and expected limits at 95% CL for the (a) $\mathrm{VLL}_e^{\mathrm{S}}$, (b) $\mathrm{VLL}_e^{\mathrm{D}}$, (c) $\mathrm{VLL}_\mu^{\mathrm{S}}$, and (d) $\mathrm{VLL}_\mu^{\mathrm{D}}$ models, as a function of the mass of the VLL. The inner and outer bands around the expected limit are the $\pm 1\sigma$ and $\pm 2\sigma$ variations including all uncertainties, respectively. The theoretical prediction for the signal production cross-section is also shown as a red solid line. Expected limits on the signal cross-section from the individual channels are shown in dashed lines for 2ℓOS (long-dashed), 3ℓ (short-dashed), and 4ℓ (dot-dashed).

JHEP05(2025)075

9 Conclusions

A search for a doublet or singlet vector-like lepton coupling to the Standard Model first- and second-generation leptons is presented. The search is based on a data sample of proton-proton collisions recorded at $\sqrt{s} = 13$ TeV by the ATLAS detector during Run 2 of the LHC, corresponding to an integrated luminosity of $140\,\text{fb}^{-1}$. The search is performed in the multilepton (two, three, and four light leptons) final state. A deep-neural-network-based categorisation is performed to enhance the purity of the various signal types and to discriminate signal against the SM background. The dominant backgrounds originate from $t\bar{t}$, $Z+\text{jets}$, $t\bar{t}W$, $t\bar{t}Z$, and VV, and are estimated from Monte-Carlo simulation and normalised to data in a simultaneous fit of the signal and control regions. The data are found to be consistent with the Standard Model predictions and exclusion limits are set on the mass of the vector-like electrons and muons, excluding masses below 1220 GeV (1270 GeV) and 320 GeV (400 GeV) for vector-like electrons (muons) in the doublet and singlet scenarios at 95% confidence level, respectively. These are the most stringent limits on vector-like electrons and muons to date, improving the previous mass exclusion limits set with the Run 1 data for the singlet scenario by 140 GeV (230 GeV) for vector-like electrons (muons) and setting limits on the doublet scenario for the first time.

Acknowledgments

We thank CERN for the very successful operation of the LHC and its injectors, as well as the support staff at CERN and at our institutions worldwide without whom ATLAS could not be operated efficiently.

The crucial computing support from all WLCG partners is acknowledged gratefully, in particular from CERN, the ATLAS Tier-1 facilities at TRIUMF/SFU (Canada), NDGF (Denmark, Norway, Sweden), CC-IN2P3 (France), KIT/GridKA (Germany), INFN-CNAF (Italy), NL-T1 (Netherlands), PIC (Spain), RAL (U.K.) and BNL (U.S.A.), the Tier-2 facilities worldwide and large non-WLCG resource providers. Major contributors of computing resources are listed in ref. [134].

We gratefully acknowledge the support of ANPCyT, Argentina; YerPhI, Armenia; ARC, Australia; BMWFW and FWF, Austria; ANAS, Azerbaijan; CNPq and FAPESP, Brazil; NSERC, NRC and CFI, Canada; CERN; ANID, Chile; CAS, MOST and NSFC, China; Minciencias, Colombia; MEYS CR, Czech Republic; DNRF and DNSRC, Denmark; IN2P3-CNRS and CEA-DRF/IRFU, France; SRNSFG, Georgia; BMBF, HGF and MPG, Germany; GSRI, Greece; RGC and Hong Kong SAR, China; ICHEP and Academy of Sciences and Humanities, Israel; INFN, Italy; MEXT and JSPS, Japan; CNRST, Morocco; NWO, Netherlands; RCN, Norway; MNiSW, Poland; FCT, Portugal; MNE/IFA, Romania; MSTDI, Serbia; MSSR, Slovakia; ARIS and MVZI, Slovenia; DSI/NRF, South Africa; MICIU/AEI, Spain; SRC and Wallenberg Foundation, Sweden; SERI, SNSF and Cantons of Bern and Geneva, Switzerland; NSTC, Taipei; TENMAK, Türkiye; STFC/UKRI, United Kingdom; DOE and NSF, United States of America.

Individual groups and members have received support from BCKDF, CANARIE, CRC and DRAC, Canada; CERN-CZ, FORTE and PRIMUS, Czech Republic; COST, ERC, ERDF,

JHEP05(2025)075

Horizon 2020, ICSC-NextGenerationEU and Marie Skłodowska-Curie Actions, European Union; Investissements d'Avenir Labex, Investissements d'Avenir Idex and ANR, France; DFG and AvH Foundation, Germany; Herakleitos, Thales and Aristeia programmes co-financed by EU-ESF and the Greek NSRF, Greece; BSF-NSF and MINERVA, Israel; NCN and NAWA, Poland; La Caixa Banking Foundation, CERCA Programme Generalitat de Catalunya and PROMETEO and GenT Programmes Generalitat Valenciana, Spain; Göran Gustafssons Stiftelse, Sweden; The Royal Society and Leverhulme Trust, United Kingdom.

In addition, individual members wish to acknowledge support from Armenia: Yerevan Physics Institute (FAPERJ); CERN: European Organization for Nuclear Research (CERN DOCT); Chile: Agencia Nacional de Investigación y Desarrollo (FONDECYT 1230812, FONDECYT 1230987, FONDECYT 1240864); China: Chinese Ministry of Science and Technology (MOST-2023YFA1605700, MOST-2023YFA1609300), National Natural Science Foundation of China (NSFC — 12175119, NSFC 12275265, NSFC-12075060); Czech Republic: Czech Science Foundation (GACR — 24-11373S), Ministry of Education Youth and Sports (FORTE CZ.02.01.01/00/22_008/0004632), PRIMUS Research Programme (PRIMUS/21/SCI/017); EU: H2020 European Research Council (ERC — 101002463); European Union: European Research Council (ERC — 948254, ERC 101089007, ERC, BARD, 101116429), Horizon 2020 Framework Programme (MUCCA — CHIST-ERA-19-XAI-00), European Union, Future Artificial Intelligence Research (FAIR-NextGenerationEU PE00000013), Italian Center for High Performance Computing, Big Data and Quantum Computing (ICSC, NextGenerationEU); France: Agence Nationale de la Recherche (ANR-20-CE31-0013, ANR-21-CE31-0013, ANR-21-CE31-0022, ANR-22-EDIR-0002); Germany: Baden-Württemberg Stiftung (BW Stiftung-Postdoc Eliteprogramme), Deutsche Forschungsgemeinschaft (DFG — 469666862, DFG — CR 312/5-2); Italy: Istituto Nazionale di Fisica Nucleare (ICSC, NextGenerationEU), Ministero dell'Università e della Ricerca (NextGenEU PRIN20223N7F8K M4C2.1.1); Japan: Japan Society for the Promotion of Science (JSPS KAKENHI JP22H01227, JSPS KAKENHI JP22H04944, JSPS KAKENHI JP22KK0227, JSPS KAKENHI JP23KK0245); Netherlands: Netherlands Organisation for Scientific Research (NWO Veni 2020 — VI.Veni.202.179); Norway: Research Council of Norway (RCN-314472); Poland: Ministry of Science and Higher Education (IDUB AGH, POB8, D4 no 9722), Polish National Agency for Academic Exchange (PPN/PPO/2020/1/00002/U/00001), Polish National Science Centre (NCN 2021/42/E/ST2/00350, NCN OPUS 2023/51/B/ST2/02507, NCN OPUS nr 2022/47/B/ST2/03059, NCN UMO-2019/34/E/ST2/00393, NCN & H2020 MSCA 945339, UMO-2020/37/B/ST2/01043, UMO-2021/40/C/ST2/00187, UMO-2022/47/O/ST2/00148, UMO-2023/49/B/ST2/04085, UMO-2023/51/B/ST2/00920); Slovenia: Slovenian Research Agency (ARIS grant J1-3010); Spain: Generalitat Valenciana (Artemisa, FEDER, IDIFEDER/2018/048), Ministry of Science and Innovation (MCIN & NextGenEU PCI2022-135018-2, MICIN & FEDER PID2021-125273NB, RYC2019-028510-I, RYC2020-030254-I, RYC2021-031273-I, RYC2022-038164-I); Sweden: Carl Trygger Foundation (Carl Trygger Foundation CTS 22:2312), Swedish Research Council (Swedish Research Council 2023-04654, VR 2018-00482, VR 2021-03651, VR 2022-03845, VR 2022-04683, VR 2023-03403), Knut and Alice Wallenberg Foundation (KAW 2018.0458, KAW 2019.0447, KAW 2022.0358);

JHEP05(2025)075

Switzerland: Swiss National Science Foundation (SNSF — PCEFP2_194658); United Kingdom: Leverhulme Trust (Leverhulme Trust RPG-2020-004), Royal Society (NIF-R1-231091); United States of America: U.S. Department of Energy (ECA DE-AC02-76SF00515), Neubauer Family Foundation.

Data Availability Statement. This article has no associated data or the data will not be deposited.

Code Availability Statement. This article has no associated code or the code will not be deposited.

References

[1] ATLAS collaboration, *Observation of a new particle in the search for the Standard Model Higgs boson with the ATLAS detector at the LHC*, *Phys. Lett. B* **716** (2012) 1 [arXiv:1207.7214] [INSPIRE].

[2] CMS collaboration, *Observation of a new boson at a mass of 125 GeV with the CMS experiment at the LHC*, *Phys. Lett. B* **716** (2012) 30 [arXiv:1207.7235] [INSPIRE].

[3] L. Evans and P. Bryant, *LHC machine*, 2008 *JINST* **3** S08001 [INSPIRE].

[4] F. del Aguila and M.J. Bowick, *The possibility of new fermions with $\Delta I = 0$ mass*, *Nucl. Phys. B* **224** (1983) 107 [INSPIRE].

[5] P.M. Fishbane, R.E. Norton and M.J. Rivard, *Experimental implications of heavy isosinglet quarks and leptons*, *Phys. Rev. D* **33** (1986) 2632 [INSPIRE].

[6] P.M. Fishbane and P.Q. Hung, *Lepton masses in a dynamical model of family symmetry*, *Z. Phys. C* **38** (1988) 649 [INSPIRE].

[7] I. Montvay, *Three mirror pairs of fermion families*, *Phys. Lett. B* **205** (1988) 315 [INSPIRE].

[8] K. Fujikawa, *A vector-like extension of the standard model*, *Prog. Theor. Phys.* **92** (1994) 1149 [hep-ph/9411258] [INSPIRE].

[9] F. del Aguila, L. Ametller, G.L. Kane and J. Vidal, *Vector like fermion and standard Higgs production at hadron colliders*, *Nucl. Phys. B* **334** (1990) 1 [INSPIRE].

[10] D.B. Kaplan, H. Georgi and S. Dimopoulos, *Composite Higgs scalars*, *Phys. Lett. B* **136** (1984) 187 [INSPIRE].

[11] K. Agashe, R. Contino and A. Pomarol, *The minimal composite Higgs model*, *Nucl. Phys. B* **719** (2005) 165 [hep-ph/0412089] [INSPIRE].

[12] K. Kong, S.C. Park and T.G. Rizzo, *A vector-like fourth generation with a discrete symmetry from split-UED*, *JHEP* **07** (2010) 059 [arXiv:1004.4635] [INSPIRE].

[13] G.-Y. Huang, K. Kong and S.C. Park, *Bounds on the fermion-bulk masses in models with universal extra dimensions*, *JHEP* **06** (2012) 099 [arXiv:1204.0522] [INSPIRE].

[14] S.P. Martin, *Extra vector-like matter and the lightest Higgs scalar boson mass in low-energy supersymmetry*, *Phys. Rev. D* **81** (2010) 035004 [arXiv:0910.2732] [INSPIRE].

JHEP05(2025)075

[15] S. Zheng, *Minimal vector-like model in supersymmetric unification*, *Eur. Phys. J. C* **80** (2020) 273 [arXiv:1904.10145] [INSPIRE].

[16] R. Nevzorov, *E_6 inspired supersymmetric models with exact custodial symmetry*, *Phys. Rev. D* **87** (2013) 015029 [arXiv:1205.5967] [INSPIRE].

[17] I. Dorsner, S. Fajfer and I. Mustać, *Light vector-like fermions in a minimal $SU(\,)5$ setup*, *Phys. Rev. D* **89** (2014) 115004 [arXiv:1401.6870] [INSPIRE].

[18] A. Joglekar and J.L. Rosner, *Searching for signatures of E_6*, *Phys. Rev. D* **96** (2017) 015026 [arXiv:1607.06900] [INSPIRE].

[19] K. Agashe, T. Okui and R. Sundrum, *A common origin for neutrino anarchy and charged hierarchies*, *Phys. Rev. Lett.* **102** (2009) 101801 [arXiv:0810.1277] [INSPIRE].

[20] M. Redi, *Leptons in composite MFV*, *JHEP* **09** (2013) 060 [arXiv:1306.1525] [INSPIRE].

[21] P. Schwaller, T.M.P. Tait and R. Vega-Morales, *Dark matter and vectorlike leptons from gauged lepton number*, *Phys. Rev. D* **88** (2013) 035001 [arXiv:1305.1108] [INSPIRE].

[22] J. Halverson, N. Orlofsky and A. Pierce, *Vectorlike leptons as the tip of the dark matter iceberg*, *Phys. Rev. D* **90** (2014) 015002 [arXiv:1403.1592] [INSPIRE].

[23] S. Bahrami et al., *Dark matter and collider studies in the left-right symmetric model with vectorlike leptons*, *Phys. Rev. D* **95** (2017) 095024 [arXiv:1612.06334] [INSPIRE].

[24] S. Bhattacharya, P. Ghosh, N. Sahoo and N. Sahu, *Mini review on vector-like leptonic dark matter, neutrino mass, and collider signatures*, *Front. in Phys.* **7** (2019) 80 [arXiv:1812.06505] [INSPIRE].

[25] L. Susskind, *Dynamics of spontaneous symmetry breaking in the Weinberg-Salam theory*, *Phys. Rev. D* **20** (1979) 2619 [INSPIRE].

[26] Muon g-2 collaboration, *Final report of the muon E821 anomalous magnetic moment measurement at BNL*, *Phys. Rev. D* **73** (2006) 072003 [hep-ex/0602035] [INSPIRE].

[27] Muon g-2 collaboration, *Measurement of the positive muon anomalous magnetic moment to 0.20 ppm*, *Phys. Rev. Lett.* **131** (2023) 161802 [arXiv:2308.06230] [INSPIRE].

[28] R.H. Parker et al., *Measurement of the fine-structure constant as a test of the Standard Model*, *Science* **360** (2018) 191 [arXiv:1812.04130] [INSPIRE].

[29] L. Morel, Z. Yao, P. Cladé and S. Guellati-Khélifa, *Determination of the fine-structure constant with an accuracy of 81 parts per trillion*, *Nature* **588** (2020) 61 [INSPIRE].

[30] X. Fan, T.G. Myers, B.A.D. Sukra and G. Gabrielse, *Measurement of the electron magnetic moment*, *Phys. Rev. Lett.* **130** (2023) 071801 [arXiv:2209.13084] [INSPIRE].

[31] B. Belfatto, R. Beradze and Z. Berezhiani, *The CKM unitarity problem: a trace of new physics at the TeV scale?*, *Eur. Phys. J. C* **80** (2020) 149 [arXiv:1906.02714] [INSPIRE].

[32] Y. Grossman, E. Passemar and S. Schacht, *On the statistical treatment of the Cabibbo angle anomaly*, *JHEP* **07** (2020) 068 [arXiv:1911.07821] [INSPIRE].

[33] A. Crivellin, F. Kirk, C.A. Manzari and M. Montull, *Global electroweak fit and vector-like leptons in light of the Cabibbo angle anomaly*, *JHEP* **12** (2020) 166 [arXiv:2008.01113] [INSPIRE].

[34] M. Endo, K. Hamaguchi, S. Iwamoto and N. Yokozaki, *Higgs mass and muon anomalous magnetic moment in supersymmetric models with vector-like matters*, *Phys. Rev. D* **84** (2011) 075017 [arXiv:1108.3071] [INSPIRE].

JHEP05(2025)075

[35] R. Dermisek and A. Raval, *Explanation of the muon g-2 anomaly with vectorlike leptons and its implications for Higgs decays*, *Phys. Rev. D* **88** (2013) 013017 [arXiv:1305.3522] [INSPIRE].

[36] E. Megias, M. Quiros and L. Salas, $g_\mu - 2$ *from vector-like leptons in warped space*, *JHEP* **05** (2017) 016 [arXiv:1701.05072] [INSPIRE].

[37] G. Hiller, C. Hormigos-Feliu, D.F. Litim and T. Steudtner, *Model building from asymptotic safety with Higgs and flavor portals*, *Phys. Rev. D* **102** (2020) 095023 [arXiv:2008.08606] [INSPIRE].

[38] P. Dehghani, M. Frank and B. Fuks, *Collider imprint of vector-like leptons in light of anomalous magnetic moment and neutrino data*, *Eur. Phys. J. C* **84** (2024) 1284 [arXiv:2403.11862] [INSPIRE].

[39] ATLAS collaboration, *Exploration at the high-energy frontier: ATLAS run 2 searches investigating the exotic jungle beyond the Standard Model*, *Phys. Rept.* **1116** (2025) 301 [arXiv:2403.09292] [INSPIRE].

[40] CMS collaboration, *Review of searches for vector-like quarks, vector-like leptons, and heavy neutral leptons in proton-proton collisions at* $\sqrt{s} = 13$ *TeV at the CMS experiment*, *Phys. Rept.* **1115** (2025) 570 [arXiv:2405.17605] [INSPIRE].

[41] N. Kumar and S.P. Martin, *Vectorlike leptons at the Large Hadron Collider*, *Phys. Rev. D* **92** (2015) 115018 [arXiv:1510.03456] [INSPIRE].

[42] P.N. Bhattiprolu and S.P. Martin, *Prospects for vectorlike leptons at future proton-proton colliders*, *Phys. Rev. D* **100** (2019) 015033 [arXiv:1905.00498] [INSPIRE].

[43] M.S. Chanowitz and M.K. Gaillard, *The TeV physics of strongly interacting W's and Z's*, *Nucl. Phys. B* **261** (1985) 379 [INSPIRE].

[44] L3 collaboration, *Search for heavy neutral and charged leptons in* e^+e^- *annihilation at LEP*, *Phys. Lett. B* **517** (2001) 75 [hep-ex/0107015] [INSPIRE].

[45] ATLAS collaboration, *Search for heavy lepton resonances decaying to a Z boson and a lepton in pp collisions at* $\sqrt{s} = 8$ *TeV with the ATLAS detector*, *JHEP* **09** (2015) 108 [arXiv:1506.01291] [INSPIRE].

[46] ATLAS collaboration, *Search for third-generation vector-like leptons in pp collisions at* $\sqrt{s} = 13$ *TeV with the ATLAS detector*, *JHEP* **07** (2023) 118 [arXiv:2303.05441] [INSPIRE].

[47] CMS collaboration, *Inclusive nonresonant multilepton probes of new phenomena at* $\sqrt{s} = 13$ *TeV*, *Phys. Rev. D* **105** (2022) 112007 [arXiv:2202.08676] [INSPIRE].

[48] ATLAS collaboration, *Measurements of differential cross-sections in four-lepton events in 13 TeV proton-proton collisions with the ATLAS detector*, *JHEP* **07** (2021) 005 [arXiv:2103.01918] [INSPIRE].

[49] ATLAS collaboration, *The ATLAS experiment at the CERN Large Hadron Collider*, 2008 *JINST* **3** S08003 [INSPIRE].

[50] ATLAS IBL collaboration, *Production and integration of the ATLAS Insertable B-Layer*, 2018 *JINST* **13** T05008 [arXiv:1803.00844] [INSPIRE].

[51] G. Avoni et al., *The new LUCID-2 detector for luminosity measurement and monitoring in ATLAS*, 2018 *JINST* **13** P07017 [INSPIRE].

[52] ATLAS collaboration, *Performance of the ATLAS trigger system in 2015*, *Eur. Phys. J. C* **77** (2017) 317 [arXiv:1611.09661] [INSPIRE].

JHEP05(2025)075

[53] ATLAS collaboration, *Software and computing for run 3 of the ATLAS experiment at the LHC*, *Eur. Phys. J. C* **85** (2025) 234 [arXiv:2404.06335] [INSPIRE].

[54] ATLAS collaboration, *ATLAS data quality operations and performance for 2015–2018 data-taking*, 2020 *JINST* **15** P04003 [arXiv:1911.04632] [INSPIRE].

[55] ATLAS collaboration, *ATLAS Pythia 8 tunes to 7 TeV data*, ATL-PHYS-PUB-2014-021, CERN, Geneva, Switzerland (2014).

[56] J. Bellm et al., *Herwig 7.0/Herwig++ 3.0 release note*, *Eur. Phys. J. C* **76** (2016) 196 [arXiv:1512.01178] [INSPIRE].

[57] T. Gleisberg et al., *Event generation with SHERPA 1.1*, *JHEP* **02** (2009) 007 [arXiv:0811.4622] [INSPIRE].

[58] T. Gleisberg and S. Höche, *Comix, a new matrix element generator*, *JHEP* **12** (2008) 039 [arXiv:0808.3674] [INSPIRE].

[59] F. Buccioni et al., *OpenLoops 2*, *Eur. Phys. J. C* **79** (2019) 866 [arXiv:1907.13071] [INSPIRE].

[60] F. Cascioli, P. Maierhöfer and S. Pozzorini, *Scattering amplitudes with OpenLoops*, *Phys. Rev. Lett.* **108** (2012) 111601 [arXiv:1111.5206] [INSPIRE].

[61] A. Denner, S. Dittmaier and L. Hofer, *Collier: a fortran-based Complex One-Loop LIbrary in Extended Regularizations*, *Comput. Phys. Commun.* **212** (2017) 220 [arXiv:1604.06792] [INSPIRE].

[62] S. Schumann and F. Krauss, *A parton shower algorithm based on Catani-Seymour dipole factorisation*, *JHEP* **03** (2008) 038 [arXiv:0709.1027] [INSPIRE].

[63] S. Höche, F. Krauss, M. Schönherr and F. Siegert, *A critical appraisal of NLO+PS matching methods*, *JHEP* **09** (2012) 049 [arXiv:1111.1220] [INSPIRE].

[64] S. Höche, F. Krauss, M. Schönherr and F. Siegert, *QCD matrix elements + parton showers: the NLO case*, *JHEP* **04** (2013) 027 [arXiv:1207.5030] [INSPIRE].

[65] S. Catani, F. Krauss, R. Kuhn and B.R. Webber, *QCD matrix elements + parton showers*, *JHEP* **11** (2001) 063 [hep-ph/0109231] [INSPIRE].

[66] S. Höche, F. Krauss, S. Schumann and F. Siegert, *QCD matrix elements and truncated showers*, *JHEP* **05** (2009) 053 [arXiv:0903.1219] [INSPIRE].

[67] T. Sjöstrand, S. Mrenna and P.Z. Skands, *A brief introduction to PYTHIA 8.1*, *Comput. Phys. Commun.* **178** (2008) 852 [arXiv:0710.3820] [INSPIRE].

[68] ATLAS collaboration, *Further ATLAS tunes of PYTHIA 6 and PYTHIA 8*, ATL-PHYS-PUB-2011-014, CERN, Geneva, Switzerland (2011).

[69] P. Golonka and Z. Was, *PHOTOS Monte Carlo: a precision tool for QED corrections in Z and W decays*, *Eur. Phys. J. C* **45** (2006) 97 [hep-ph/0506026] [INSPIRE].

[70] GEANT4 collaboration, *GEANT4 — a simulation toolkit*, *Nucl. Instrum. Meth. A* **506** (2003) 250 [INSPIRE].

[71] ATLAS collaboration, *The ATLAS simulation infrastructure*, *Eur. Phys. J. C* **70** (2010) 823 [arXiv:1005.4568] [INSPIRE].

[72] J. Alwall et al., *The automated computation of tree-level and next-to-leading order differential cross sections, and their matching to parton shower simulations*, *JHEP* **07** (2014) 079 [arXiv:1405.0301] [INSPIRE].

JHEP05(2025)075

[73] NNPDF collaboration, *Parton distributions for the LHC run II*, *JHEP* **04** (2015) 040 [arXiv:1410.8849] [INSPIRE].

[74] T. Sjöstrand et al., *An introduction to PYTHIA 8.2*, *Comput. Phys. Commun.* **191** (2015) 159 [arXiv:1410.3012] [INSPIRE].

[75] S. Frixione, P. Nason and G. Ridolfi, *A positive-weight next-to-leading-order Monte Carlo for heavy flavour hadroproduction*, *JHEP* **09** (2007) 126 [arXiv:0707.3088] [INSPIRE].

[76] P. Nason, *A new method for combining NLO QCD with shower Monte Carlo algorithms*, *JHEP* **11** (2004) 040 [hep-ph/0409146] [INSPIRE].

[77] S. Frixione, P. Nason and C. Oleari, *Matching NLO QCD computations with parton shower simulations: the POWHEG method*, *JHEP* **11** (2007) 070 [arXiv:0709.2092] [INSPIRE].

[78] S. Alioli, P. Nason, C. Oleari and E. Re, *A general framework for implementing NLO calculations in shower Monte Carlo programs: the POWHEG BOX*, *JHEP* **06** (2010) 043 [arXiv:1002.2581] [INSPIRE].

[79] E. Re, *Single-top Wt-channel production matched with parton showers using the POWHEG method*, *Eur. Phys. J. C* **71** (2011) 1547 [arXiv:1009.2450] [INSPIRE].

[80] R. Frederix, E. Re and P. Torrielli, *Single-top t-channel hadroproduction in the four-flavour scheme with POWHEG and aMC@NLO*, *JHEP* **09** (2012) 130 [arXiv:1207.5391] [INSPIRE].

[81] S. Alioli, P. Nason, C. Oleari and E. Re, *NLO single-top production matched with shower in POWHEG: s- and t-channel contributions*, *JHEP* **09** (2009) 111 [*Erratum ibid.* **02** (2010) 011] [arXiv:0907.4076] [INSPIRE].

[82] D.J. Lange, *The EvtGen particle decay simulation package*, *Nucl. Instrum. Meth. A* **462** (2001) 152 [INSPIRE].

[83] ATLAS collaboration, *Studies on top-quark Monte Carlo modelling for Top2016*, ATL-PHYS-PUB-2016-020, CERN, Geneva, Switzerland (2016).

[84] M. Beneke, P. Falgari, S. Klein and C. Schwinn, *Hadronic top-quark pair production with NNLL threshold resummation*, *Nucl. Phys. B* **855** (2012) 695 [arXiv:1109.1536] [INSPIRE].

[85] M. Cacciari et al., *Top-pair production at hadron colliders with next-to-next-to-leading logarithmic soft-gluon resummation*, *Phys. Lett. B* **710** (2012) 612 [arXiv:1111.5869] [INSPIRE].

[86] P. Bärnreuther, M. Czakon and A. Mitov, *Percent level precision physics at the Tevatron: first genuine NNLO QCD corrections to $q\bar{q} \to t\bar{t} + X$*, *Phys. Rev. Lett.* **109** (2012) 132001 [arXiv:1204.5201] [INSPIRE].

[87] M. Czakon and A. Mitov, *NNLO corrections to top-pair production at hadron colliders: the all-fermionic scattering channels*, *JHEP* **12** (2012) 054 [arXiv:1207.0236] [INSPIRE].

[88] M. Czakon and A. Mitov, *NNLO corrections to top pair production at hadron colliders: the quark-gluon reaction*, *JHEP* **01** (2013) 080 [arXiv:1210.6832] [INSPIRE].

[89] M. Czakon, P. Fiedler and A. Mitov, *Total top-quark pair-production cross section at hadron colliders through $O(\alpha_S^4)$*, *Phys. Rev. Lett.* **110** (2013) 252004 [arXiv:1303.6254] [INSPIRE].

[90] M. Czakon and A. Mitov, *Top++: a program for the calculation of the top-pair cross-section at hadron colliders*, *Comput. Phys. Commun.* **185** (2014) 2930 [arXiv:1112.5675] [INSPIRE].

[91] S. Catani et al., *Vector boson production at hadron colliders: a fully exclusive QCD calculation at NNLO*, *Phys. Rev. Lett.* **103** (2009) 082001 [arXiv:0903.2120] [INSPIRE].

JHEP05(2025)075

[92] SHERPA collaboration, *Event generation with Sherpa 2.2*, *SciPost Phys.* **7** (2019) 034 [arXiv:1905.09127] [INSPIRE].

[93] S. Kallweit et al., *NLO QCD+EW predictions for V+jets including off-shell vector-boson decays and multijet merging*, *JHEP* **04** (2016) 021 [arXiv:1511.08692] [INSPIRE].

[94] R. Frederix, D. Pagani and M. Zaro, *Large NLO corrections in $t\bar{t}W^{\pm}$ and $t\bar{t}t\bar{t}$ hadroproduction from supposedly subleading EW contributions*, *JHEP* **02** (2018) 031 [arXiv:1711.02116] [INSPIRE].

[95] S. Frixione et al., *Single-top hadroproduction in association with a W boson*, *JHEP* **07** (2008) 029 [arXiv:0805.3067] [INSPIRE].

[96] J. Pumplin et al., *New generation of parton distributions with uncertainties from global QCD analysis*, *JHEP* **07** (2002) 012 [hep-ph/0201195] [INSPIRE].

[97] NNPDF collaboration, *Parton distributions from high-precision collider data*, *Eur. Phys. J. C* **77** (2017) 663 [arXiv:1706.00428] [INSPIRE].

[98] ATLAS collaboration, *Vertex reconstruction performance of the ATLAS detector at $\sqrt{s} = 13$ TeV*, ATL-PHYS-PUB-2015-026, CERN, Geneva, Switzerland (2015).

[99] ATLAS collaboration, *Electron and photon performance measurements with the ATLAS detector using the 2015–2017 LHC proton-proton collision data*, 2019 *JINST* **14** P12006 [arXiv:1908.00005] [INSPIRE].

[100] ATLAS collaboration, *Muon reconstruction and identification efficiency in ATLAS using the full run 2 pp collision data set at $\sqrt{s} = 13$ TeV*, *Eur. Phys. J. C* **81** (2021) 578 [arXiv:2012.00578] [INSPIRE].

[101] ATLAS collaboration, *Evidence for the associated production of the Higgs boson and a top quark pair with the ATLAS detector*, *Phys. Rev. D* **97** (2018) 072003 [arXiv:1712.08891] [INSPIRE].

[102] ATLAS collaboration, *Jet reconstruction and performance using particle flow with the ATLAS detector*, *Eur. Phys. J. C* **77** (2017) 466 [arXiv:1703.10485] [INSPIRE].

[103] M. Cacciari, G.P. Salam and G. Soyez, *The anti-k_t jet clustering algorithm*, *JHEP* **04** (2008) 063 [arXiv:0802.1189] [INSPIRE].

[104] M. Cacciari, G.P. Salam and G. Soyez, *FastJet user manual*, *Eur. Phys. J. C* **72** (2012) 1896 [arXiv:1111.6097] [INSPIRE].

[105] ATLAS collaboration, *Jet energy scale and resolution measured in proton-proton collisions at $\sqrt{s} = 13$ TeV with the ATLAS detector*, *Eur. Phys. J. C* **81** (2021) 689 [arXiv:2007.02645] [INSPIRE].

[106] ATLAS collaboration, *Performance of pile-up mitigation techniques for jets in pp collisions at $\sqrt{s} = 8$ TeV using the ATLAS detector*, *Eur. Phys. J. C* **76** (2016) 581 [arXiv:1510.03823] [INSPIRE].

[107] ATLAS collaboration, *Selection of jets produced in 13 TeV proton-proton collisions with the ATLAS detector*, ATLAS-CONF-2015-029, CERN, Geneva, Switzerland (2015).

[108] ATLAS collaboration, *ATLAS flavour-tagging algorithms for the LHC run 2 pp collision dataset*, *Eur. Phys. J. C* **83** (2023) 681 [arXiv:2211.16345] [INSPIRE].

[109] ATLAS collaboration, *ATLAS b-jet identification performance and efficiency measurement with $t\bar{t}$ events in pp collisions at $\sqrt{s} = 13$ TeV*, *Eur. Phys. J. C* **79** (2019) 970 [arXiv:1907.05120] [INSPIRE].

JHEP05(2025)075

[110] ATLAS collaboration, *Measurement of the c-jet mistagging efficiency in $t\bar{t}$ events using pp collision data at $\sqrt{s} = 13$ TeV collected with the ATLAS detector*, *Eur. Phys. J. C* **82** (2022) 95 [arXiv:2109.10627] [INSPIRE].

[111] ATLAS collaboration, *Calibration of the light-flavour jet mistagging efficiency of the b-tagging algorithms with Z+jets events using 139 fb^{-1} of ATLAS proton-proton collision data at $\sqrt{s} = 13$ TeV*, *Eur. Phys. J. C* **83** (2023) 728 [arXiv:2301.06319] [INSPIRE].

[112] ATLAS collaboration, *The performance of missing transverse momentum reconstruction and its significance with the ATLAS detector using 140 fb^{-1} of $\sqrt{s} = 13$ TeV pp collisions*, arXiv:2402.05858 [INSPIRE].

[113] ATLAS collaboration, *Performance of the ATLAS muon triggers in run 2*, 2020 *JINST* **15** P09015 [arXiv:2004.13447] [INSPIRE].

[114] ATLAS collaboration, *Performance of electron and photon triggers in ATLAS during LHC run 2*, *Eur. Phys. J. C* **80** (2020) 47 [arXiv:1909.00761] [INSPIRE].

[115] F. Chollet et al., *Keras*, https://github.com/fchollet/keras (2015).

[116] M. Abadi et al., *TensorFlow: large-scale machine learning on heterogeneous distributed systems*, arXiv:1603.04467 [INSPIRE].

[117] D.P. Kingma and J. Ba, *Adam: a method for stochastic optimization*, arXiv:1412.6980 [INSPIRE].

[118] M. Czakon et al., *Top-pair production at the LHC through NNLO QCD and NLO EW*, *JHEP* **10** (2017) 186 [arXiv:1705.04105] [INSPIRE].

[119] ATLAS collaboration, *Measurement of the total and differential cross-sections of $t\bar{t}W$ production in pp collisions at $\sqrt{s} = 13$ TeV with the ATLAS detector*, *JHEP* **05** (2024) 131 [arXiv:2401.05299] [INSPIRE].

[120] ATLAS collaboration, *Luminosity determination in pp collisions at $\sqrt{s} = 13$ TeV using the ATLAS detector at the LHC*, *Eur. Phys. J. C* **83** (2023) 982 [arXiv:2212.09379] [INSPIRE].

[121] ATLAS collaboration, *Muon reconstruction performance of the ATLAS detector in proton-proton collision data at $\sqrt{s} = 13$ TeV*, *Eur. Phys. J. C* **76** (2016) 292 [arXiv:1603.05598] [INSPIRE].

[122] ATLAS collaboration, *Studies of the muon momentum calibration and performance of the ATLAS detector with pp collisions at $\sqrt{s} = 13$ TeV*, *Eur. Phys. J. C* **83** (2023) 686 [arXiv:2212.07338] [INSPIRE].

[123] F. Febres Cordero, M. Kraus and L. Reina, *Top-quark pair production in association with a $W^{\pm}$ gauge boson in the POWHEG-BOX*, *Phys. Rev. D* **103** (2021) 094014 [arXiv:2101.11808] [INSPIRE].

[124] ATLAS collaboration, *Studies on the improvement of the matching uncertainty definition in top-quark processes simulated with Powheg+Pythia 8*, ATL-PHYS-PUB-2023-029, CERN, Geneva, Switzerland (2023).

[125] LHC Higgs Cross Section Working Group collaboration, *Handbook of LHC Higgs cross sections: 4. Deciphering the nature of the Higgs sector*, arXiv:1610.07922 [DOI:10.23731/CYRM-2017-002] [INSPIRE].

[126] ATLAS collaboration, *Observation of the associated production of a top quark and a Z boson in pp collisions at $\sqrt{s} = 13$ TeV with the ATLAS detector*, *JHEP* **07** (2020) 124 [arXiv:2002.07546] [INSPIRE].

JHEP05(2025)075

[127] J. Butterworth et al., *PDF4LHC recommendations for LHC run II*, *J. Phys. G* **43** (2016) 023001 [arXiv:1510.03865] [INSPIRE].

[128] ROOT collaboration, *HistFactory: a tool for creating statistical models for use with RooFit and RooStats*, CERN-OPEN-2012-016, New York U., New York, NY, U.S.A. (2012) [DOI:10.17181/CERN-OPEN-2012-016].

[129] J.S. Conway, *Incorporating nuisance parameters in likelihoods for multisource spectra*, in the proceedings of the *PHYSTAT 2011*, (2011) [DOI:10.5170/CERN-2011-006.115] [arXiv:1103.0354] [INSPIRE].

[130] W. Verkerke and D.P. Kirkby, *The RooFit toolkit for data modeling*, *eConf C* **0303241** (2003) MOLT007 [physics/0306116] [INSPIRE].

[131] G. Cowan, K. Cranmer, E. Gross and O. Vitells, *Asymptotic formulae for likelihood-based tests of new physics*, *Eur. Phys. J. C* **71** (2011) 1554 [*Erratum ibid.* **73** (2013) 2501] [arXiv:1007.1727] [INSPIRE].

[132] T. Junk, *Confidence level computation for combining searches with small statistics*, *Nucl. Instrum. Meth. A* **434** (1999) 435 [hep-ex/9902006] [INSPIRE].

[133] A.L. Read, *Presentation of search results: the CL_s technique*, *J. Phys. G* **28** (2002) 2693 [INSPIRE].

[134] ATLAS collaboration, *ATLAS computing acknowledgements*, ATL-SOFT-PUB-2025-001, CERN, Geneva, Switzerland (2025).

The ATLAS collaboration

G. Aad[104], E. Aakvaag[17], B. Abbott[123], S. Abdelhameed[119a], K. Abeling[56], N.J. Abicht[50], S.H. Abidi[30], M. Aboelela[46], A. Aboulhorma[36e], H. Abramowicz[155], Y. Abulaiti[120], B.S. Acharya[70a,70b,m], A. Ackermann[64a], C. Adam Bourdarios[4], L. Adamczyk[87a], S.V. Addepalli[147], M.J. Addison[103], J. Adelman[118], A. Adiguzel[22c], T. Adye[137], A.A. Affolder[139], Y. Afik[41], M.N. Agaras[13], A. Aggarwal[102], C. Agheorghiesei[28c], F. Ahmadov[40,ac], S. Ahuja[97], X. Ai[63e], G. Aielli[77a,77b], A. Aikot[167], M. Ait Tamlihat[36e], B. Aitbenchikh[36a], M. Akbiyik[102], T.P.A. Åkesson[100], A.V. Akimov[149], D. Akiyama[172], N.N. Akolkar[25], S. Aktas[22a], G.L. Alberghi[24b], J. Albert[169], P. Albicocco[54], G.L. Albouy[61], S. Alderweireldt[53], Z.L. Alegria[124], M. Aleksa[37], I.N. Aleksandrov[40], C. Alexa[28b], T. Alexopoulos[10], F. Alfonsi[24b], M. Algren[57], M. Alhroob[171], B. Ali[135], H.M.J. Ali[93,v], S. Ali[32], S.W. Alibocus[94], M. Aliev[34c], G. Alimonti[72a], W. Alkakhi[56], C. Allaire[67], B.M.M. Allbrooke[150], J.S. Allen[103], J.F. Allen[53], C.A. Allendes Flores[140f], P.P. Allport[21], A. Aloisio[73a,73b], F. Alonso[92], C. Alpigiani[142], Z.M.K. Alsolami[93], A. Alvarez Fernandez[102], M. Alves Cardoso[57], M.G. Alviggi[73a,73b], M. Aly[103], Y. Amaral Coutinho[84b], A. Ambler[106], C. Amelung[37], M. Amerl[103], C.G. Ames[111], D. Amidei[108], B. Amini[55], K. Amirie[158], A. Amirkhanov[39], S.P. Amor Dos Santos[133a], K.R. Amos[167], D. Amperiadou[156], S. An[85], V. Ananiev[128], C. Anastopoulos[143], T. Andeen[11], J.K. Anders[37], A.C. Anderson[60], A. Andreazza[72a,72b], S. Angelidakis[9], A. Angerami[43], A.V. Anisenkov[39], A. Annovi[75a], C. Antel[57], E. Antipov[149], M. Antonelli[54], F. Anulli[76a], M. Aoki[85], T. Aoki[157], M.A. Aparo[150], L. Aperio Bella[49], C. Appelt[155], A. Apyan[27], S.J. Arbiol Val[88], C. Arcangeletti[54], A.T.H. Arce[52], J-F. Arguin[110], S. Argyropoulos[156], J.-H. Arling[49], O. Arnaez[4], H. Arnold[149], G. Artoni[76a,76b], H. Asada[113], K. Asai[121], S. Asai[157], N.A. Asbah[37], R.A. Ashby Pickering[171], A.M. Aslam[97], K. Assamagan[30], R. Astalos[29a], K.S.V. Astrand[100], S. Atashi[162], R.J. Atkin[34a], H. Atmani[36f], P.A. Atmasiddha[131], K. Augsten[135], A.D. Auriol[42], V.A. Austrup[103], G. Avolio[37], K. Axiotis[57], G. Azuelos[110,ag], D. Babal[29b], H. Bachacou[138], K. Bachas[156,q], A. Bachiu[35], E. Bachmann[51], A. Badea[41], T.M. Baer[108], P. Bagnaia[76a,76b], M. Bahmani[19], D. Bahner[55], K. Bai[126], J.T. Baines[137], L. Baines[96], O.K. Baker[176], E. Bakos[16], D. Bakshi Gupta[8], L.E. Balabram Filho[84b], V. Balakrishnan[123], R. Balasubramanian[4], E.M. Baldin[39], P. Balek[87a], E. Ballabene[24b,24a], F. Balli[138], L.M. Baltes[64a], W.K. Balunas[33], J. Balz[102], I. Bamwidhi[119b], E. Banas[88], M. Bandieramonte[132], A. Bandyopadhyay[25], S. Bansal[25], L. Barak[155], M. Barakat[49], E.L. Barberio[107], D. Barberis[58b,58a], M. Barbero[104], M.Z. Barel[117], T. Barillari[112], M-S. Barisits[37], T. Barklow[147], P. Baron[125], D.A. Baron Moreno[103], A. Baroncelli[63a], A.J. Barr[129], J.D. Barr[98], F. Barreiro[101], J. Barreiro Guimarães da Costa[14], M.G. Barros Teixeira[133a], S. Barsov[39], F. Bartels[64a], R. Bartoldus[147], A.E. Barton[93], P. Bartos[29a], A. Basan[102], M. Baselga[50], S. Bashiri[88], A. Bassalat[67,b], M.J. Basso[159a], S. Bataju[46], R. Bate[168], R.L. Bates[60], S. Batlamous[101], M. Battaglia[139], D. Battulga[19], M. Bauce[76a,76b], M. Bauer[80], P. Bauer[25], L.T. Bazzano Hurrell[31], J.B. Beacham[52], T. Beau[130], J.Y. Beaucamp[92], P.H. Beauchemin[161], P. Bechtle[25], H.P. Beck[20,p], K. Becker[171], A.J. Beddall[83], V.A. Bednyakov[40], C.P. Bee[149], L.J. Beemster[16], M. Begalli[84d],

JHEP05(2025)075

M. Begel[30], J.K. Behr[49], J.F. Beirer[37], F. Beisiegel[25], M. Belfkir[119b], G. Bella[155], L. Bellagamba[24b], A. Bellerive[35], P. Bellos[21], K. Beloborodov[39], D. Benchekroun[36a], F. Bendebba[36a], Y. Benhammou[155], K.C. Benkendorfer[62], L. Beresford[49], M. Beretta[54], E. Bergeaas Kuutmann[165], N. Berger[4], B. Bergmann[135], J. Beringer[18a], G. Bernardi[5], C. Bernius[147], F.U. Bernlochner[25], F. Bernon[37], A. Berrocal Guardia[13], T. Berry[97], P. Berta[136], A. Berthold[51], S. Bethke[112], A. Betti[76a,76b], A.J. Bevan[96], N.K. Bhalla[55], S. Bharthuar[112], S. Bhatta[149], D.S. Bhattacharya[170], P. Bhattarai[147], Z.M. Bhatti[120], K.D. Bhide[55], V.S. Bhopatkar[124], R.M. Bianchi[132], G. Bianco[24b,24a], O. Biebel[111], M. Biglietti[78a], C.S. Billingsley[46], Y. Bimgdi[36f], M. Bindi[56], A. Bingham[175], A. Bingul[22b], C. Bini[76a,76b], G.A. Bird[33], M. Birman[173], M. Biros[136], S. Biryukov[150], T. Bisanz[50], E. Bisceglie[45b,45a], J.P. Biswal[137], D. Biswas[145], I. Bloch[49], A. Blue[60], U. Blumenschein[96], J. Blumenthal[102], V.S. Bobrovnikov[39], M. Boehler[55], B. Boehm[170], D. Bogavac[37], A.G. Bogdanchikov[39], L.S. Boggia[130], V. Boisvert[97], P. Bokan[37], T. Bold[87a], M. Bomben[5], M. Bona[96], M. Boonekamp[138], A.G. Borbély[60], I.S. Bordulev[39], G. Borissov[93], D. Bortoletto[129], D. Boscherini[24b], M. Bosman[13], K. Bouaouda[36a], N. Bouchhar[167], L. Boudet[4], J. Boudreau[132], E.V. Bouhova-Thacker[93], D. Boumediene[42], R. Bouquet[58b,58a], A. Boveia[122], J. Boyd[37], D. Boye[30], I.R. Boyko[40], L. Bozianu[57], J. Bracinik[21], N. Brahimi[4], G. Brandt[175], O. Brandt[33], B. Brau[105], J.E. Brau[126], R. Brener[173], L. Brenner[117], R. Brenner[165], S. Bressler[173], G. Brianti[79a,79b], D. Britton[60], D. Britzger[112], I. Brock[25], R. Brock[109], G. Brooijmans[43], A.J. Brooks[69], E.M. Brooks[159b], E. Brost[30], L.M. Brown[169,159a], L.E. Bruce[62], T.L. Bruckler[129], P.A. Bruckman de Renstrom[88], B. Brüers[49], A. Bruni[24b], G. Bruni[24b], D. Brunner[48a,48b], M. Bruschi[24b], N. Bruscino[76a,76b], T. Buanes[17], Q. Buat[142], D. Buchin[112], A.G. Buckley[60], O. Bulekov[39], B.A. Bullard[147], S. Burdin[94], C.D. Burgard[50], A.M. Burger[37], B. Burghgrave[8], O. Burlayenko[55], J. Burleson[166], J.T.P. Burr[33], J.C. Burzynski[146], E.L. Busch[43], V. Büscher[102], P.J. Bussey[60], J.M. Butler[26], C.M. Buttar[60], J.M. Butterworth[98], W. Buttinger[137], C.J. Buxo Vazquez[109], A.R. Buzykaev[39], S. Cabrera Urbán[167], L. Cadamuro[67], D. Caforio[59], H. Cai[132], Y. Cai[24b,114c,24a], Y. Cai[114a], V.M.M. Cairo[37], O. Cakir[3a], N. Calace[37], P. Calafiura[18a], G. Calderini[130], P. Calfayan[35], G. Callea[60], L.P. Caloba[84b], D. Calvet[42], S. Calvet[42], R. Camacho Toro[130], S. Camarda[37], D. Camarero Munoz[27], P. Camarri[77a,77b], M.T. Camerlingo[73a,73b], D. Cameron[37], C. Camincher[169], M. Campanelli[98], A. Camplani[44], V. Canale[73a,73b], A.C. Canbay[3a], E. Canonero[97], J. Cantero[167], Y. Cao[166], F. Capocasa[27], M. Capua[45b,45a], A. Carbone[72a,72b], R. Cardarelli[77a], J.C.J. Cardenas[8], M.P. Cardiff[27], G. Carducci[45b,45a], T. Carli[37], G. Carlino[73a], J.I. Carlotto[13], B.T. Carlson[132,r], E.M. Carlson[169], J. Carmignani[94], L. Carminati[72a,72b], A. Carnelli[138], M. Carnesale[37], S. Caron[116], E. Carquin[140f], I.B. Carr[107], S. Carrá[72a], G. Carratta[24b,24a], A.M. Carroll[126], M.P. Casado[13,i], M. Caspar[49], F.L. Castillo[4], L. Castillo Garcia[13], V. Castillo Gimenez[167], N.F. Castro[133a,133e], A. Catinaccio[37], J.R. Catmore[128], T. Cavaliere[4], V. Cavaliere[30], L.J. Caviedes Betancourt[23b], Y.C. Cekmecelioglu[49], E. Celebi[83], S. Cella[37], V. Cepaitis[57], K. Cerny[125], A.S. Cerqueira[84a], A. Cerri[150], L. Cerrito[77a,77b], F. Cerutti[18a], B. Cervato[145], A. Cervelli[24b], G. Cesarini[54], S.A. Cetin[83], P.M. Chabrillat[130],

JHEP05(2025)075

J. Chan[18a], W.Y. Chan[157], J.D. Chapman[33], E. Chapon[138], B. Chargeishvili[153b], D.G. Charlton[21], C. Chauhan[136], Y. Che[114a], S. Chekanov[6], S.V. Chekulaev[159a], G.A. Chelkov[40,a], B. Chen[155], B. Chen[169], H. Chen[114a], H. Chen[30], J. Chen[63c], J. Chen[146], M. Chen[129], S. Chen[89], S.J. Chen[114a], X. Chen[63c], X. Chen[15,af], Y. Chen[63a], C.L. Cheng[174], H.C. Cheng[65a], S. Cheong[147], A. Cheplakov[40], E. Cheremushkina[49], E. Cherepanova[117], R. Cherkaoui El Moursli[36e], E. Cheu[7], K. Cheung[66], L. Chevalier[138], V. Chiarella[54], G. Chiarelli[75a], N. Chiedde[104], G. Chiodini[71a], A.S. Chisholm[21], A. Chitan[28b], M. Chitishvili[167], M.V. Chizhov[40,s], K. Choi[11], Y. Chou[142], E.Y.S. Chow[116], K.L. Chu[173], M.C. Chu[65a], X. Chu[14,114c], Z. Chubinidze[54], J. Chudoba[134], J.J. Chwastowski[88], D. Cieri[112], K.M. Ciesla[87a], V. Cindro[95], A. Ciocio[18a], F. Cirotto[73a,73b], Z.H. Citron[173], M. Citterio[72a], D.A. Ciubotaru[28b], A. Clark[57], P.J. Clark[53], N. Clarke Hall[98], C. Clarry[158], S.E. Clawson[49], C. Clement[48a,48b], Y. Coadou[104], M. Cobal[70a,70c], A. Coccaro[58b], R.F. Coelho Barrue[133a], R. Coelho Lopes De Sa[105], S. Coelli[72a], L.S. Colangeli[158], B. Cole[43], J. Collot[61], P. Conde Muiño[133a,133g], M.P. Connell[34c], S.H. Connell[34c], E.I. Conroy[129], F. Conventi[73a,ah], H.G. Cooke[21], A.M. Cooper-Sarkar[129], F.A. Corchia[24b,24a], A. Cordeiro Oudot Choi[130], L.D. Corpe[42], M. Corradi[76a,76b], F. Corriveau[106,aa], A. Cortes-Gonzalez[19], M.J. Costa[167], F. Costanza[4], D. Costanzo[143], B.M. Cote[122], J. Couthures[4], G. Cowan[97], K. Cranmer[174], L. Cremer[50], D. Cremonini[24b,24a], S. Crépé-Renaudin[61], F. Crescioli[130], M. Cristinziani[145], M. Cristoforetti[79a,79b], V. Croft[117], J.E. Crosby[124], G. Crosetti[45b,45a], A. Cueto[101], H. Cui[98], Z. Cui[7], W.R. Cunningham[60], F. Curcio[167], J.R. Curran[53], P. Czodrowski[37], M.J. Da Cunha Sargedas De Sousa[58b,58a], J.V. Da Fonseca Pinto[84b], C. Da Via[103], W. Dabrowski[87a], T. Dado[37], S. Dahbi[152], T. Dai[108], D. Dal Santo[20], C. Dallapiccola[105], M. Dam[44], G. D'amen[30], V. D'Amico[111], J. Damp[102], J.R. Dandoy[35], D. Dannheim[37], M. Danninger[146], V. Dao[149], G. Darbo[58b], S.J. Das[30], F. Dattola[49], S. D'Auria[72a,72b], A. D'Avanzo[73a,73b], T. Davidek[136], I. Dawson[96], H.A. Day-hall[135], K. De[8], C. De Almeida Rossi[158], R. De Asmundis[73a], N. De Biase[49], S. De Castro[24b,24a], N. De Groot[116], P. de Jong[117], H. De la Torre[118], A. De Maria[114a], A. De Salvo[76a], U. De Sanctis[77a,77b], F. De Santis[71a,71b], A. De Santo[150], J.B. De Vivie De Regie[61], J. Debevc[95], D.V. Dedovich[40], J. Degens[94], A.M. Deiana[46], J. Del Peso[101], L. Delagrange[130], F. Deliot[138], C.M. Delitzsch[50], M. Della Pietra[73a,73b], D. Della Volpe[57], A. Dell'Acqua[37], L. Dell'Asta[72a,72b], M. Delmastro[4], C.C. Delogu[102], P.A. Delsart[61], S. Demers[176], M. Demichev[40], S.P. Denisov[39], H. Denizli[22a], L. D'Eramo[42], D. Derendarz[88], F. Derue[130], P. Dervan[94], K. Desch[25], C. Deutsch[25], F.A. Di Bello[58b,58a], A. Di Ciaccio[77a,77b], L. Di Ciaccio[4], A. Di Domenico[76a,76b], C. Di Donato[73a,73b], A. Di Girolamo[37], G. Di Gregorio[37], A. Di Luca[79a,79b], B. Di Micco[78a,78b], R. Di Nardo[78a,78b], K.F. Di Petrillo[41], M. Diamantopoulou[35], F.A. Dias[117], T. Dias Do Vale[146], M.A. Diaz[140a,140b], A.R. Didenko[40], M. Didenko[167], E.B. Diehl[108], S. Díez Cornell[49], C. Diez Pardos[145], C. Dimitriadi[148], A. Dimitrievska[21], A. Dimri[149], J. Dingfelder[25], T. Dingley[129], I-M. Dinu[28b], S.J. Dittmeier[64b], F. Dittus[37], M. Divisek[136], B. Dixit[94], F. Djama[104], T. Djobava[153b], C. Doglioni[103,100], A. Dohnalova[29a], Z. Dolezal[136], K. Domijan[87a], K.M. Dona[41], M. Donadelli[84d],

JHEP05(2025)075

B. Dong[109], J. Donini[42], A. D'Onofrio[73a,73b], M. D'Onofrio[94], J. Dopke[137], A. Doria[73a], N. Dos Santos Fernandes[133a], P. Dougan[103], M.T. Dova[92], A.T. Doyle[60], M.A. Draguet[129], M.P. Drescher[56], E. Dreyer[173], I. Drivas-koulouris[10], M. Drnevich[120], M. Drozdova[57], D. Du[63a], T.A. du Pree[117], F. Dubinin[39], M. Dubovsky[29a], E. Duchovni[173], G. Duckeck[111], O.A. Ducu[28b], D. Duda[53], A. Dudarev[37], E.R. Duden[27], M. D'uffizi[103], L. Duflot[67], M. Dührssen[37], I. Duminica[28g], A.E. Dumitriu[28b], M. Dunford[64a], S. Dungs[50], K. Dunne[48a,48b], A. Duperrin[104], H. Duran Yildiz[3a], M. Düren[59], A. Durglishvili[153b], D. Duvnjak[35], B.L. Dwyer[118], G.I. Dyckes[18a], M. Dyndal[87a], B.S. Dziedzic[37], Z.O. Earnshaw[150], G.H. Eberwein[129], B. Eckerova[29a], S. Eggebrecht[56], E. Egidio Purcino De Souza[84e], L.F. Ehrke[57], G. Eigen[17], K. Einsweiler[18a], T. Ekelof[165], P.A. Ekman[100], S. El Farkh[36b], Y. El Ghazali[63a], H. El Jarrari[37], A. El Moussaouy[36a], V. Ellajosyula[165], M. Ellert[165], F. Ellinghaus[175], N. Ellis[37], J. Elmsheuser[30], M. Elsawy[119a], M. Elsing[37], D. Emeliyanov[137], Y. Enari[85], I. Ene[18a], S. Epari[13], P.A. Erland[88], D. Ernani Martins Neto[88], M. Errenst[175], M. Escalier[67], C. Escobar[167], E. Etzion[155], G. Evans[133a,133b], H. Evans[69], L.S. Evans[97], A. Ezhilov[39], S. Ezzarqtouni[36a], F. Fabbri[24b,24a], L. Fabbri[24b,24a], G. Facini[98], V. Fadeyev[139], R.M. Fakhrutdinov[39], D. Fakoudis[102], S. Falciano[76a], L.F. Falda Ulhoa Coelho[133a], F. Fallavollita[112], G. Falsetti[45b,45a], J. Faltova[136], C. Fan[166], K.Y. Fan[65b], Y. Fan[14], Y. Fang[14,114c], M. Fanti[72a,72b], M. Faraj[70a,70b], Z. Farazpay[99], A. Farbin[8], A. Farilla[78a], T. Farooque[109], J.N. Farr[176], S.M. Farrington[137,53], F. Fassi[36e], D. Fassouliotis[9], M. Faucci Giannelli[77a,77b], W.J. Fawcett[33], L. Fayard[67], P. Federic[136], P. Federicova[134], O.L. Fedin[39,a], M. Feickert[174], L. Feligioni[104], D.E. Fellers[126], C. Feng[63b], Z. Feng[117], M.J. Fenton[162], L. Ferencz[49], R.A.M. Ferguson[93], P. Fernandez Martinez[68], M.J.V. Fernoux[104], J. Ferrando[93], A. Ferrari[165], P. Ferrari[117,116], R. Ferrari[74a], D. Ferrere[57], C. Ferretti[108], M.P. Fewell[1], D. Fiacco[76a,76b], F. Fiedler[102], P. Fiedler[135], S. Filimonov[39], A. Filipčič[95], E.K. Filmer[159a], F. Filthaut[116], M.C.N. Fiolhais[133a,133c,c], L. Fiorini[167], W.C. Fisher[109], T. Fitschen[103], P.M. Fitzhugh[138], I. Fleck[145], P. Fleischmann[108], T. Flick[175], M. Flores[34d,ad], L.R. Flores Castillo[65a], L. Flores Sanz De Acedo[37], F.M. Follega[79a,79b], N. Fomin[33], J.H. Foo[158], A. Formica[138], A.C. Forti[103], E. Fortin[37], A.W. Fortman[18a], L. Fountas[9,j], D. Fournier[67], H. Fox[93], P. Francavilla[75a,75b], S. Francescato[62], S. Franchellucci[57], M. Franchini[24b,24a], S. Franchino[64a], D. Francis[37], L. Franco[116], V. Franco Lima[37], L. Franconi[49], M. Franklin[62], G. Frattari[27], Y.Y. Frid[155], J. Friend[60], N. Fritzsche[37], A. Froch[57], D. Froidevaux[37], J.A. Frost[129], Y. Fu[109], S. Fuenzalida Garrido[140f], M. Fujimoto[104], K.Y. Fung[65a], E. Furtado De Simas Filho[84e], M. Furukawa[157], J. Fuster[167], A. Gaa[56], A. Gabrielli[24b,24a], A. Gabrielli[158], P. Gadow[37], G. Gagliardi[58b,58a], L.G. Gagnon[18a], S. Gaid[164], S. Galantzan[155], J. Gallagher[1], E.J. Gallas[129], A.L. Gallen[165], B.J. Gallop[137], K.K. Gan[122], S. Ganguly[157], Y. Gao[53], A. Garabaglu[142], F.M. Garay Walls[140a,140b], B. Garcia[30], C. García[167], A. Garcia Alonso[117], A.G. Garcia Caffaro[176], J.E. García Navarro[167], M. Garcia-Sciveres[18a], G.L. Gardner[131], R.W. Gardner[41], N. Garelli[161], R.B. Garg[147], J.M. Gargan[53], C.A. Garner[158], C.M. Garvey[34a], V.K. Gassmann[161], G. Gaudio[74a], V. Gautam[13], P. Gauzzi[76a,76b], J. Gavranovic[95], I.L. Gavrilenko[39], A. Gavrilyuk[39], C. Gay[168], G. Gaycken[126],

JHEP05(2025)075

E.N. Gazis[10], A. Gekow[122], C. Gemme[58b], M.H. Genest[61], A.D. Gentry[115], S. George[97], W.F. George[21], T. Geralis[47], A.A. Gerwin[123], P. Gessinger-Befurt[37], M.E. Geyik[175], M. Ghani[171], K. Ghorbanian[96], A. Ghosal[145], A. Ghosh[162], A. Ghosh[7], B. Giacobbe[24b], S. Giagu[76a,76b], T. Giani[117], A. Giannini[63a], S.M. Gibson[97], M. Gignac[139], D.T. Gil[87b], A.K. Gilbert[87a], B.J. Gilbert[43], D. Gillberg[35], G. Gilles[117], L. Ginabat[130], D.M. Gingrich[2,ag], M.P. Giordani[70a,70c], P.F. Giraud[138], G. Giugliarelli[70a,70c], D. Giugni[72a], F. Giuli[77a,77b], I. Gkialas[9,j], L.K. Gladilin[39], C. Glasman[101], G. Glemža[49], M. Glisic[126], I. Gnesi[45b], Y. Go[30], M. Goblirsch-Kolb[37], B. Gocke[50], D. Godin[110], B. Gokturk[22a], S. Goldfarb[107], T. Golling[57], M.G.D. Gololo[34c], D. Golubkov[39], J.P. Gombas[109], A. Gomes[133a,133b], G. Gomes Da Silva[145], A.J. Gomez Delegido[167], R. Gonçalo[133a], L. Gonella[21], A. Gongadze[153c], F. Gonnella[21], J.L. Gonski[147], R.Y. González Andana[53], S. González de la Hoz[167], R. Gonzalez Lopez[94], C. Gonzalez Renteria[18a], M.V. Gonzalez Rodrigues[49], R. Gonzalez Suarez[165], S. Gonzalez-Sevilla[57], L. Goossens[37], B. Gorini[37], E. Gorini[71a,71b], A. Gorišek[95], T.C. Gosart[131], A.T. Goshaw[52], M.I. Gostkin[40], S. Goswami[124], C.A. Gottardo[37], S.A. Gotz[111], M. Gouighri[36b], A.G. Goussiou[142], N. Govender[34c], R.P. Grabarczyk[129], I. Grabowska-Bold[87a], K. Graham[35], E. Gramstad[128], S. Grancagnolo[71a,71b], C.M. Grant[1,138], P.M. Gravila[28f], F.G. Gravili[71a,71b], H.M. Gray[18a], M. Greco[112], M.J. Green[1], C. Grefe[25], A.S. Grefsrud[17], I.M. Gregor[49], K.T. Greif[162], P. Grenier[147], S.G. Grewe[112], A.A. Grillo[139], K. Grimm[32], S. Grinstein[13,w], J.-F. Grivaz[67], E. Gross[173], J. Grosse-Knetter[56], L. Guan[108], J.G.R. Guerrero Rojas[167], G. Guerrieri[37], R. Gugel[102], J.A.M. Guhit[108], A. Guida[19], E. Guilloton[171], S. Guindon[37], F. Guo[14,114c], J. Guo[63c], L. Guo[49], L. Guo[114b,u], Y. Guo[108], A. Gupta[50], R. Gupta[132], S. Gurbuz[25], S.S. Gurdasani[49], G. Gustavino[76a,76b], P. Gutierrez[123], L.F. Gutierrez Zagazeta[131], M. Gutsche[51], C. Gutschow[98], C. Gwenlan[129], C.B. Gwilliam[94], E.S. Haaland[128], A. Haas[120], M. Habedank[60], C. Haber[18a], H.K. Hadavand[8], A. Hadef[51], A.I. Hagan[93], J.J. Hahn[145], E.H. Haines[98], M. Haleem[170], J. Haley[124], G.D. Hallewell[104], L. Halser[20], K. Hamano[169], M. Hamer[25], E.J. Hampshire[97], J. Han[63b], L. Han[114a], L. Han[63a], S. Han[18a], K. Hanagaki[85], M. Hance[139], D.A. Hangal[43], H. Hanif[146], M.D. Hank[131], J.B. Hansen[44], P.H. Hansen[44], D. Harada[57], T. Harenberg[175], S. Harkusha[177], M.L. Harris[105], Y.T. Harris[25], J. Harrison[13], N.M. Harrison[122], P.F. Harrison[171], N.M. Hartman[112], N.M. Hartmann[111], R.Z. Hasan[97,137], Y. Hasegawa[144], F. Haslbeck[129], S. Hassan[17], R. Hauser[109], C.M. Hawkes[21], R.J. Hawkings[37], Y. Hayashi[157], D. Hayden[109], C. Hayes[108], R.L. Hayes[117], C.P. Hays[129], J.M. Hays[96], H.S. Hayward[94], F. He[63a], M. He[14,114c], Y. He[49], Y. He[98], N.B. Heatley[96], V. Hedberg[100], A.L. Heggelund[128], C. Heidegger[55], K.K. Heidegger[55], J. Heilman[35], S. Heim[49], T. Heim[18a], J.G. Heinlein[131], J.J. Heinrich[126], L. Heinrich[112,ae], J. Hejbal[134], A. Held[174], S. Hellesund[17], C.M. Helling[168], S. Hellman[48a,48b], R.C.W. Henderson[93], L. Henkelmann[33], A.M. Henriques Correia[37], H. Herde[100], Y. Hernández Jiménez[149], L.M. Herrmann[25], T. Herrmann[51], G. Herten[55], R. Hertenberger[111], L. Hervas[37], M.E. Hesping[102], N.P. Hessey[159a], J. Hessler[112], M. Hidaoui[36b], N. Hidic[136], E. Hill[158], S.J. Hillier[21], J.R. Hinds[109], F. Hinterkeuser[25], M. Hirose[127], S. Hirose[160], D. Hirschbuehl[175], T.G. Hitchings[103], B. Hiti[95], J. Hobbs[149], R. Hobincu[28e], N. Hod[173],

JHEP05(2025)075

M.C. Hodgkinson[143], B.H. Hodkinson[129], A. Hoecker[37], D.D. Hofer[108], J. Hofer[167], M. Holzbock[37], L.B.A.H. Hommels[33], B.P. Honan[103], J.J. Hong[69], J. Hong[63c], T.M. Hong[132], B.H. Hooberman[166], W.H. Hopkins[6], M.C. Hoppesch[166], Y. Horii[113], M.E. Horstmann[112], S. Hou[152], M.R. Housenga[166], A.S. Howard[95], J. Howarth[60], J. Hoya[6], M. Hrabovsky[125], T. Hryn'ova[4], P.J. Hsu[66], S.-C. Hsu[142], T. Hsu[67], M. Hu[18a], Q. Hu[63a], S. Huang[33], X. Huang[14,114c], Y. Huang[143], Y. Huang[114b], Y. Huang[102], Y. Huang[14], Z. Huang[103], Z. Hubacek[135], M. Huebner[25], F. Huegging[25], T.B. Huffman[129], M. Hufnagel Maranha De Faria[84a], C.A. Hugli[49], M. Huhtinen[37], S.K. Huiberts[17], R. Hulsken[106], C.E. Hultquist[18a], N. Huseynov[12,g], J. Huston[109], J. Huth[62], R. Hyneman[7], G. Iacobucci[57], G. Iakovidis[30], L. Iconomidou-Fayard[67], J.P. Iddon[37], P. Iengo[73a,73b], R. Iguchi[157], Y. Iiyama[157], T. Iizawa[129], Y. Ikegami[85], D. Iliadis[156], N. Ilic[158], H. Imam[84c], G. Inacio Goncalves[84d], S.A. Infante Cabanas[140c], T. Ingebretsen Carlson[48a,48b], J.M. Inglis[96], G. Introzzi[74a,74b], M. Iodice[78a], V. Ippolito[76a,76b], R.K. Irwin[94], M. Ishino[157], W. Islam[174], C. Issever[19], S. Istin[22a,al], H. Ito[172], R. Iuppa[79a,79b], A. Ivina[173], V. Izzo[73a], P. Jacka[134], P. Jackson[1], C.S. Jagfeld[111], G. Jain[159a], P. Jain[49], K. Jakobs[55], T. Jakoubek[173], J. Jamieson[60], W. Jang[157], M. Javurkova[105], P. Jawahar[103], L. Jeanty[126], J. Jejelava[153a], P. Jenni[55,f], C.E. Jessiman[35], C. Jia[63b], H. Jia[168], J. Jia[149], X. Jia[14,114c], Z. Jia[114a], C. Jiang[53], Q. Jiang[65b], S. Jiggins[49], J. Jimenez Pena[13], S. Jin[114a], A. Jinaru[28b], O. Jinnouchi[141], P. Johansson[143], K.A. Johns[7], J.W. Johnson[139], F.A. Jolly[49], D.M. Jones[150], E. Jones[49], K.S. Jones[8], P. Jones[33], R.W.L. Jones[93], T.J. Jones[94], H.L. Joos[56,37], R. Joshi[122], J. Jovicevic[16], X. Ju[18a], J.J. Junggeburth[37], T. Junkermann[64a], A. Juste Rozas[13,w], M.K. Juzek[88], S. Kabana[140e], A. Kaczmarska[88], M. Kado[112], H. Kagan[122], M. Kagan[147], A. Kahn[131], C. Kahra[102], T. Kaji[157], E. Kajomovitz[154], N. Kakati[173], I. Kalaitzidou[55], N.J. Kang[139], D. Kar[34g], K. Karava[129], E. Karentzos[25], O. Karkout[117], S.N. Karpov[40], Z.M. Karpova[40], V. Kartvelishvili[93], A.N. Karyukhin[39], E. Kasimi[156], J. Katzy[49], S. Kaur[35], K. Kawade[144], M.P. Kawale[123], C. Kawamoto[89], T. Kawamoto[63a], E.F. Kay[37], F.I. Kaya[161], S. Kazakos[109], V.F. Kazanin[39], Y. Ke[149], J.M. Keaveney[34a], R. Keeler[169], G.V. Kehris[62], J.S. Keller[35], J.J. Kempster[150], O. Kepka[134], J. Kerr[159b], B.P. Kerridge[137], B.P. Kerševan[95], L. Keszeghova[29a], R.A. Khan[132], A. Khanov[124], A.G. Kharlamov[39], T. Kharlamova[39], E.E. Khoda[142], M. Kholodenko[133a], T.J. Khoo[19], G. Khoriauli[170], J. Khubua[153b,*], Y.A.R. Khwaira[130], B. Kibirige[34g], D. Kim[6], D.W. Kim[48a,48b], Y.K. Kim[41], N. Kimura[98], M.K. Kingston[56], A. Kirchhoff[56], C. Kirfel[25], F. Kirfel[25], J. Kirk[137], A.E. Kiryunin[112], S. Kita[160], C. Kitsaki[10], O. Kivernyk[25], M. Klassen[161], C. Klein[35], L. Klein[170], M.H. Klein[46], S.B. Klein[57], U. Klein[94], A. Klimentov[30], T. Klioutchnikova[37], P. Kluit[117], S. Kluth[112], E. Kneringer[80], T.M. Knight[158], A. Knue[50], M. Kobel[51], D. Kobylianskii[173], S.F. Koch[129], M. Kocian[147], P. Kodyš[136], D.M. Koeck[126], P.T. Koenig[25], T. Koffas[35], O. Kolay[51], I. Koletsou[4], T. Komarek[88], K. Köneke[56], A.X.Y. Kong[1], T. Kono[121], N. Konstantinidis[98], P. Kontaxakis[57], B. Konya[100], R. Kopeliansky[43], S. Koperny[87a], K. Korcyl[88], K. Kordas[156,e], A. Korn[98], S. Korn[56], I. Korolkov[13], N. Korotkova[39], B. Kortman[117], O. Kortner[112], S. Kortner[112], W.H. Kostecka[118], V.V. Kostyukhin[145], A. Kotsokechagia[37], A. Kotwal[52], A. Koulouris[37], A. Kourkoumeli-Charalampidi[74a,74b],

JHEP05(2025)075

C. Kourkoumelis[9], E. Kourlitis[112], O. Kovanda[126], R. Kowalewski[169], W. Kozanecki[126], A.S. Kozhin[39], V.A. Kramarenko[39], G. Kramberger[95], P. Kramer[25], M.W. Krasny[130], A. Krasznahorkay[105], A.C. Kraus[118], J.W. Kraus[175], J.A. Kremer[49], T. Kresse[51], L. Kretschmann[175], J. Kretzschmar[94], K. Kreul[19], P. Krieger[158], K. Krizka[21], K. Kroeninger[50], H. Kroha[112], J. Kroll[134], J. Kroll[131], K.S. Krowpman[109], U. Kruchonak[40], H. Krüger[25], N. Krumnack[82], M.C. Kruse[52], O. Kuchinskaia[39], S. Kuday[3a], S. Kuehn[37], R. Kuesters[55], T. Kuhl[49], V. Kukhtin[40], Y. Kulchitsky[40], S. Kuleshov[140d,140b], M. Kumar[34g], N. Kumari[49], P. Kumari[159b], A. Kupco[134], T. Kupfer[50], A. Kupich[39], O. Kuprash[55], H. Kurashige[86], L.L. Kurchaninov[159a], O. Kurdysh[67], Y.A. Kurochkin[38], A. Kurova[39], M. Kuze[141], A.K. Kvam[105], J. Kvita[125], N.G. Kyriacou[108], L.A.O. Laatu[104], C. Lacasta[167], F. Lacava[76a,76b], H. Lacker[19], D. Lacour[130], N.N. Lad[98], E. Ladygin[40], A. Lafarge[42], B. Laforge[130], T. Lagouri[176], F.Z. Lahbabi[36a], S. Lai[56], J.E. Lambert[169], S. Lammers[69], W. Lampl[7], C. Lampoudis[156,e], G. Lamprinoudis[102], A.N. Lancaster[118], E. Lançon[30], U. Landgraf[55], M.P.J. Landon[96], V.S. Lang[55], O.K.B. Langrekken[128], A.J. Lankford[162], F. Lanni[37], K. Lantzsch[25], A. Lanza[74a], M. Lanzac Berrocal[167], J.F. Laporte[138], T. Lari[72a], F. Lasagni Manghi[24b], M. Lassnig[37], V. Latonova[134], S.D. Lawlor[143], Z. Lawrence[103], R. Lazaridou[171], M. Lazzaroni[72a,72b], H.D.M. Le[109], E.M. Le Boulicaut[176], L.T. Le Pottier[18a], B. Leban[24b,24a], M. LeBlanc[103], F. Ledroit-Guillon[61], S.C. Lee[152], T.F. Lee[94], L.L. Leeuw[34c,aj], M. Lefebvre[169], C. Leggett[18a], G. Lehmann Miotto[37], M. Leigh[57], W.A. Leight[105], W. Leinonen[116], A. Leisos[156,t], M.A.L. Leite[84c], C.E. Leitgeb[19], R. Leitner[136], K.J.C. Leney[46], T. Lenz[25], S. Leone[75a], C. Leonidopoulos[53], A. Leopold[148], J.H. Lepage Bourbonnais[35], R. Les[109], C.G. Lester[33], M. Levchenko[39], J. Levêque[4], L.J. Levinson[173], G. Levrini[24b,24a], M.P. Lewicki[88], C. Lewis[142], D.J. Lewis[4], L. Lewitt[143], A. Li[30], B. Li[63b], C. Li[108], C-Q. Li[112], H. Li[63a], H. Li[63b], H. Li[114a], H. Li[15], H. Li[63b], J. Li[63c], K. Li[14], L. Li[63c], R. Li[176], S. Li[14,114c], S. Li[63d,63c,d], T. Li[5], X. Li[106], Z. Li[157], Z. Li[14,114c], Z. Li[63a], S. Liang[14,114c], Z. Liang[14], M. Liberatore[138], B. Liberti[77a], K. Lie[65c], J. Lieber Marin[84e], H. Lien[69], H. Lin[108], L. Linden[111], R.E. Lindley[7], J.H. Lindon[2], J. Ling[62], E. Lipeles[131], A. Lipniacka[17], A. Lister[168], J.D. Little[69], B. Liu[14], B.X. Liu[114b], D. Liu[63d,63c], E.H.L. Liu[21], J.K.K. Liu[33], K. Liu[63d], K. Liu[63d,63c], M. Liu[63a], M.Y. Liu[63a], P. Liu[14], Q. Liu[63d,142,63c], X. Liu[63a], X. Liu[63b], Y. Liu[114b,114c], Y.L. Liu[63b], Y.W. Liu[63a], S.L. Lloyd[96], E.M. Lobodzinska[49], P. Loch[7], E. Lodhi[158], T. Lohse[19], K. Lohwasser[143], E. Loiacono[49], J.D. Lomas[21], J.D. Long[43], I. Longarini[162], R. Longo[166], A. Lopez Solis[49], N.A. Lopez-canelas[7], N. Lorenzo Martinez[4], A.M. Lory[111], M. Losada[119a], G. Löschcke Centeno[150], O. Loseva[39], X. Lou[48a,48b], X. Lou[14,114c], A. Lounis[67], P.A. Love[93], G. Lu[14,114c], M. Lu[67], S. Lu[131], Y.J. Lu[152], H.J. Lubatti[142], C. Luci[76a,76b], F.L. Lucio Alves[114a], F. Luehring[69], O. Lukianchuk[67], B.S. Lunday[131], O. Lundberg[148], B. Lund-Jensen[148,*], N.A. Luongo[6], M.S. Lutz[37], A.B. Lux[26], D. Lynn[30], R. Lysak[134], E. Lytken[100], V. Lyubushkin[40], T. Lyubushkina[40], M.M. Lyukova[149], M.Firdaus M. Soberi[53], H. Ma[30], K. Ma[63a], L.L. Ma[63b], W. Ma[63a], Y. Ma[124], J.C. MacDonald[102], P.C. Machado De Abreu Farias[84e], R. Madar[42], T. Madula[98], J. Maeda[86], T. Maeno[30], P.T. Mafa[34c,k], H. Maguire[143], V. Maiboroda[138],

JHEP05(2025)075

A. Maio[133a,133b,133d], K. Maj[87a], O. Majersky[49], S. Majewski[126], R. Makhmanazarov[39], N. Makovec[67], V. Maksimovic[16], B. Malaescu[130], Pa. Malecki[88], V.P. Maleev[39], F. Malek[61,o], M. Mali[95], D. Malito[97], U. Mallik[81,*], S. Maltezos[10], S. Malyukov[40], J. Mamuzic[13], G. Mancini[54], M.N. Mancini[27], G. Manco[74a,74b], J.P. Mandalia[96], S.S. Mandarry[150], I. Mandić[95], L. Manhaes de Andrade Filho[84a], I.M. Maniatis[173], J. Manjarres Ramos[91], D.C. Mankad[173], A. Mann[111], S. Manzoni[37], L. Mao[63c], X. Mapekula[34c], A. Marantis[156,t], G. Marchiori[5], M. Marcisovsky[134], C. Marcon[72a], M. Marinescu[21], S. Marium[49], M. Marjanovic[123], A. Markhoos[55], M. Markovitch[67], M.K. Maroun[105], E.J. Marshall[93], Z. Marshall[18a], S. Marti-Garcia[167], J. Martin[98], T.A. Martin[137], V.J. Martin[53], B. Martin dit Latour[17], L. Martinelli[76a,76b], M. Martinez[13,w], P. Martinez Agullo[167], V.I. Martinez Outschoorn[105], P. Martinez Suarez[13], S. Martin-Haugh[137], G. Martinovicova[136], V.S. Martoiu[28b], A.C. Martyniuk[98], A. Marzin[37], D. Mascione[79a,79b], L. Masetti[102], J. Masik[103], A.L. Maslennikov[39], S.L. Mason[43], P. Massarotti[73a,73b], P. Mastrandrea[75a,75b], A. Mastroberardino[45b,45a], T. Masubuchi[127], T.T. Mathew[126], J. Matousek[136], D.M. Mattern[50], J. Maurer[28b], T. Maurin[60], A.J. Maury[67], B. Maček[95], D.A. Maximov[39], A.E. May[103], R. Mazini[34g], I. Maznas[118], M. Mazza[109], S.M. Mazza[139], E. Mazzeo[72a,72b], J.P. Mc Gowan[169], S.P. Mc Kee[108], C.A. Mc Lean[6], C.C. McCracken[168], E.F. McDonald[107], A.E. McDougall[117], L.F. Mcelhinney[93], J.A. Mcfayden[150], R.P. McGovern[131], R.P. Mckenzie[34g], T.C. Mclachlan[49], D.J. Mclaughlin[98], S.J. McMahon[137], C.M. Mcpartland[94], R.A. McPherson[169,aa], S. Mehlhase[111], A. Mehta[94], D. Melini[167], B.R. Mellado Garcia[34g], A.H. Melo[56], F. Meloni[49], A.M. Mendes Jacques Da Costa[103], H.Y. Meng[158], L. Meng[93], S. Menke[112], M. Mentink[37], E. Meoni[45b,45a], G. Mercado[118], S. Merianos[156], C. Merlassino[70a,70c], C. Meroni[72a,72b], J. Metcalfe[6], A.S. Mete[6], E. Meuser[102], C. Meyer[69], J-P. Meyer[138], R.P. Middleton[137], L. Mijović[53], G. Mikenberg[173], M. Mikestikova[134], M. Mikuž[95], H. Mildner[102], A. Milic[37], D.W. Miller[41], E.H. Miller[147], L.S. Miller[35], A. Milov[173], D.A. Milstead[48a,48b], T. Min[114a], A.A. Minaenko[39], I.A. Minashvili[153b], A.I. Mincer[120], B. Mindur[87a], M. Mineev[40], Y. Mino[89], L.M. Mir[13], M. Miralles Lopez[60], M. Mironova[18a], M.C. Missio[116], A. Mitra[171], V.A. Mitsou[167], Y. Mitsumori[113], O. Miu[158], P.S. Miyagawa[96], T. Mkrtchyan[64a], M. Mlinarevic[98], T. Mlinarevic[98], M. Mlynarikova[37], S. Mobius[20], P. Mogg[111], M.H. Mohamed Farook[115], A.F. Mohammed[14,114c], S. Mohapatra[43], G. Mokgatitswane[34g], L. Moleri[173], B. Mondal[145], S. Mondal[135], K. Mönig[49], E. Monnier[104], L. Monsonis Romero[167], J. Montejo Berlingen[13], A. Montella[48a,48b], M. Montella[122], F. Montereali[78a,78b], F. Monticelli[92], S. Monzani[70a,70c], A. Morancho Tarda[44], N. Morange[67], A.L. Moreira De Carvalho[49], M. Moreno Llácer[167], C. Moreno Martinez[57], J.M. Moreno Perez[23b], P. Morettini[58b], S. Morgenstern[37], M. Morii[62], M. Morinaga[157], M. Moritsu[90], F. Morodei[76a,76b], P. Moschovakos[37], B. Moser[129], M. Mosidze[153b], T. Moskalets[46], P. Moskvitina[116], J. Moss[32,l], P. Moszkowicz[87a], A. Moussa[36d], Y. Moyal[173], E.J.W. Moyse[105], O. Mtintsilana[34g], S. Muanza[104], J. Mueller[132], D. Muenstermann[93], R. Müller[37], G.A. Mullier[165], A.J. Mullin[33], J.J. Mullin[131], A.E. Mulski[62], D.P. Mungo[158], D. Munoz Perez[167], F.J. Munoz Sanchez[103], M. Murin[103], W.J. Murray[171,137], M. Muškinja[95], C. Mwewa[30], A.G. Myagkov[39,a],

JHEP05(2025)075

A.J. Myers[8], G. Myers[108], M. Myska[135], B.P. Nachman[18a], K. Nagai[129], K. Nagano[85], R. Nagasaka[157], J.L. Nagle[30,ai], E. Nagy[104], A.M. Nairz[37], Y. Nakahama[85], K. Nakamura[85], K. Nakkalil[5], H. Nanjo[127], E.A. Narayanan[46], Y. Narukawa[157], I. Naryshkin[39], L. Nasella[72a,72b], S. Nasri[119b], C. Nass[25], G. Navarro[23a], J. Navarro-Gonzalez[167], A. Nayaz[19], P.Y. Nechaeva[39], S. Nechaeva[24b,24a], F. Nechansky[134], L. Nedic[129], T.J. Neep[21], A. Negri[74a,74b], M. Negrini[24b], C. Nellist[117], C. Nelson[106], K. Nelson[108], S. Nemecek[134], M. Nessi[37,h], M.S. Neubauer[166], F. Neuhaus[102], J. Newell[94], P.R. Newman[21], Y.W.Y. Ng[166], B. Ngair[119a], H.D.N. Nguyen[110], R.B. Nickerson[129], R. Nicolaidou[138], J. Nielsen[139], M. Niemeyer[56], J. Niermann[37], N. Nikiforou[37], V. Nikolaenko[39,a], I. Nikolic-Audit[130], P. Nilsson[30], I. Ninca[49], G. Ninio[155], A. Nisati[76a], N. Nishu[2], R. Nisius[112], N. Nitika[70a,70c], J-E. Nitschke[51], E.K. Nkadimeng[34g], T. Nobe[157], T. Nommensen[151], M.B. Norfolk[143], B.J. Norman[35], M. Noury[36a], J. Novak[95], T. Novak[95], R. Novotny[115], L. Nozka[125], K. Ntekas[162], N.M.J. Nunes De Moura Junior[84b], J. Ocariz[130], A. Ochi[86], I. Ochoa[133a], S. Oerdek[49,x], J.T. Offermann[41], A. Ogrodnik[136], A. Oh[103], C.C. Ohm[148], H. Oide[85], R. Oishi[157], M.L. Ojeda[37], Y. Okumura[157], L.F. Oleiro Seabra[133a], I. Oleksiyuk[57], S.A. Olivares Pino[140d], G. Oliveira Correa[13], D. Oliveira Damazio[30], J.L. Oliver[162], Ö.O. Öncel[55], A.P. O'Neill[20], A. Onofre[133a,133e], P.U.E. Onyisi[11], M.J. Oreglia[41], D. Orestano[78a,78b], R.S. Orr[158], L.M. Osojnak[131], Y. Osumi[113], G. Otero y Garzon[31], H. Otono[90], P.S. Ott[64a], G.J. Ottino[18a], M. Ouchrif[36d], F. Ould-Saada[128], T. Ovsiannikova[142], M. Owen[60], R.E. Owen[137], V.E. Ozcan[22a], F. Ozturk[88], N. Ozturk[8], S. Ozturk[83], H.A. Pacey[129], A. Pacheco Pages[13], C. Padilla Aranda[13], G. Padovano[76a,76b], S. Pagan Griso[18a], G. Palacino[69], A. Palazzo[71a,71b], J. Pampel[25], J. Pan[176], T. Pan[65a], D.K. Panchal[11], C.E. Pandini[117], J.G. Panduro Vazquez[137], H.D. Pandya[1], H. Pang[138], P. Pani[49], G. Panizzo[70a,70c], L. Panwar[130], L. Paolozzi[57], S. Parajuli[166], A. Paramonov[6], C. Paraskevopoulos[54], D. Paredes Hernandez[65b], A. Pareti[74a,74b], K.R. Park[43], T.H. Park[112], F. Parodi[58b,58a], J.A. Parsons[43], U. Parzefall[55], B. Pascual Dias[110], L. Pascual Dominguez[101], E. Pasqualucci[76a], S. Passaggio[58b], F. Pastore[97], P. Patel[88], U.M. Patel[52], J.R. Pater[103], T. Pauly[37], F. Pauwels[136], C.I. Pazos[161], M. Pedersen[128], R. Pedro[133a], S.V. Peleganchuk[39], O. Penc[37], E.A. Pender[53], S. Peng[15], G.D. Penn[176], K.E. Penski[111], M. Penzin[39], B.S. Peralva[84d], A.P. Pereira Peixoto[142], L. Pereira Sanchez[147], D.V. Perepelitsa[30,ai], G. Perera[105], E. Perez Codina[159a], M. Perganti[10], H. Pernegger[37], S. Perrella[76a,76b], O. Perrin[42], K. Peters[49], R.F.Y. Peters[103], B.A. Petersen[37], T.C. Petersen[44], E. Petit[104], V. Petousis[135], C. Petridou[156,e], T. Petru[136], A. Petrukhin[145], M. Pettee[18a], A. Petukhov[83], K. Petukhova[37], R. Pezoa[140f], L. Pezzotti[37], G. Pezzullo[176], A.J. Pfleger[37], T.M. Pham[174], T. Pham[107], P.W. Phillips[137], G. Piacquadio[149], E. Pianori[18a], F. Piazza[126], R. Piegaia[31], D. Pietreanu[28b], A.D. Pilkington[103], M. Pinamonti[70a,70c], J.L. Pinfold[2], B.C. Pinheiro Pereira[133a], J. Pinol Bel[13], A.E. Pinto Pinoargote[138,138], L. Pintucci[70a,70c], K.M. Piper[150], A. Pirttikoski[57], D.A. Pizzi[35], L. Pizzimento[65b], M.-A. Pleier[30], V. Pleskot[136], E. Plotnikova[40], G. Poddar[96], R. Poettgen[100], L. Poggioli[130], S. Polacek[136], G. Polesello[74a], A. Poley[146,159a], A. Polini[24b], C.S. Pollard[171], Z.B. Pollock[122], E. Pompa Pacchi[123], N.I. Pond[98], D. Ponomarenko[69],

JHEP05(2025)075

L. Pontecorvo[37], S. Popa[28a], G.A. Popeneciu[28d], A. Poreba[37], D.M. Portillo Quintero[159a], S. Pospisil[135], M.A. Postill[143], P. Postolache[28c], K. Potamianos[171], P.A. Potepa[87a], I.N. Potrap[40], C.J. Potter[33], H. Potti[151], J. Poveda[167], M.E. Pozo Astigarraga[37], A. Prades Ibanez[77a,77b], J. Pretel[169], D. Price[103], M. Primavera[71a], L. Primomo[70a,70c], M.A. Principe Martin[101], R. Privara[125], T. Procter[60], M.L. Proffitt[142], N. Proklova[131], K. Prokofiev[65c], G. Proto[112], J. Proudfoot[6], M. Przybycien[87a], W.W. Przygoda[87b], A. Psallidas[47], J.E. Puddefoot[143], D. Pudzha[55], D. Pyatiizbyantseva[39], J. Qian[108], R. Qian[109], D. Qichen[103], Y. Qin[13], T. Qiu[53], A. Quadt[56], M. Queitsch-Maitland[103], G. Quetant[57], R.P. Quinn[168], G. Rabanal Bolanos[62], D. Rafanoharana[55], F. Raffaeli[77a,77b], F. Ragusa[72a,72b], J.L. Rainbolt[41], J.A. Raine[57], S. Rajagopalan[30], E. Ramakoti[39], L. Rambelli[58b,58a], I.A. Ramirez-Berend[35], K. Ran[49,114c], D.S. Rankin[131], N.P. Rapheeha[34g], H. Rasheed[28b], V. Raskina[130], D.F. Rassloff[64a], A. Rastogi[18a], S. Rave[102], S. Ravera[58b,58a], B. Ravina[37], I. Ravinovich[173], M. Raymond[37], A.L. Read[128], N.P. Readioff[143], D.M. Rebuzzi[74a,74b], A.S. Reed[112], K. Reeves[27], J.A. Reidelsturz[175], D. Reikher[126], A. Rej[50], C. Rembser[37], H. Ren[63a], M. Renda[28b], F. Renner[49], A.G. Rennie[162], A.L. Rescia[49], S. Resconi[72a], M. Ressegotti[58b,58a], S. Rettie[37], W.F. Rettie[35], J.G. Reyes Rivera[109], E. Reynolds[18a], O.L. Rezanova[39], P. Reznicek[136], H. Riani[36d], N. Ribaric[52], E. Ricci[79a,79b], R. Richter[112], S. Richter[48a,48b], E. Richter-Was[87b], M. Ridel[130], S. Ridouani[36d], P. Rieck[120], P. Riedler[37], E.M. Riefel[48a,48b], J.O. Rieger[117], M. Rijssenbeek[149], M. Rimoldi[37], L. Rinaldi[24b,24a], P. Rincke[56], M.P. Rinnagel[111], G. Ripellino[165], I. Riu[13], J.C. Rivera Vergara[169], F. Rizatdinova[124], E. Rizvi[96], B.R. Roberts[18a], S.S. Roberts[139], D. Robinson[33], M. Robles Manzano[102], A. Robson[60], A. Rocchi[77a,77b], C. Roda[75a,75b], S. Rodriguez Bosca[37], Y. Rodriguez Garcia[23a], A.M. Rodríguez Vera[118], S. Roe[37], J.T. Roemer[37], O. Røhne[128], R.A. Rojas[37], C.P.A. Roland[130], J. Roloff[30], A. Romaniouk[80], E. Romano[74a,74b], M. Romano[24b], A.C. Romero Hernandez[166], N. Rompotis[94], L. Roos[130], S. Rosati[76a], B.J. Rosser[41], E. Rossi[129], E. Rossi[73a,73b], L.P. Rossi[62], L. Rossini[55], R. Rosten[122], M. Rotaru[28b], B. Rottler[55], C. Rougier[91], D. Rousseau[67], D. Rousso[49], S. Roy-Garand[158], A. Rozanov[104], Z.M.A. Rozario[60], Y. Rozen[154], A. Rubio Jimenez[167], V.H. Ruelas Rivera[19], T.A. Ruggeri[1], A. Ruggiero[129], A. Ruiz-Martinez[167], A. Rummler[37], Z. Rurikova[55], N.A. Rusakovich[40], H.L. Russell[169], G. Russo[76a,76b], J.P. Rutherfoord[7], S. Rutherford Colmenares[33], M. Rybar[136], E.B. Rye[128], A. Ryzhov[46], J.A. Sabater Iglesias[57], H.F-W. Sadrozinski[139], F. Safai Tehrani[76a], S. Saha[1], M. Sahinsoy[83], A. Saibel[167], M. Saimpert[138], M. Saito[157], T. Saito[157], A. Sala[72a,72b], D. Salamani[37], A. Salnikov[147], J. Salt[167], A. Salvador Salas[155], D. Salvatore[45b,45a], F. Salvatore[150], A. Salzburger[37], D. Sammel[55], E. Sampson[93], D. Sampsonidis[156,e], D. Sampsonidou[126], J. Sánchez[167], V. Sanchez Sebastian[167], H. Sandaker[128], C.O. Sander[49], J.A. Sandesara[105], M. Sandhoff[175], C. Sandoval[23b], L. Sanfilippo[64a], D.P.C. Sankey[137], T. Sano[89], A. Sansoni[54], L. Santi[37,76b], C. Santoni[42], H. Santos[133a,133b], A. Santra[173], E. Sanzani[24b,24a], K.A. Saoucha[164], J.G. Saraiva[133a,133d], J. Sardain[7], O. Sasaki[85], K. Sato[160], C. Sauer[37], E. Sauvan[4], P. Savard[158,ag], R. Sawada[157], C. Sawyer[137], L. Sawyer[99], C. Sbarra[24b], A. Sbrizzi[24b,24a], T. Scanlon[98], J. Schaarschmidt[142], U. Schäfer[102], A.C. Schaffer[67,46], D. Schaile[111], R.D. Schamberger[149],

JHEP05(2025)075

C. Scharf[19], M.M. Schefer[20], V.A. Schegelsky[39], D. Scheirich[136], M. Schernau[140e], C. Scheulen[57], C. Schiavi[58b,58a], M. Schioppa[45b,45a], B. Schlag[147], S. Schlenker[37], J. Schmeing[175], M.A. Schmidt[175], K. Schmieden[102], C. Schmitt[102], N. Schmitt[102], S. Schmitt[49], L. Schoeffel[138], A. Schoening[64b], P.G. Scholer[35], E. Schopf[129], M. Schott[25], J. Schovancova[37], S. Schramm[57], T. Schroer[57], H-C. Schultz-Coulon[64a], M. Schumacher[55], B.A. Schumm[139], Ph. Schune[138], H.R. Schwartz[139], A. Schwartzman[147], T.A. Schwarz[108], Ph. Schwemling[138], R. Schwienhorst[109], F.G. Sciacca[20], A. Sciandra[30], G. Sciolla[27], F. Scuri[75a], C.D. Sebastiani[94], K. Sedlaczek[118], S.C. Seidel[115], A. Seiden[139], B.D. Seidlitz[43], C. Seitz[49], J.M. Seixas[84b], G. Sekhniaidze[73a], L. Selem[61], N. Semprini-Cesari[24b,24a], A. Semushin[177,39], D. Sengupta[57], V. Senthilkumar[167], L. Serin[67], M. Sessa[77a,77b], H. Severini[123], F. Sforza[58b,58a], A. Sfyrla[57], Q. Sha[14], E. Shabalina[56], H. Shaddix[118], A.H. Shah[33], R. Shaheen[148], J.D. Shahinian[131], D. Shaked Renous[173], L.Y. Shan[14], M. Shapiro[18a], A. Sharma[37], A.S. Sharma[168], P. Sharma[30], P.B. Shatalov[39], K. Shaw[150], S.M. Shaw[103], Q. Shen[63c], D.J. Sheppard[146], P. Sherwood[98], L. Shi[98], X. Shi[14], S. Shimizu[85], C.O. Shimmin[176], I.P.J. Shipsey[129,*], S. Shirabe[90], M. Shiyakova[40,y], M.J. Shochet[41], D.R. Shope[128], B. Shrestha[123], S. Shrestha[122,ak], I. Shreyber[39], M.J. Shroff[169], P. Sicho[134], A.M. Sickles[166], E. Sideras Haddad[34g,163], A.C. Sidley[117], A. Sidoti[24b], F. Siegert[51], Dj. Sijacki[16], F. Sili[92], J.M. Silva[53], I. Silva Ferreira[84b], M.V. Silva Oliveira[30], S.B. Silverstein[48a], S. Simion[67], R. Simoniello[37], E.L. Simpson[103], H. Simpson[150], L.R. Simpson[108], S. Simsek[83], S. Sindhu[56], P. Sinervo[158], S.N. Singh[27], S. Singh[30], S. Sinha[49], S. Sinha[103], M. Sioli[24b,24a], I. Siral[37], E. Sitnikova[49], J. Sjölin[48a,48b], A. Skaf[56], E. Skorda[21], P. Skubic[123], M. Slawinska[88], I. Slazyk[17], V. Smakhtin[173], B.H. Smart[137], S.Yu. Smirnov[39], Y. Smirnov[39], L.N. Smirnova[39,a], O. Smirnova[100], A.C. Smith[43], D.R. Smith[162], E.A. Smith[41], J.L. Smith[103], M.B. Smith[35], R. Smith[147], H. Smitmanns[102], M. Smizanska[93], K. Smolek[135], A.A. Snesarev[39], H.L. Snoek[117], S. Snyder[30], R. Sobie[169,aa], A. Soffer[155], C.A. Solans Sanchez[37], E.Yu. Soldatov[39], U. Soldevila[167], A.A. Solodkov[39], S. Solomon[27], A. Soloshenko[40], K. Solovieva[55], O.V. Solovyanov[42], P. Sommer[51], A. Sonay[13], W.Y. Song[159b], A. Sopczak[135], A.L. Sopio[53], F. Sopkova[29b], J.D. Sorenson[115], I.R. Sotarriva Alvarez[141], V. Sothilingam[64a], O.J. Soto Sandoval[140c,140b], S. Sottocornola[69], R. Soualah[164], Z. Soumaimi[36e], D. South[49], N. Soybelman[173], S. Spagnolo[71a,71b], M. Spalla[112], D. Sperlich[55], B. Spisso[73a,73b], D.P. Spiteri[60], M. Spousta[136], E.J. Staats[35], R. Stamen[64a], E. Stanecka[88], W. Stanek-Maslouska[49], M.V. Stange[51], B. Stanislaus[18a], M.M. Stanitzki[49], B. Stapf[49], E.A. Starchenko[39], G.H. Stark[139], J. Stark[91], P. Staroba[134], P. Starovoitov[164], R. Staszewski[88], G. Stavropoulos[47], A. Stefl[37], P. Steinberg[30], B. Stelzer[146,159a], H.J. Stelzer[132], O. Stelzer-Chilton[159a], H. Stenzel[59], T.J. Stevenson[150], G.A. Stewart[37], J.R. Stewart[124], M.C. Stockton[37], G. Stoicea[28b], M. Stolarski[133a], S. Stonjek[112], A. Straessner[51], J. Strandberg[148], S. Strandberg[48a,48b], M. Stratmann[175], M. Strauss[123], T. Strebler[104], P. Strizenec[29b], R. Ströhmer[170], D.M. Strom[126], R. Stroynowski[46], A. Strubig[48a,48b], S.A. Stucci[30], B. Stugu[17], J. Stupak[123], N.A. Styles[49], D. Su[147], S. Su[63a], W. Su[63d], X. Su[63a], D. Suchy[29a], K. Sugizaki[157], V.V. Sulin[39], M.J. Sullivan[94], D.M.S. Sultan[129], L. Sultanaliyeva[39], S. Sultansoy[3b], S. Sun[174], W. Sun[14], O. Sunneborn Gudnadottir[165],

JHEP05(2025)075

N. Sur[104], M.R. Sutton[150], H. Suzuki[160], M. Svatos[134], M. Swiatlowski[159a], T. Swirski[170], I. Sykora[29a], M. Sykora[136], T. Sykora[136], D. Ta[102], K. Tackmann[49,x], A. Taffard[162], R. Tafirout[159a], J.S. Tafoya Vargas[67], Y. Takubo[85], M. Talby[104], A.A. Talyshev[39], K.C. Tam[65b], N.M. Tamir[155], A. Tanaka[157], J. Tanaka[157], R. Tanaka[67], M. Tanasini[149], Z. Tao[168], S. Tapia Araya[140f], S. Tapprogge[102], A. Tarek Abouelfadl Mohamed[109], S. Tarem[154], K. Tariq[14], G. Tarna[28b], G.F. Tartarelli[72a], M.J. Tartarin[91], P. Tas[136], M. Tasevsky[134], E. Tassi[45b,45a], A.C. Tate[166], G. Tateno[157], Y. Tayalati[36e,z], G.N. Taylor[107], W. Taylor[159b], P. Teixeira-Dias[97], J.J. Teoh[158], K. Terashi[157], J. Terron[101], S. Terzo[13], M. Testa[54], R.J. Teuscher[158,aa], A. Thaler[80], O. Theiner[57], T. Theveneaux-Pelzer[104], O. Thielmann[175], D.W. Thomas[97], J.P. Thomas[21], E.A. Thompson[18a], P.D. Thompson[21], E. Thomson[131], R.E. Thornberry[46], C. Tian[63a], Y. Tian[57], V. Tikhomirov[39,a], Yu.A. Tikhonov[39], S. Timoshenko[39], D. Timoshyn[136], E.X.L. Ting[1], P. Tipton[176], A. Tishelman-Charny[30], S.H. Tlou[34g], K. Todome[141], S. Todorova-Nova[136], S. Todt[51], L. Toffolin[70a,70c], M. Togawa[85], J. Tojo[90], S. Tokár[29a], O. Toldaiev[69], G. Tolkachev[104], M. Tomoto[85,113], L. Tompkins[147,n], E. Torrence[126], H. Torres[91], E. Torró Pastor[167], M. Toscani[31], C. Tosciri[41], M. Tost[11], D.R. Tovey[143], T. Trefzger[170], A. Tricoli[30], I.M. Trigger[159a], S. Trincaz-Duvoid[130], D.A. Trischuk[27], A. Tropina[40], L. Truong[34c], M. Trzebinski[88], A. Trzupek[88], F. Tsai[149], M. Tsai[108], A. Tsiamis[156], P.V. Tsiareshka[40], S. Tsigaridas[159a], A. Tsirigotis[156,t], V. Tsiskaridze[158], E.G. Tskhadadze[153a], M. Tsopoulou[156], Y. Tsujikawa[89], I.I. Tsukerman[39], V. Tsulaia[18a], S. Tsuno[85], K. Tsuri[121], D. Tsybychev[149], Y. Tu[65b], A. Tudorache[28b], V. Tudorache[28b], S. Turchikhin[58b,58a], I. Turk Cakir[3a], R. Turra[72a], T. Turtuvshin[40,ab], P.M. Tuts[43], S. Tzamarias[156,e], E. Tzovara[102], F. Ukegawa[160], P.A. Ulloa Poblete[140c,140b], E.N. Umaka[30], G. Unal[37], A. Undrus[30], G. Unel[162], J. Urban[29b], P. Urrejola[140a], G. Usai[8], R. Ushioda[141], M. Usman[110], F. Ustuner[53], Z. Uysal[83], V. Vacek[135], B. Vachon[106], T. Vafeiadis[37], A. Vaitkus[98], C. Valderanis[111], E. Valdes Santurio[48a,48b], M. Valente[159a], S. Valentinetti[24b,24a], A. Valero[167], E. Valiente Moreno[167], A. Vallier[91], J.A. Valls Ferrer[167], D.R. Van Arneman[117], T.R. Van Daalen[142], A. Van Der Graaf[50], P. Van Gemmeren[6], M. Van Rijnbach[37], S. Van Stroud[98], I. Van Vulpen[117], P. Vana[136], M. Vanadia[77a,77b], U.M. Vande Voorde[148], W. Vandelli[37], E.R. Vandewall[124], D. Vannicola[155], L. Vannoli[54], R. Vari[76a], E.W. Varnes[7], C. Varni[18b], D. Varouchas[67], L. Varriale[167], K.E. Varvell[151], M.E. Vasile[28b], L. Vaslin[85], A. Vasyukov[40], L.M. Vaughan[124], R. Vavricka[102], T. Vazquez Schroeder[13], J. Veatch[32], V. Vecchio[103], M.J. Veen[105], I. Veliscek[30], L.M. Veloce[158], F. Veloso[133a,133c], S. Veneziano[76a], A. Ventura[71a,71b], S. Ventura Gonzalez[138], A. Verbytskyi[112], M. Verducci[75a,75b], C. Vergis[96], M. Verissimo De Araujo[84b], W. Verkerke[117], J.C. Vermeulen[117], C. Vernieri[147], M. Vessella[162], M.C. Vetterli[146,ag], A. Vgenopoulos[102], N. Viaux Maira[140f], T. Vickey[143], O.E. Vickey Boeriu[143], G.H.A. Viehhauser[129], L. Vigani[64b], M. Vigl[112], M. Villa[24b,24a], M. Villaplana Perez[167], E.M. Villhauer[53], E. Vilucchi[54], M.G. Vincter[35], A. Visibile[117], C. Vittori[37], I. Vivarelli[24b,24a], E. Voevodina[112], F. Vogel[111], J.C. Voigt[51], P. Vokac[135], Yu. Volkotrub[87b], E. Von Toerne[25], B. Vormwald[37], K. Vorobev[39], M. Vos[167], K. Voss[145], M. Vozak[117], L. Vozdecky[123], N. Vranjes[16], M. Vranjes Milosavljevic[16], M. Vreeswijk[117], N.K. Vu[63d,63c], R. Vuillermet[37], O. Vujinovic[102], I. Vukotic[41], I.K. Vyas[35], S. Wada[160],

JHEP05(2025)075

C. Wagner[147], J.M. Wagner[18a], W. Wagner[175], S. Wahdan[175], H. Wahlberg[92], C.H. Waits[123], J. Walder[137], R. Walker[111], W. Walkowiak[145], A. Wall[131], E.J. Wallin[100], T. Wamorkar[18a], A.Z. Wang[139], C. Wang[102], C. Wang[11], H. Wang[18a], J. Wang[65c], P. Wang[103], P. Wang[98], R. Wang[62], R. Wang[6], S.M. Wang[152], S. Wang[14], T. Wang[63a], W.T. Wang[81], W. Wang[14], X. Wang[166], X. Wang[63c], Y. Wang[114a], Y. Wang[63a], Z. Wang[108], Z. Wang[63d,52,63c], Z. Wang[108], C. Wanotayaroj[85], A. Warburton[106], R.J. Ward[21], A.L. Warnerbring[145], N. Warrack[60], S. Waterhouse[97], A.T. Watson[21], H. Watson[53], M.F. Watson[21], E. Watton[60,137], G. Watts[142], B.M. Waugh[98], J.M. Webb[55], C. Weber[30], H.A. Weber[19], M.S. Weber[20], S.M. Weber[64a], C. Wei[63a], Y. Wei[55], A.R. Weidberg[129], E.J. Weik[120], J. Weingarten[50], C. Weiser[55], C.J. Wells[49], T. Wenaus[30], B. Wendland[50], T. Wengler[37], N.S. Wenke[112], N. Wermes[25], M. Wessels[64a], A.M. Wharton[93], A.S. White[62], A. White[8], M.J. White[1], D. Whiteson[162], L. Wickremasinghe[127], W. Wiedenmann[174], M. Wielers[137], C. Wiglesworth[44], D.J. Wilbern[123], H.G. Wilkens[37], J.J.H. Wilkinson[33], D.M. Williams[43], H.H. Williams[131], S. Williams[33], S. Willocq[105], B.J. Wilson[103], D.J. Wilson[103], P.J. Windischhofer[41], F.I. Winkel[31], F. Winklmeier[126], B.T. Winter[55], M. Wittgen[147], M. Wobisch[99], T. Wojtkowski[61], Z. Wolffs[117], J. Wollrath[37], M.W. Wolter[88], H. Wolters[133a,133c], M.C. Wong[139], E.L. Woodward[43], S.D. Worm[49], B.K. Wosiek[88], K.W. Woźniak[88], S. Wozniewski[56], K. Wraight[60], C. Wu[21], M. Wu[114b], M. Wu[116], S.L. Wu[174], X. Wu[57], X. Wu[63a], Y. Wu[63a], Z. Wu[4], J. Wuerzinger[112,ae], T.R. Wyatt[103], B.M. Wynne[53], S. Xella[44], L. Xia[114a], M. Xia[15], M. Xie[63a], A. Xiong[126], J. Xiong[18a], D. Xu[14], H. Xu[63a], L. Xu[63a], R. Xu[131], T. Xu[108], Y. Xu[142], Z. Xu[53], Z. Xu[114a], B. Yabsley[151], S. Yacoob[34a], Y. Yamaguchi[85], E. Yamashita[157], H. Yamauchi[160], T. Yamazaki[18a], Y. Yamazaki[86], S. Yan[60], Z. Yan[105], H.J. Yang[63c,63d], H.T. Yang[63a], S. Yang[63a], T. Yang[65c], X. Yang[37], X. Yang[14], Y. Yang[46], Y. Yang[63a], W-M. Yao[18a], H. Ye[56], J. Ye[14], S. Ye[30], X. Ye[63a], Y. Yeh[98], I. Yeletskikh[40], B. Yeo[18b], M.R. Yexley[98], T.P. Yildirim[129], P. Yin[43], K. Yorita[172], S. Younas[28b], C.J.S. Young[37], C. Young[147], N.D. Young[126], C. Yu[14,114c], Y. Yu[63a], J. Yuan[14,114c], M. Yuan[108], R. Yuan[63d,63c], L. Yue[98], M. Zaazoua[63a], B. Zabinski[88], I. Zahir[36a], Z.K. Zak[88], T. Zakareishvili[167], S. Zambito[57], J.A. Zamora Saa[140d,140b], J. Zang[157], D. Zanzi[55], R. Zanzottera[72a,72b], O. Zaplatilek[135], C. Zeitnitz[175], H. Zeng[14], J.C. Zeng[166], D.T. Zenger Jr[27], O. Zenin[39], T. Ženiš[29a], S. Zenz[96], S. Zerradi[36a], D. Zerwas[67], M. Zhai[14,114c], D.F. Zhang[143], J. Zhang[63b], J. Zhang[6], K. Zhang[14,114c], L. Zhang[63a], L. Zhang[114a], P. Zhang[14,114c], R. Zhang[174], S. Zhang[91], T. Zhang[157], X. Zhang[63c], Y. Zhang[142], Y. Zhang[98], Y. Zhang[114a], Z. Zhang[18a], Z. Zhang[63b], Z. Zhang[67], H. Zhao[142], T. Zhao[63b], Y. Zhao[35], Z. Zhao[63a], Z. Zhao[63a], A. Zhemchugov[40], J. Zheng[114a], K. Zheng[166], X. Zheng[63a], Z. Zheng[147], D. Zhong[166], B. Zhou[108], H. Zhou[7], N. Zhou[63c], Y. Zhou[15], Y. Zhou[114a], Y. Zhou[7], C.G. Zhu[63b], J. Zhu[108], X. Zhu[63d], Y. Zhu[63c], Y. Zhu[63a], X. Zhuang[14], K. Zhukov[69], N.I. Zimine[40], J. Zinsser[64b], M. Ziolkowski[145], L. Živković[16], A. Zoccoli[24b,24a], K. Zoch[62], T.G. Zorbas[143], O. Zormpa[47], W. Zou[43], L. Zwalinski[37]

[1] *Department of Physics, University of Adelaide, Adelaide; Australia*
[2] *Department of Physics, University of Alberta, Edmonton AB; Canada*
[3] [(a)] *Department of Physics, Ankara University, Ankara;* [(b)] *Division of Physics, TOBB University of*

JHEP05(2025)075

Economics and Technology, Ankara; Türkiye
[4] *LAPP, Université Savoie Mont Blanc, CNRS/IN2P3, Annecy; France*
[5] *APC, Université Paris Cité, CNRS/IN2P3, Paris; France*
[6] *High Energy Physics Division, Argonne National Laboratory, Argonne IL; United States of America*
[7] *Department of Physics, University of Arizona, Tucson AZ; United States of America*
[8] *Department of Physics, University of Texas at Arlington, Arlington TX; United States of America*
[9] *Physics Department, National and Kapodistrian University of Athens, Athens; Greece*
[10] *Physics Department, National Technical University of Athens, Zografou; Greece*
[11] *Department of Physics, University of Texas at Austin, Austin TX; United States of America*
[12] *Institute of Physics, Azerbaijan Academy of Sciences, Baku; Azerbaijan*
[13] *Institut de Física d'Altes Energies (IFAE), Barcelona Institute of Science and Technology, Barcelona; Spain*
[14] *Institute of High Energy Physics, Chinese Academy of Sciences, Beijing; China*
[15] *Physics Department, Tsinghua University, Beijing; China*
[16] *Institute of Physics, University of Belgrade, Belgrade; Serbia*
[17] *Department for Physics and Technology, University of Bergen, Bergen; Norway*
[18] [(a)] *Physics Division, Lawrence Berkeley National Laboratory, Berkeley CA;* [(b)] *University of California, Berkeley CA; United States of America*
[19] *Institut für Physik, Humboldt Universität zu Berlin, Berlin; Germany*
[20] *Albert Einstein Center for Fundamental Physics and Laboratory for High Energy Physics, University of Bern, Bern; Switzerland*
[21] *School of Physics and Astronomy, University of Birmingham, Birmingham; United Kingdom*
[22] [(a)] *Department of Physics, Bogazici University, Istanbul;* [(b)] *Department of Physics Engineering, Gaziantep University, Gaziantep;* [(c)] *Department of Physics, Istanbul University, Istanbul; Türkiye*
[23] [(a)] *Facultad de Ciencias y Centro de Investigaciónes, Universidad Antonio Nariño, Bogotá;* [(b)] *Departamento de Física, Universidad Nacional de Colombia, Bogotá; Colombia*
[24] [(a)] *Dipartimento di Fisica e Astronomia A. Righi, Università di Bologna, Bologna;* [(b)] *INFN Sezione di Bologna; Italy*
[25] *Physikalisches Institut, Universität Bonn, Bonn; Germany*
[26] *Department of Physics, Boston University, Boston MA; United States of America*
[27] *Department of Physics, Brandeis University, Waltham MA; United States of America*
[28] [(a)] *Transilvania University of Brasov, Brasov;* [(b)] *Horia Hulubei National Institute of Physics and Nuclear Engineering, Bucharest;* [(c)] *Department of Physics, Alexandru Ioan Cuza University of Iasi, Iasi;* [(d)] *National Institute for Research and Development of Isotopic and Molecular Technologies, Physics Department, Cluj-Napoca;* [(e)] *National University of Science and Technology Politechnica, Bucharest;* [(f)] *West University in Timisoara, Timisoara;* [(g)] *Faculty of Physics, University of Bucharest, Bucharest; Romania*
[29] [(a)] *Faculty of Mathematics, Physics and Informatics, Comenius University, Bratislava;* [(b)] *Department of Subnuclear Physics, Institute of Experimental Physics of the Slovak Academy of Sciences, Kosice; Slovak Republic*
[30] *Physics Department, Brookhaven National Laboratory, Upton NY; United States of America*
[31] *Universidad de Buenos Aires, Facultad de Ciencias Exactas y Naturales, Departamento de Física, y CONICET, Instituto de Física de Buenos Aires (IFIBA), Buenos Aires; Argentina*
[32] *California State University, CA; United States of America*
[33] *Cavendish Laboratory, University of Cambridge, Cambridge; United Kingdom*
[34] [(a)] *Department of Physics, University of Cape Town, Cape Town;* [(b)] *iThemba Labs, Western Cape;* [(c)] *Department of Mechanical Engineering Science, University of Johannesburg, Johannesburg;* [(d)] *National Institute of Physics, University of the Philippines Diliman (Philippines);* [(e)] *University of South Africa, Department of Physics, Pretoria;* [(f)] *University of Zululand, KwaDlangezwa;* [(g)] *School of Physics, University of the Witwatersrand, Johannesburg; South Africa*
[35] *Department of Physics, Carleton University, Ottawa ON; Canada*
[36] [(a)] *Faculté des Sciences Ain Chock, Université Hassan II de Casablanca;* [(b)] *Faculté des Sciences, Université Ibn-Tofail, Kénitra;* [(c)] *Faculté des Sciences Semlalia, Université Cadi Ayyad, LPHEA-Marrakech;* [(d)] *LPMR, Faculté des Sciences, Université Mohamed Premier, Oujda;* [(e)] *Faculté des sciences, Université Mohammed*

JHEP05(2025)075

V, Rabat;[f] Institute of Applied Physics, Mohammed VI Polytechnic University, Ben Guerir; Morocco
[37] CERN, Geneva; Switzerland
[38] Affiliated with an institute formerly covered by a cooperation agreement with CERN
[39] Affiliated with an institute covered by a cooperation agreement with CERN
[40] Affiliated with an international laboratory covered by a cooperation agreement with CERN
[41] Enrico Fermi Institute, University of Chicago, Chicago IL; United States of America
[42] LPC, Université Clermont Auvergne, CNRS/IN2P3, Clermont-Ferrand; France
[43] Nevis Laboratory, Columbia University, Irvington NY; United States of America
[44] Niels Bohr Institute, University of Copenhagen, Copenhagen; Denmark
[45] [a] Dipartimento di Fisica, Università della Calabria, Rende;[b] INFN Gruppo Collegato di Cosenza, Laboratori Nazionali di Frascati; Italy
[46] Physics Department, Southern Methodist University, Dallas TX; United States of America
[47] National Centre for Scientific Research "Demokritos", Agia Paraskevi; Greece
[48] [a] Department of Physics, Stockholm University;[b] Oskar Klein Centre, Stockholm; Sweden
[49] Deutsches Elektronen-Synchrotron DESY, Hamburg and Zeuthen; Germany
[50] Fakultät Physik, Technische Universität Dortmund, Dortmund; Germany
[51] Institut für Kern- und Teilchenphysik, Technische Universität Dresden, Dresden; Germany
[52] Department of Physics, Duke University, Durham NC; United States of America
[53] SUPA — School of Physics and Astronomy, University of Edinburgh, Edinburgh; United Kingdom
[54] INFN e Laboratori Nazionali di Frascati, Frascati; Italy
[55] Physikalisches Institut, Albert-Ludwigs-Universität Freiburg, Freiburg; Germany
[56] II. Physikalisches Institut, Georg-August-Universität Göttingen, Göttingen; Germany
[57] Département de Physique Nucléaire et Corpusculaire, Université de Genève, Genève; Switzerland
[58] [a] Dipartimento di Fisica, Università di Genova, Genova;[b] INFN Sezione di Genova; Italy
[59] II. Physikalisches Institut, Justus-Liebig-Universität Giessen, Giessen; Germany
[60] SUPA — School of Physics and Astronomy, University of Glasgow, Glasgow; United Kingdom
[61] LPSC, Université Grenoble Alpes, CNRS/IN2P3, Grenoble INP, Grenoble; France
[62] Laboratory for Particle Physics and Cosmology, Harvard University, Cambridge MA; United States of America
[63] [a] Department of Modern Physics and State Key Laboratory of Particle Detection and Electronics, University of Science and Technology of China, Hefei;[b] Institute of Frontier and Interdisciplinary Science and Key Laboratory of Particle Physics and Particle Irradiation (MOE), Shandong University, Qingdao;[c] State Key Laboratory of Dark Matter Physics, School of Physics and Astronomy, Shanghai Jiao Tong University, Key Laboratory for Particle Astrophysics and Cosmology (MOE), SKLPPC, Shanghai;[d] State Key Laboratory of Dark Matter Physics, Tsung-Dao Lee Institute, Shanghai Jiao Tong University, Shanghai;[e] School of Physics, Zhengzhou University; China
[64] [a] Kirchhoff-Institut für Physik, Ruprecht-Karls-Universität Heidelberg, Heidelberg;[b] Physikalisches Institut, Ruprecht-Karls-Universität Heidelberg, Heidelberg; Germany
[65] [a] Department of Physics, Chinese University of Hong Kong, Shatin, N.T., Hong Kong;[b] Department of Physics, University of Hong Kong, Hong Kong;[c] Department of Physics and Institute for Advanced Study, Hong Kong University of Science and Technology, Clear Water Bay, Kowloon, Hong Kong; China
[66] Department of Physics, National Tsing Hua University, Hsinchu; Taiwan
[67] IJCLab, Université Paris-Saclay, CNRS/IN2P3, 91405, Orsay; France
[68] Centro Nacional de Microelectrónica (IMB-CNM-CSIC), Barcelona; Spain
[69] Department of Physics, Indiana University, Bloomington IN; United States of America
[70] [a] INFN Gruppo Collegato di Udine, Sezione di Trieste, Udine;[b] ICTP, Trieste;[c] Dipartimento Politecnico di Ingegneria e Architettura, Università di Udine, Udine; Italy
[71] [a] INFN Sezione di Lecce;[b] Dipartimento di Matematica e Fisica, Università del Salento, Lecce; Italy
[72] [a] INFN Sezione di Milano;[b] Dipartimento di Fisica, Università di Milano, Milano; Italy
[73] [a] INFN Sezione di Napoli;[b] Dipartimento di Fisica, Università di Napoli, Napoli; Italy
[74] [a] INFN Sezione di Pavia;[b] Dipartimento di Fisica, Università di Pavia, Pavia; Italy
[75] [a] INFN Sezione di Pisa;[b] Dipartimento di Fisica E. Fermi, Università di Pisa, Pisa; Italy
[76] [a] INFN Sezione di Roma;[b] Dipartimento di Fisica, Sapienza Università di Roma, Roma; Italy

JHEP05(2025)075

[77] [(a)] INFN Sezione di Roma Tor Vergata; [(b)] Dipartimento di Fisica, Università di Roma Tor Vergata, Roma; Italy
[78] [(a)] INFN Sezione di Roma Tre; [(b)] Dipartimento di Matematica e Fisica, Università Roma Tre, Roma; Italy
[79] [(a)] INFN-TIFPA; [(b)] Università degli Studi di Trento, Trento; Italy
[80] Universität Innsbruck, Department of Astro and Particle Physics, Innsbruck; Austria
[81] University of Iowa, Iowa City IA; United States of America
[82] Department of Physics and Astronomy, Iowa State University, Ames IA; United States of America
[83] Istinye University, Sariyer, Istanbul; Türkiye
[84] [(a)] Departamento de Engenharia Elétrica, Universidade Federal de Juiz de Fora (UFJF), Juiz de Fora; [(b)] Universidade Federal do Rio De Janeiro COPPE/EE/IF, Rio de Janeiro; [(c)] Instituto de Física, Universidade de São Paulo, São Paulo; [(d)] Rio de Janeiro State University, Rio de Janeiro; [(e)] Federal University of Bahia, Bahia; Brazil
[85] KEK, High Energy Accelerator Research Organization, Tsukuba; Japan
[86] Graduate School of Science, Kobe University, Kobe; Japan
[87] [(a)] AGH University of Krakow, Faculty of Physics and Applied Computer Science, Krakow; [(b)] Marian Smoluchowski Institute of Physics, Jagiellonian University, Krakow; Poland
[88] Institute of Nuclear Physics Polish Academy of Sciences, Krakow; Poland
[89] Faculty of Science, Kyoto University, Kyoto; Japan
[90] Research Center for Advanced Particle Physics and Department of Physics, Kyushu University, Fukuoka; Japan
[91] L2IT, Université de Toulouse, CNRS/IN2P3, UPS, Toulouse; France
[92] Instituto de Física La Plata, Universidad Nacional de La Plata and CONICET, La Plata; Argentina
[93] Physics Department, Lancaster University, Lancaster; United Kingdom
[94] Oliver Lodge Laboratory, University of Liverpool, Liverpool; United Kingdom
[95] Department of Experimental Particle Physics, Jožef Stefan Institute and Department of Physics, University of Ljubljana, Ljubljana; Slovenia
[96] Department of Physics and Astronomy, Queen Mary University of London, London; United Kingdom
[97] Department of Physics, Royal Holloway University of London, Egham; United Kingdom
[98] Department of Physics and Astronomy, University College London, London; United Kingdom
[99] Louisiana Tech University, Ruston LA; United States of America
[100] Fysiska institutionen, Lunds universitet, Lund; Sweden
[101] Departamento de Física Teorica C-15 and CIAFF, Universidad Autónoma de Madrid, Madrid; Spain
[102] Institut für Physik, Universität Mainz, Mainz; Germany
[103] School of Physics and Astronomy, University of Manchester, Manchester; United Kingdom
[104] CPPM, Aix-Marseille Université, CNRS/IN2P3, Marseille; France
[105] Department of Physics, University of Massachusetts, Amherst MA; United States of America
[106] Department of Physics, McGill University, Montreal QC; Canada
[107] School of Physics, University of Melbourne, Victoria; Australia
[108] Department of Physics, University of Michigan, Ann Arbor MI; United States of America
[109] Department of Physics and Astronomy, Michigan State University, East Lansing MI; United States of America
[110] Group of Particle Physics, University of Montreal, Montreal QC; Canada
[111] Fakultät für Physik, Ludwig-Maximilians-Universität München, München; Germany
[112] Max-Planck-Institut für Physik (Werner-Heisenberg-Institut), München; Germany
[113] Graduate School of Science and Kobayashi-Maskawa Institute, Nagoya University, Nagoya; Japan
[114] [(a)] Department of Physics, Nanjing University, Nanjing; [(b)] School of Science, Shenzhen Campus of Sun Yat-sen University; [(c)] University of Chinese Academy of Science (UCAS), Beijing; China
[115] Department of Physics and Astronomy, University of New Mexico, Albuquerque NM; United States of America
[116] Institute for Mathematics, Astrophysics and Particle Physics, Radboud University/Nikhef, Nijmegen; Netherlands
[117] Nikhef National Institute for Subatomic Physics and University of Amsterdam, Amsterdam; Netherlands
[118] Department of Physics, Northern Illinois University, DeKalb IL; United States of America

JHEP05(2025)075

[119] [(a)] New York University Abu Dhabi, Abu Dhabi;[(b)] United Arab Emirates University, Al Ain; United Arab Emirates
[120] Department of Physics, New York University, New York NY; United States of America
[121] Ochanomizu University, Otsuka, Bunkyo-ku, Tokyo; Japan
[122] Ohio State University, Columbus OH; United States of America
[123] Homer L. Dodge Department of Physics and Astronomy, University of Oklahoma, Norman OK; United States of America
[124] Department of Physics, Oklahoma State University, Stillwater OK; United States of America
[125] Palacký University, Joint Laboratory of Optics, Olomouc; Czech Republic
[126] Institute for Fundamental Science, University of Oregon, Eugene, OR; United States of America
[127] Graduate School of Science, Osaka University, Osaka; Japan
[128] Department of Physics, University of Oslo, Oslo; Norway
[129] Department of Physics, Oxford University, Oxford; United Kingdom
[130] LPNHE, Sorbonne Université, Université Paris Cité, CNRS/IN2P3, Paris; France
[131] Department of Physics, University of Pennsylvania, Philadelphia PA; United States of America
[132] Department of Physics and Astronomy, University of Pittsburgh, Pittsburgh PA; United States of America
[133] [(a)] Laboratório de Instrumentação e Física Experimental de Partículas — LIP, Lisboa;[(b)] Departamento de Física, Faculdade de Ciências, Universidade de Lisboa, Lisboa;[(c)] Departamento de Física, Universidade de Coimbra, Coimbra;[(d)] Centro de Física Nuclear da Universidade de Lisboa, Lisboa;[(e)] Departamento de Física, Escola de Ciências, Universidade do Minho, Braga;[(f)] Departamento de Física Teórica y del Cosmos, Universidad de Granada, Granada (Spain);[(g)] Departamento de Física, Instituto Superior Técnico, Universidade de Lisboa, Lisboa; Portugal
[134] Institute of Physics of the Czech Academy of Sciences, Prague; Czech Republic
[135] Czech Technical University in Prague, Prague; Czech Republic
[136] Charles University, Faculty of Mathematics and Physics, Prague; Czech Republic
[137] Particle Physics Department, Rutherford Appleton Laboratory, Didcot; United Kingdom
[138] IRFU, CEA, Université Paris-Saclay, Gif-sur-Yvette; France
[139] Santa Cruz Institute for Particle Physics, University of California Santa Cruz, Santa Cruz CA; United States of America
[140] [(a)] Departamento de Física, Pontificia Universidad Católica de Chile, Santiago;[(b)] Millennium Institute for Subatomic physics at high energy frontier (SAPHIR), Santiago;[(c)] Instituto de Investigación Multidisciplinario en Ciencia y Tecnología, y Departamento de Física, Universidad de La Serena;[(d)] Universidad Andres Bello, Department of Physics, Santiago;[(e)] Instituto de Alta Investigación, Universidad de Tarapacá, Arica;[(f)] Departamento de Física, Universidad Técnica Federico Santa María, Valparaíso; Chile
[141] Department of Physics, Institute of Science, Tokyo; Japan
[142] Department of Physics, University of Washington, Seattle WA; United States of America
[143] Department of Physics and Astronomy, University of Sheffield, Sheffield; United Kingdom
[144] Department of Physics, Shinshu University, Nagano; Japan
[145] Department Physik, Universität Siegen, Siegen; Germany
[146] Department of Physics, Simon Fraser University, Burnaby BC; Canada
[147] SLAC National Accelerator Laboratory, Stanford CA; United States of America
[148] Department of Physics, Royal Institute of Technology, Stockholm; Sweden
[149] Departments of Physics and Astronomy, Stony Brook University, Stony Brook NY; United States of America
[150] Department of Physics and Astronomy, University of Sussex, Brighton; United Kingdom
[151] School of Physics, University of Sydney, Sydney; Australia
[152] Institute of Physics, Academia Sinica, Taipei; Taiwan
[153] [(a)] E. Andronikashvili Institute of Physics, Iv. Javakhishvili Tbilisi State University, Tbilisi;[(b)] High Energy Physics Institute, Tbilisi State University, Tbilisi;[(c)] University of Georgia, Tbilisi; Georgia
[154] Department of Physics, Technion, Israel Institute of Technology, Haifa; Israel
[155] Raymond and Beverly Sackler School of Physics and Astronomy, Tel Aviv University, Tel Aviv; Israel
[156] Department of Physics, Aristotle University of Thessaloniki, Thessaloniki; Greece

JHEP05(2025)075

[157] International Center for Elementary Particle Physics and Department of Physics, University of Tokyo, Tokyo; Japan
[158] Department of Physics, University of Toronto, Toronto ON; Canada
[159] [(a)] TRIUMF, Vancouver BC; [(b)] Department of Physics and Astronomy, York University, Toronto ON; Canada
[160] Division of Physics and Tomonaga Center for the History of the Universe, Faculty of Pure and Applied Sciences, University of Tsukuba, Tsukuba; Japan
[161] Department of Physics and Astronomy, Tufts University, Medford MA; United States of America
[162] Department of Physics and Astronomy, University of California Irvine, Irvine CA; United States of America
[163] University of West Attica, Athens; Greece
[164] University of Sharjah, Sharjah; United Arab Emirates
[165] Department of Physics and Astronomy, University of Uppsala, Uppsala; Sweden
[166] Department of Physics, University of Illinois, Urbana IL; United States of America
[167] Instituto de Física Corpuscular (IFIC), Centro Mixto Universidad de Valencia — CSIC, Valencia; Spain
[168] Department of Physics, University of British Columbia, Vancouver BC; Canada
[169] Department of Physics and Astronomy, University of Victoria, Victoria BC; Canada
[170] Fakultät für Physik und Astronomie, Julius-Maximilians-Universität Würzburg, Würzburg; Germany
[171] Department of Physics, University of Warwick, Coventry; United Kingdom
[172] Waseda University, Tokyo; Japan
[173] Department of Particle Physics and Astrophysics, Weizmann Institute of Science, Rehovot; Israel
[174] Department of Physics, University of Wisconsin, Madison WI; United States of America
[175] Fakultät für Mathematik und Naturwissenschaften, Fachgruppe Physik, Bergische Universität Wuppertal, Wuppertal; Germany
[176] Department of Physics, Yale University, New Haven CT; United States of America
[177] Yerevan Physics Institute, Yerevan; Armenia

[a] Also Affiliated with an institute covered by a cooperation agreement with CERN
[b] Also at An-Najah National University, Nablus; Palestine
[c] Also at Borough of Manhattan Community College, City University of New York, New York NY; United States of America
[d] Also at Center for High Energy Physics, Peking University; China
[e] Also at Center for Interdisciplinary Research and Innovation (CIRI-AUTH), Thessaloniki; Greece
[f] Also at CERN, Geneva; Switzerland
[g] Also at CMD-AC UNEC Research Center, Azerbaijan State University of Economics (UNEC); Azerbaijan
[h] Also at Département de Physique Nucléaire et Corpusculaire, Université de Genève, Genève; Switzerland
[i] Also at Departament de Fisica de la Universitat Autonoma de Barcelona, Barcelona; Spain
[j] Also at Department of Financial and Management Engineering, University of the Aegean, Chios; Greece
[k] Also at Department of Mathematical Sciences, University of South Africa, Johannesburg; South Africa
[l] Also at Department of Physics, California State University, Sacramento; United States of America
[m] Also at Department of Physics, King's College London, London; United Kingdom
[n] Also at Department of Physics, Stanford University, Stanford CA; United States of America
[o] Also at Department of Physics, Stellenbosch University; South Africa
[p] Also at Department of Physics, University of Fribourg, Fribourg; Switzerland
[q] Also at Department of Physics, University of Thessaly; Greece
[r] Also at Department of Physics, Westmont College, Santa Barbara; United States of America
[s] Also at Faculty of Physics, Sofia University, 'St. Kliment Ohridski', Sofia; Bulgaria
[t] Also at Hellenic Open University, Patras; Greece
[u] Also at Henan University; China
[v] Also at Imam Mohammad Ibn Saud Islamic University; Saudi Arabia
[w] Also at Institucio Catalana de Recerca i Estudis Avancats, ICREA, Barcelona; Spain
[x] Also at Institut für Experimentalphysik, Universität Hamburg, Hamburg; Germany
[y] Also at Institute for Nuclear Research and Nuclear Energy (INRNE) of the Bulgarian Academy of Sciences, Sofia; Bulgaria

JHEP05(2025)075

[z] Also at Institute of Applied Physics, Mohammed VI Polytechnic University, Ben Guerir; Morocco
[aa] Also at Institute of Particle Physics (IPP); Canada
[ab] Also at Institute of Physics and Technology, Mongolian Academy of Sciences, Ulaanbaatar; Mongolia
[ac] Also at Institute of Physics, Azerbaijan Academy of Sciences, Baku; Azerbaijan
[ad] Also at National Institute of Physics, University of the Philippines Diliman (Philippines); Philippines
[ae] Also at Technical University of Munich, Munich; Germany
[af] Also at The Collaborative Innovation Center of Quantum Matter (CICQM), Beijing; China
[ag] Also at TRIUMF, Vancouver BC; Canada
[ah] Also at Università di Napoli Parthenope, Napoli; Italy
[ai] Also at University of Colorado Boulder, Department of Physics, Colorado; United States of America
[aj] Also at University of the Western Cape; South Africa
[ak] Also at Washington College, Chestertown, MD; United States of America
[al] Also at Yeditepe University, Physics Department, Istanbul; Türkiye
[*] Deceased

JHEP05(2025)075